

A FEASIBILITY STUDY OF AN EXPERIMENT FOR DETERMINING  
THE PROPERTIES OF THE MARS ATMOSPHERE

VOLUME I - SUMMARY

By Steven Georgiev

Distribution of this report is provided in the interest of  
information exchange. Responsibility for the contents  
resides in the author or organization that prepared it.

Prepared under Contract No. NAS 2-2970 by  
AVCO CORPORATION  
Lowell, Mass.

for Ames Research Center

NATIONAL AERONAUTICS AND SPACE ADMINISTRATION

---

For sale by the Clearinghouse for Federal Scientific and Technical Information  
Springfield, Virginia 22151 - CFSTI price \$3.00

## BOOK INDEX

VOLUME	I	SUMMARY -- NASA CR 530
VOLUME	II	PROBE SYSTEM SELECTION AND DESIGN -- NASA CR 73004
VOLUME	III	SUBSYSTEM AND TECHNICAL ANALYSES -- NASA CR 73005
Book	1	Trajectories and Avionics
Book	2	Mechanics and Design
VOLUME	IV	STERILIZATION ANALYSIS -- NASA CR 73006
VOLUME	V	PROBE DEVELOPMENT PLAN -- NASA CR 73007
VOLUME	VI	VENUS PROBE ANALYSIS AND DESIGN -- NASA CR 73008

## PREFACE

This report presents the results of a feasibility study of a Mars Atmospheric Probe whose purpose is to accurately determine the properties of the Mars atmosphere. In addition, the ability of such a small probe vehicle for determining the Venus atmosphere properties was also briefly examined.

The final report consists of six volumes, namely:

- Volume I Summary -- NASA CR 530
- Volume II Probe System Selection and Design -- NASA CR 73004
- Volume III Subsystem and Technical Analyses -- NASA CR 73005
  - Book 1 Trajectories and Avionics
  - Book 2 Mechanics and Design
- Volume IV Sterilization Analysis -- NASA CR 73006
- Volume V Probe Development Plan -- NASA CR 73007
- Volume VI Venus Probe Analysis and Design -- NASA CR 73008

This volume contains a summary of the Mars Atmosphere Probe study program results. The study ground rules and constraints are minimized first, followed by a description of the Probe System design, selection and performance. A summary of the probe sterilization analyses is contained in Section 6.0 which is followed by a brief description of several alternate mission modes considered during the study. Finally, a suggested earth-entry test program and an overall Probe development plan are summarized.

## ACKNOWLEDGMENT

The principal study leaders for this program were:

- W. J. Coderre, Systems Analysis
- H. B. Winkler, Vehicle Engineering and Analysis
- R. I. Moskowitz, Telecommunications and Instrumentation
- H. M. Burnham, Vehicle Design
- T. H. Rider, Sterilization
- L. E. Donadio, Program Planning and Schedules.

## CONTENTS

1. 0 Introduction .....	1
2. 0 Mission Requirements and Constraints .....	2
2. 1 Mission Objectives .....	2
2. 2 Mission Ground Rules and Constraints .....	2
2. 2. 1 Atmospheric Reconstruction .....	2
2. 2. 2 Range of Model Atmospheres .....	3
2. 2. 3 Range of Launch Opportunities and Mars Entry Conditions .....	3
2. 2. 4 Relay Communications Constraints .....	6
2. 2. 5 Probe-Spacecraft Separation Constraints .....	6
2. 2. 6 Probe-Spacecraft Integration Constraints .....	7
2. 2. 7 Planetary Quarantine Constraint .....	8
3. 0 Mission Profile .....	10
3. 1 Launch to Probe-Spacecraft Separation Sequence .....	10
3. 2 Probe-Spacecraft Separation Sequence .....	10
3. 3 Probe Entry Sequence .....	11
4. 0 Probe System Design Description .....	15
4. 1 Overall Probe System Description .....	15
4. 2 The Entry Probe .....	15
4. 2. 1 Probe Shell Structure .....	20
4. 2. 2 Probe Heat Protection and Thermal Control .....	20
4. 2. 3 Probe Instrumentation Components .....	21
4. 2. 4 Probe Telecommunications Components .....	27
4. 3 The Probe Separation, Stabilization, and Propulsion Subsystem .....	54
4. 3. 1 Probe Separation and Stabilization .....	54
4. 3. 2 Probe Propulsion .....	57
4. 3. 3 Probe Safing, Sequencing, and Initiation .....	58
4. 4 The Probe Sterilization Canister .....	65
4. 5 Probe-Spacecraft Integration .....	67
4. 5. 1 Probe-Spacecraft Electrical Interface .....	67
4. 5. 2 Probe-Spacecraft Mechanical Integration .....	67

## CONTENTS (Cont'd)

5.0 Probe System Selection and Performance .....	71
5.1 Probe Instrumentation Payload Selection .....	71
5.2 Launch Window, Approach Trajectory, and Probe- Spacecraft Separation Conditions Selection .....	73
5.2.1 Launch Window Selection .....	73
5.2.2 Effects of Approach Velocity and Probe Separation Conditions .....	75
5.3 Probe Separation System Selection and Performance .....	81
5.4 Probe Ballistic Coefficient, Probe Configuration, and Entry Trajectory Selection .....	82
5.4.1 Effect of Ballistic Coefficient and Entry Angle on Communications Time .....	85
5.4.2 Effect of Ballistic Coefficient on Ambient Pressure and Temperature Measurements .....	87
5.4.3 Probe Configuration Selection .....	87
5.5 Telecommunications System Selection and Performance .....	89
5.5.1 Telecommunications System Selection .....	89
5.5.2 System Performance .....	96
6.0 Probe Sterilization Analysis .....	99
6.1 Major Considerations in Selection of Sterilization Techniques .....	99
6.1.1 Contamination and Decontamination Factors .....	101
6.1.2 System Physical Characteristics .....	104
6.1.3 Methods of Analysis .....	104
6.2 Results and Conclusions .....	108
6.2.1 Biological Burden Estimates .....	108
6.2.2 Assay Requirements .....	112
6.2.3 Terminal Sterilization .....	112
6.2.4 Post-sterilization Maintenance .....	116
6.2.5 Sterilization Effects on Materials and Components .....	116

## CONTENTS (Concl'd)

7.0 Alternate Mission Modes .....	119
7.1 The 1971 Launch Opportunity .....	119
7.2 Minimum Ballistic Coefficient Probe Design .....	120
7.3 Probe Deployment from Out-of-Orbit .....	120
8.0 Earth-Entry Test Program .....	122
8.1 Booster and Trajectory Selection .....	122
8.2 Probe Design and Booster Integration .....	125
9.0 References .....	129

## TABLES

Tables	I	Model Atmosphere Properties .....	4
	II	Probe System Weight Breakdown .....	19
	III	Probe Scientific Data List .....	22
	IV	Probe Engineering Data List .....	23
	V	Data Acquisition Summary .....	24
	VI	Probe Transmitting Antenna Design Requirements ..	32
	VII	Probe Transmitter Design Requirements .....	33
	VIII	Probe Power Subsystem Characteristics .....	42
	IX	Spacecraft Receiving Antenna Design Requirements .....	43
	X	Spacecraft Receiver Characteristics .....	45
	XI	Spacecraft Data Handling Characteristics (sample and encode technique) .....	49
	XII	Spacecraft Data Handling Characteristics (synchronous detection technique) .....	50
	XIII	Probe Rocket Motor Characteristics .....	59
	XIV	Sequence of Primary Events During Probe Separation and Propulsion .....	62
	XV	Modulation Techniques Comparison .....	95
	XVI	Biological Burden Contamination and Decontamination Factors .....	102
	XVII	Part and Material Burden Estimates .....	103
	XVIII	Physical Characteristics of the Mars Probe System .....	105
	XIX	Computer Program Inputs .....	107

TABLES (Concl'd)

Tables	XX	Summary of Biological Burden Estimates (millions of organisms) .....	109
	XXI	Statistical Method Description .....	113
	XXII	Assay Accuracies .....	113
	XXIII	Overall Assay Accuracies .....	113

## ILLUSTRATIONS

Figure	1	Probe Separation Sequence .....	12
	2	Probe Entry Sequence .....	13
	3a	Probe Reference Design .....	16
	3b	Probe Reference Design .....	17
	4	Three-Dimensional Probe Cut Away View .....	18
	5	Probe Telecommunications Block Diagram .....	29
	6	Spacecraft Telecommunications (receiving) Block Diagram .....	30
	7	Probe Data Handling Block Diagram .....	37
	8	Data Payout and Sampling Format .....	39
	9	Data Frame Sequence .....	40
	10	Spacecraft Receiver Block Diagram .....	46
	11	Spacecraft Data Handling Block Diagram .....	52
	12	Probe Separation Assembly .....	56
	13	Probe Safing, Sequencing, and Initiation Block Diagram .....	63
	14	Electrical Interface Schematic .....	68
	15	Probe-Spacecraft Agena Mating and Integration .....	69
	16	Interplanetary Trajectory Characteristics Summary ....	74
	17	Planetary Approach Geometry .....	76
	18	Probe Separation and Planetary Entry Geometry .....	77
	19	Effect of Probe-to-Spacecraft Lead Time and Planetary Approach Velocity on Relay Communications Range .....	79
	20	Effect of Lead Time and Approach Velocity on the Probe Entry Angle Dispersion .....	80

## ILLUSTRATIONS (Cont'd)

Figure	21	Effect of Spin/Thrust Parameter on Thrust Application Angle Error .....	83
	22	Effect of Probe Spin Rate and Initial Entry Angle of Attack on Angle-of-Attack Convergence .....	84
	23	Available Communications Time (time from 10,000 ft/sec velocity to impact) .....	86
	24	Probe Mach Number at Impact .....	88
	25	Probe Payload Comparison for Different Probe Configurations .....	90
	26	Effect of Probe Diameter on Achievable Probe Ballistic Coefficient .....	91
	27	Communications Performance Margin as a Function of Frequency .....	93
	28	Antenna Breakdown Correlation .....	94
	29	Effect of Receiving-Antenna Gain and Relay Communications Range on Achieving 10-Decibel Communications Margin .....	97
	30	Constant Margin Contours .....	98
	31	Considerations in the Selection of Sterilization Techniques .....	100
	32	Computer Program Schematic .....	106
	33	Pre-sterilization Burden Estimates .....	111
	34	Burden Assignment Assay Requirements .....	114
	35	Terminal Sterilization Configuration .....	115
	36	Post-sterilization Maintenance .....	117
	37	Earth-Entry Test Trajectory (shallow entry, thick atmosphere simulation) .....	123

ILLUSTRATIONS (Concl'd)

Figure	38	Earth-Entry Test Trajectory (vertical entry, thin atmosphere simulation) .....	124
	39	Probe-Scout and Probe-Mariner Spacecraft Integration Comparison .....	126
	40	Probe-Scout Mechanical Interface Definition .....	127

## 1.0 INTRODUCTION

The structure and composition of the Mars' atmosphere can be determined from measurements made during entry of a Probe vehicle (Reference 1-6). The pressure, temperature, and density profiles with altitude can be obtained with good accuracy from acceleration measurements at high speeds and measurements of ambient pressure and temperature in the terminal descent phase. Radiometric observations of selected wavelengths from the emission spectrum of the shock layer provide information on the composition of the atmosphere. A conceptual design of a small probe vehicle to make these measurements was described in Reference 2.

The purpose of the present study, carried out for the NASA/Ames Research Center, was to determine the feasibility of such a Mars' atmosphere probe through a study, in some detail, of the Probe Systems design and performance. The study was carried out in sufficient detail to establish the engineering feasibility of the Probe and to arrive at a preliminary design of the total Probe System together with a definition of all subsystem performance characteristics and specifications. In addition, a preliminary program plan for the development of the Probe System has been prepared, together with the associated schedules and estimated costs.

## 2.0 MISSION REQUIREMENTS AND CONSTRAINTS

Although the mission objectives remained well defined during the course of the study, many of the mission ground rules and constraints changed as additional atmospheric data was obtained from the Mariner IV Occultation Experiment and as the possible class of "bus" spacecraft was expanded to include both Voyager and Mariner class spacecraft. A summary of the most important mission objectives and constraints is given below.

### 2.1 MISSION OBJECTIVES

The basic mission objectives consist of determining accurately as a function of altitude the following characteristics of the Martian atmosphere:

- Ambient Density
- Ambient Pressure
- Ambient Temperature
- Composition

In addition to providing these data for scientific purposes, the information on surface pressure, atmospheric scale height and composition (all being obtained as part of the above measurement objectives) has an important bearing on the optimum design of large, survivable landers. This is particularly true for the low surface pressure, low scale height, atmospheric models where the landed payload is a strong function of the surface pressure and scale height.

As will be discussed later, the required data can be obtained with an instrumentation complement consisting of three axis accelerometers, pressure gages, total temperature gages, an optical radiometer and a mass spectrometer.

### 2.2 MISSION GROUND RULES AND CONSTRAINTS

The most important mission constraints arise from the atmospheric reconstruction requirements, the range of atmospheres considered, the range of spacecraft-Probe separation and planet approach and entry trajectory conditions, the Probe-to-spacecraft relay communications requirements, the Probe-spacecraft integration requirements and the requirement for planetary quarantine which imposes sterilization requirements on the probe entry vehicle.

#### 2.2.1 Atmospheric Reconstruction

To reconstruct the atmosphere with the greatest accuracy from the accelerometer measurements, it is desirable to minimize the dispersion in entry angle (and to enter at high entry angles so that dispersion in the entry angle is relatively less important).

At low altitudes, the ambient pressure and temperature measurements can be made most accurately at subsonic speeds. These requirements conflict since for the low density, low scale height atmospheres it is very difficult to achieve subsonic impact velocities for steep entry angles. Therefore it is desirable to design the Probe with a very low ballistic coefficient ( $M/C_D A$ ) in order to obtain some subsonic measurements in the low density atmospheres. (As discussed below, a low  $M/C_D A$  also greatly facilitates the Probe-spacecraft relay communications). It should be pointed out, however, that accurate atmospheric reconstruction can be obtained without recourse to the pressure and temperature measurements at low altitudes as long as the integration of the accelerometer bias errors is not great. This is the case for steep entry into the low density atmospheres where the flight times are short and the deceleration is quite high all the way up to impact. Thus the pressure and temperature measurements are included primarily to cover the contingency of a higher density atmosphere (or entry at a shallow angle) where bias error accumulation would degrade the low altitude density accuracy. For such a case, a low  $M/C_D A$  vehicle would reach subsonic speeds near impact thus resulting in accurate ambient pressure and temperature measurements.

#### 2.2.2 Range of Model Atmospheres

During the initial portions of the study only the NASA Engineering Model Atmospheres 1, 2 and 3 were considered (corresponding to surface pressures of 40, 25 and 10 millibars respectively). These models are described in NASA TN D-2525<sup>7</sup>. With the advent of the Mariner IV data the study was expanded to include a number of low density model atmospheres ranging down to 5 millibars. Table I presents a summary of the characteristics of all model atmospheres considered. It was finally decided to delete the 40 millibar atmosphere as a design criterion so that the extreme design atmospheres are the Model 2(25 millibars) and the VM-8 (5 millibars). The Model 2 atmosphere results in the greatest integrated heating and longest flight time (thus determining the heat shield thickness and data storage capacity) while the VM-8 atmosphere results in the greatest deceleration loading, dynamic pressure, heat transfer rate and the shortest flight time and communications time (i.e., the time interval between emergence from communications blackout to impact). The VM-8 atmosphere sets the requirements for the Probe structure, the relay communications data rate and the Probe ballistic coefficient. Reasonable data rates can be achieved only for relatively low  $M/C_D A$ 's (i.e., less than 0.20 slug/ft<sup>2</sup>). In addition, the dynamic ranges of most instruments are determined by the VM-8 atmosphere.

#### 2.2.3 Range of Launch Opportunities and Mars Entry Conditions

Initially, only the 1969 and 1971 flyby and orbiter launch windows were considered with the Probe being deployed on its planetary impact trajectory while the spacecraft was still on its approach trajectory prior to planet encounter.

TABLE I

## MODEL-ATMOSPHERE PROPERTIES

PROPERTY	SYMBOL	DIMENSION	Model 2 TN-D-2525	Model 3 TN-D-2525	Ames A-1 Atmosphere	VM-7	VM-8
Surface Pressure	$P_o$	mb lb/ft <sup>2</sup>	25 52.3	10 20.9	7 14.6	5.0 10.4	5.0 10.4
Surface Density	$\rho_o$	(gm/cm <sup>3</sup> ) 10 <sup>5</sup> (slugs/ft <sup>3</sup> ) 10 <sup>5</sup>	3.58 6.94	2.16 4.19	1.65 3.20	0.68 1.32	1.32 2.56
Surface Temperature	$T_o$	$^{\circ}K$ $^{\circ}R$	250.0 450.0	200.0 360	220 396	275.0 495.0	200.0 360.0
Stratospheric Temp.	$T_s$	$^{\circ}K$ $^{\circ}R$	180.0 324.0	100.0 180.0	160 288	200.0 360.0	100.0 180.0
Acceleration of Gravity at Surface	$g$	cm/sec <sup>2</sup> ft/sec <sup>2</sup>	375.0 12.3	375.0 12.3	375.0 12.3	375.0 12.3	375.0 12.3
Composition							
CO <sub>2</sub> (by mass)			16.0	60.0		28.2	100.0
CO <sub>2</sub> (by vol.)	$x_c$		10.8	48.8	70.0	20.0	100.0
N <sub>2</sub> (by mass)			84.0	40.0		71.8	0.0
N <sub>2</sub> (by vol.)	$x_n$		89.2	51.2	10.0	80.0	0.0
A (by mass)			0	0		0.0	0.0
A (by vol.)	$x_a$		0	0	20.0	0.0	0.0
Molecular Weight	$M$	mol <sup>-1</sup>	29.7	35.85	41.6	31.2	44.0
Troposphere Temp. Grad.							
Adiabatic Lapse Rate	$L_1$		1.031	1.0534	1.08202	.99467	1.0843
Press. at Stratopause at 150 KM	$P_{TH}$	lb/ft <sup>2</sup>	1.454E-3	4.939E-9	8.53E-7	5.2595E-4	1.3843E-11
Thermosphere Lapse Rate	$L_2$	$^{\circ}K/ft$	6.096E-4	1.0E-20	1.0E-20	1.0E-2-	1.0E-20
Specific Heat of Mixture	$c_p$	cal/gm <sup>o</sup> C			.165	0.230	0.166
Specific heat ratio			1.4	1.4	1.42	1.38	1.37
Adiabatic Lapse Rate (troposphere)	$L_o$	$^{\circ}K/km$ $^{\circ}R/kilo ft$	-3.89 -2.14	-4.55 -2.50	-5.55 -3.05	-3.88 -2.13	-5.39 -2.96
Tropopause altitude (bottom of stratosphere)	$Z_{ST}$	km kilo ft	18.0 59.1	22.0 72.2	10.8 35.4	19.3 63.3	18.6 61.0
Stratopause altitude* top of stratosphere	$Z_{TH}$	km kilo ft	150 492.15	150 492.15	150 492.15	150 492.15	150 492.15
Inverse Scale Ht. (Stratos) $\beta$ (1/ $\beta$ )		km <sup>-1</sup> (km) ft <sup>-1</sup> x 10 <sup>5</sup>	.0714, (14.00) 2.18	.15385, (6.50) 4.695	.11765, (8.5) 3.58423	.0705, (14.18) 2.15	.199, (503) 6.07
Cont. Surf. Wind Speed	$\bar{v}$	ft/sec	**	**	**	220	220
Peak Surf. Wind Speed	$v_{max}$	ft/sec	**	**	**	556	556
Vert. Grad. of Wind Spd. $d\bar{v}/dh$		ft/sec/kilo ft.	**	**	**	2.	2.

\* Assumed for VM-series and Model 3, given for Model 2; assumed for Ames A-1  
 \*\* Not specified in TN-D-2525 or Ames A-1

During the latter part of the study, another mission mode was examined which consisted of carrying the Probe into orbit around Mars on the orbiter spacecraft and then deploying the Probe from orbit into the Mars atmosphere. Finally, during the last portion of the study very high velocity approach trajectories were examined for the 1969 opportunity. Such trajectories are attractive in that they minimize earth-to-Mars transit time and earth-to-Mars communications range. They can be achieved for Mariner-class spacecraft launched by the Atlas/Centaur booster but are beyond the Atlas/Agena capability.

For the minimum energy 1969 and 1971 opportunities, the maximum Mars entry velocities are about 22,000 and 18,000 ft/sec, respectively. For the high approach velocity 1969 trajectories, the entry velocities are about 26,000 ft/sec (corresponding to an approach velocity,  $V_{\infty}$ , of 6.5 km/sec). The entry velocities of the Probe, when deployed from an orbiting spacecraft, range from about 11,000 to 15,000 ft/sec depending on the eccentricity of the orbit. For deployment from the approach trajectory, the Probe is designed for an entry velocity as high as 26,000 ft/sec. For deployment from orbit the entry velocities are so low that the same Probe would be grossly overdesigned and a pure heat sink (non-ablation) design becomes attractive.

For entry from the approach trajectory an arbitrary lower limit of 50 degrees has been placed on the entry angle. As mentioned previously, this is done in the interests of atmospheric reconstruction accuracy since:

- a. Greater entry angle dispersion occurs for the lower entry angles.
- b. Entry angle dispersion is more effective in producing errors at the lower entry angles.

The range of entry angles for direct entry from the approach trajectory is from 50 to 90 degrees.

For the case of entry from orbit it is possible to achieve very low entry angle dispersions. Therefore it is not very crucial to limit the range of entry angles because the lower limit to the allowable entry angle is determined by skipout considerations. This results in minimum entry angles of 10 to 15 degrees.

To minimize the effects of angle of attack, it is desirable to enter at moderate initial angles of attack. For entry from the approach trajectory, the angle of attack of the spin stabilized Probe is a function of the probe-spacecraft separation conditions and ranges from 20 to 70 degrees for a wide range of separation conditions. For entry from certain orbits, it is harder to achieve moderate initial angles of attack. However, in all instances angles of attack of 90 degrees or less can be achieved by selecting the proper deployment point along the orbit.

#### 2.2.4 Relay Communications Constraints

The data obtained by the atmospheric Probe is first transmitted to the spacecraft and is then stored on board the spacecraft and transmitted to earth via the spacecraft to deep space instrumentation facility (DSIF) communications link. To assure mission success, it is necessary to obtain adequate performance from the Probe-to-spacecraft relay link. The performance of the link depends on many factors but the major mission dependent factors are the communications range (i.e., Probe-to-spacecraft distance) during entry, the range of the look-angles between the Probe transmitting and the spacecraft receiving antennas during entry, and the gain (which is related to the size) of the spacecraft receiving antenna. To maintain mission flexibility it is desirable to achieve a relay link which performs adequately over a wide range of communications distances and geometries, but without imposing excessively large receiving antenna gain requirements on the spacecraft. In addition, the relay link should be selected so as to minimize the effects of propagation anomalies (e.g., multipath, attenuation, etc.) encountered in communications during entry and descent into planetary atmospheres.

#### 2.2.5 Probe-Spacecraft Separation Constraints

At some time prior to planetary encounter (of the order of a few days) the Probe is separated from the spacecraft and given a velocity increment,  $\Delta V$ , to put it on a planetary impact trajectory, while the spacecraft is flying by the planet. The entry angle and initial angle of attack are determined by the separation conditions and the expected dispersion in the targeted entry angle is determined by the separation conditions and the accuracy (i.e., direction and magnitude) of the velocity increment. Since the velocity increment is obtained with a body-fixed solid propellant motor, it is necessary to orient and closely control the Probe attitude prior and during the motor burn (generally to within an accuracy of less than three degrees, 3-sigma from a preselected orientation). In addition, it is desirable that the Probe separation and attitude control process does not unduly disturb the spacecraft attitude control or interfere with the spacecraft operation. Thus the requirements for the Probe Separation System consists of:

- a. Accurate separation, orientation and stabilization of the Probe prior to and during the  $\Delta V$  rocket firing.
- b. Minimum perturbation to the spacecraft.
- c. Maintain attitude control during the Probe cruise phase after separation so that the Probe angle of attack at entry is known and controlled. In addition, attitude control during the cruise phase is required to establish communications between the Probe and the spacecraft for periodic checkouts of the Probe Systems during cruise and prior to entry.

### 2.2.6 Probe-Spacecraft Integration Constraints

For reasons of mission flexibility and simplicity, it is desirable to design the Probe System so that it is compatible with all spacecraft which are likely candidates for future Mars missions. Furthermore, it is desirable to minimize the requirements imposed by the Probe on the spacecraft. The major Probe-spacecraft integration and interface areas are:

- a. Mechanical Integration -- For the smaller spacecraft (such as the Mariner IV class) there are limitations on the location and mounting attitude of the Probe without major redesign and relocation of spacecraft components. This also imposes limitations on the physical size of the Probe and the size of the associated receiving antenna on the spacecraft.
  - b. Electrical Interface--The electrical interface has to provide for Probe checkout during the prelaunch-to-separation phase of the mission and must also allow for Probe commands and updating of various programer in the Probe System. Furthermore, provisions must be made for the spacecraft to furnish a small amount of power to the Probe during the spacecraft cruise phase for the Probe battery trickle charging, for thermal control maintenance of the Probe and for periodic Probe checkouts. It is desirable to maintain a relatively simple electrical interface which imposes limitations on the number and types of commands used by the Probe.
- The electronic equipment on the spacecraft necessary to implement the relay communications link consists of the receiver with its associated bit detection and synchronization gear and a data storage system to store the data prior to transmission to earth. This equipment does not impose serious requirements on the spacecraft and can be readily accomodated. The gain of the receiving antenna, however, is constrained by the allowable physical dimensions of the antenna arising from the spacecraft and booster packaging and integration constraints.
- c. Thermal Control Interface--The Probe System must be designed so that adequate spacecraft thermal control is obtained both during the interplanetary cruise prior to Probe separation, as well as for the remainder of the mission when the Probe is missing from the spacecraft. It is therefore desirable to maintain an adiabatic thermal interface between the Probe System and the spacecraft. This influences the sterilization canister and Probe-spacecraft adapter design and requires that the spacecraft supply a small amount of power to the Probe for thermal control during the interplanetary cruise phase.
  - d. Separation and Attitude Control System Interface--During the interplanetary flight the spacecraft is usually stabilized in the sun-Canopus frame. To prevent the necessity for re-acquiring lock on the sun or Canopus, the disturbance torques acting on the spacecraft during the Probe separation

process should not exceed the capabilities of the spacecraft attitude control system. For Mariner IV class spacecraft with relatively low inertia and a low thrust attitude control system, the allowable disturbance torques are quite small and require careful design of the separation system to provide compensating torques as well as preferred positioning of the Probe axis so that the separation forces act through the spacecraft center of gravity.

The attitude control of the Probe is achieved through spin stabilization. To avoid interference with the spacecraft systems, it is undesirable to fire spin rockets in the vicinity of the spacecraft (and even a cold gas spinup system may be undesirable since it may dislodge dust particles which could interfere with the Canopus sensor). This imposes additional constraints on the separation system by leading to a mechanical spinup of the Probe during the separation process. A counter-rotating device must now be incorporated to prevent the transmission of the spinup torque to the spacecraft. An alternate scheme of allowing the Probe to coast for a period of time away from the spacecraft prior to spin rocket firing does not appear attractive because the integration of even quite small tipoff rates over a period of even a few seconds results in excessively high angular errors.

#### 2.2.7 Planetary Quarantine Constraint

It is required that the probability of contaminating Mars with a viable organism be no higher than  $10^{-4}$ . This means that the Probe System has to be sterilized prior to launch and then maintained in a sterile condition throughout the mission. Sterilization is achieved by controlling the bacteriological burden on the Probe System to a total of less than  $10^8$  organisms and then subjecting the Probe System to the specified terminal heat sterilization cycle which is rated as a twelve decade kill cycle. This then results in a probability of less than  $10^{-4}$  of a viable organism on board the entry Probe. Ethylene oxide (ETO) may also be used for surface decontamination prior to the terminal sterilization cycle. To assure sterility, the Probe is sealed hermetically in a pressurized container prior to the application of the terminal sterilization cycle. It remains sealed in the container until the injection of the spacecraft into the interplanetary transfer trajectory. The canister can then be vented (or if preferable it can remain pressurized until Probe separation) but the canister is not opened until just prior to Probe-spacecraft separation.

The sterilization requirement imposes the following constraints on the Probe system design:

- a. All Probe components must survive the terminal sterilization cycle (and the related qualification cycles) and the total Probe System must function correctly after sterilization.

- b. To minimize the bacteriological burden on the Probe, final assembly and checkout should be conducted in a high-grade clean room (class 100). This influences the assembly and checkout procedures.
- c. Side effects associated with the heat sterilization cycle such as out-gassing, structural deformations, etc. must be minimized or eliminated to prevent degradation of the Probe performance due to interference with thermal control coatings, misalignments and the like.
- d. An adequate sterilization canister has to be designed and provisions made for Probe checkout and calibration while it is sealed in the canister.
- e. Assay and other monitoring techniques must be developed to monitor the presterilization burden on the Probe System and to confirm that all Probe parts were exposed to the proper temperature cycle.

### 3.0 MISSION PROFILE

To illustrate the most significant events which occur during the Probe Mission, a typical mission sequence is discussed below. For illustrative purposes the 1969 short time-of-flight (Type I) trajectories have been chosen. Similar mission profiles have been obtained for the 1969 Type II and the 1971 Type I flyby missions. In addition, mission profiles for out-of-orbit Probe deployment for a variety of orbits were examined.

#### 3.1 LAUNCH-TO-PROBE/SPACECRAFT SEPARATION SEQUENCE

For the 1969 launch opportunity, a launch period between 14 Feb and 18 Mar 1969 has been selected. For launches during this period, Type I (heliocentric transfer angles less than 180 degrees) trajectories have been chosen. These low time-of-flight trajectories, selected at or near to minimum earth launch energy conditions, have a constant planetary arrival velocity of 6.5 km/sec which results in an entry velocity of 26,000 ft/sec. To obtain the short time of flight, above-minimum launch velocities are required, with subsequently high planetary approach velocities.

The basic interplanetary mission begins with the Mariner class spacecraft and atmospheric Probe being launched from Cape Kennedy by an Atlas/Centaur launch vehicle. After injection into an interplanetary transfer orbit to Mars, the flight spacecraft (which contains the Probe) is separated from the Centaur, the solar panels are deployed and the spacecraft acquires first the sun and then the star Canopus. The spacecraft then cruises in this attitude as maintained by its active attitude control system. The first midcourse correction maneuver is applied after several days of flight and, if necessary, a second correction maneuver is executed after about 30 days of flight (for each midcourse correction the spacecraft leaves the sun/Canopus frame, is commanded to the correct attitude for rocket firing to obtain the right velocity increment, and then re-acquires the sun/Canopus frame for subsequent cruise).

After about 260 days of flight and about 10 days prior to spacecraft/Probe separation, a final trajectory verification is made, allowing the Probe separation conditions to be selected. Depending upon the spacecraft trajectory periapsis, a planetocentric separation distance (and time) is selected and when that time is reached the separation sequence begins.

Prior to separation, the Probe System performance is checked out periodically during the cruise phase.

#### 3.2 PROBE/SPACECRAFT SEPARATION SEQUENCE

Prior to launch, a fixed velocity increment, solid propellant rocket motor has been chosen for the Probe and a fixed-probe thrust application angle has been determined relative to the spacecraft velocity vector at separation. The values

for a fixed  $\Delta V$  and the fixed-thrust application angle are selected so that variations in the actual spacecraft trajectory from that calculated prior to launch can be accommodated by simply separating the Probe at different distances from the planet.

Once the separation time has been determined, timers are updated on the spacecraft to initiate the separation sequence and the Probe programmer is updated to include the time from separation to Mars atmospheric encounter.

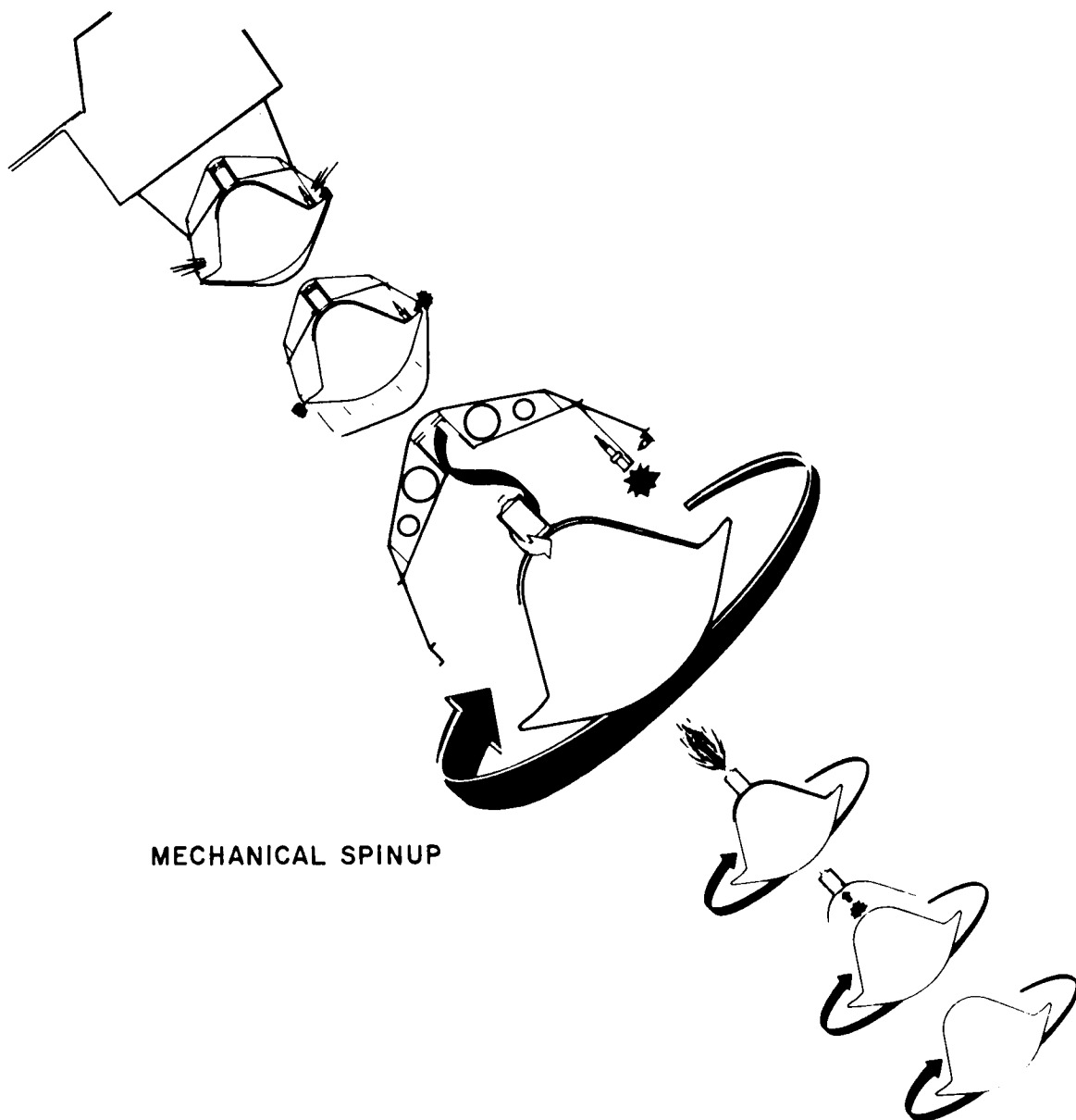
To orient the Probe in the correct direction of the thrust application angle, a spacecraft attitude maneuver is tentatively programed just prior to spacecraft/Probe separation. However a detailed analysis of the allowable mechanical mounting configuration of the Probe on the spacecraft and of the trajectory geometry at separation may indicate that either no maneuver, or merely a spacecraft maneuver about only one of its cruise-mode reference axes, is necessary. After the correct spacecraft orientation has been achieved, the physical separation sequence can start.

The separation sequence is shown schematically in Figure 1. First, the sterilization canister is vented (unless this has been already accomplished during the earlier portions of the mission). Next, the canister lid is ejected to allow the Probe to exit from the canister. Then the Probe retaining bolts are blown and the Probe is spring ejected away from the spacecraft. Spin stabilization is achieved concurrently by ejecting the Probe with a rifled tube device. To prevent significant angular-momentum transfer to the spacecraft (due to the Probe spinup), the ejection mechanism also spins up a counter-rotating flywheel which is isolated from the spacecraft (the only contact being through bearings) and which is also jettisoned after the Probe has been separated. Thus the only angular momentum acquired by the spacecraft is that transmitted through bearing friction. The linear velocity of the Probe is about 2 to 3 ft/sec and its spin rate is about 30 rpm.

Subsequent to ejection and spin stabilization the Probe is allowed to coast a safe distance away from the spacecraft (500-1000 ft) before the rocket motor is ignited so as to prevent interference with the spacecraft. The rocket burns for about 15 seconds providing a velocity increment of 75 ft/sec and after rocket motor burnout, the propulsion assembly is jettisoned and the spinning Probe continues on the planet. During the separation sequence and immediately thereafter, the Probe transmits housekeeping and acceleration data back to the spacecraft which serves as a check on the separation performance. During the subsequent cruise phase the Probe programmer turns on the Probe telemetry for periodic checkouts prior to atmospheric entry. The cruise phase lasts for about 68 hours.

### 3.3 PROBE ENTRY SEQUENCE

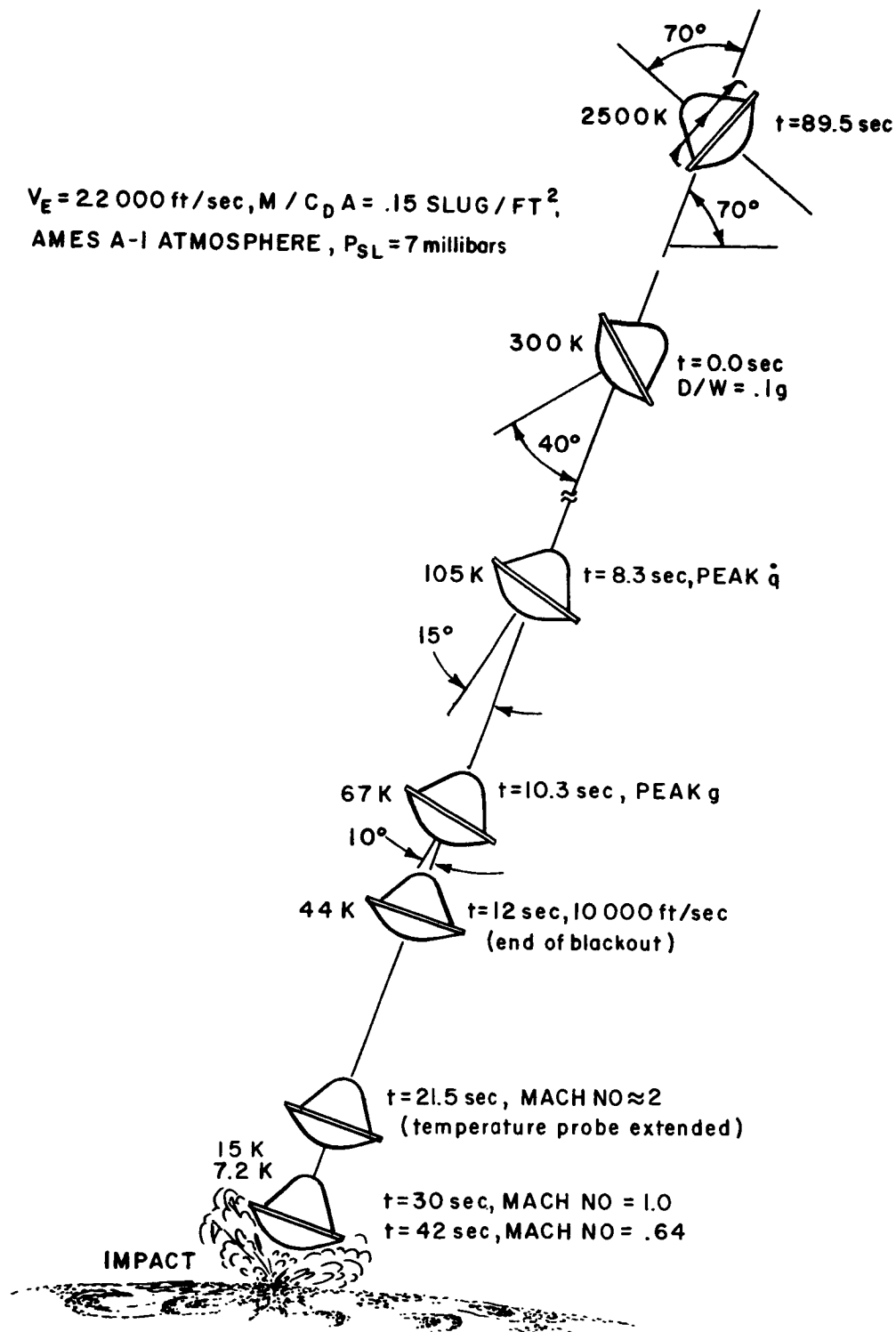
The Probe entry sequence is schematically illustrated in Figure 2 for entry onto the A-1 (7 millibar) atmosphere. About five minutes before arriving at the entry



25-1257-1A

Figure 1 PROBE SEPARATION SEQUENCE

$V_E = 22\,000 \text{ ft/sec}$ ,  $M / C_D A = .15 \text{ SLUG / FT}^2$ ,  
 AMES A-1 ATMOSPHERE,  $P_{SL} = 7 \text{ millibars}$



25- 1236-1A

Figure 2 PROBE ENTRY SEQUENCE

altitude ( $2.5 \times 10^6$  feet), a final Probe checkout occurs, triggered by the onboard timer. Then all equipment is shut off, except for a g-sensor switch. When this device senses 0.1 earth g the Probe instruments and telemetry system are turned on and data is both played out in real-time and stored for later playback. Communications blackout is conservatively assumed to exist from 0.1 g until the Probe velocity has decreased to 10,000 ft/sec.

The most important data collected during the blackout period are the accelerometer measurements and the optical radiometer measurements of the bow shock radiation. (Although quite difficult, mass spectrometer measurements can also be obtained, if desired, during this entry period.) At peak g the initial angle of attack of the Probe has converged to about 10 degrees so that angle-of-attack effects are relatively unimportant. After emergence from blackout, the blackout data is interleaved with the real-time data and transmitted to the spacecraft. The real-time data now includes the mass spectrometer, the pressure and the temperature data, as well as the accelerometer data (the optical radiometer only operates during the high velocity portion of the entry, i. e., near peak heating). It should be noted that even though the pressure and temperature instruments are sampled regularly, their readings are only meaningful at low velocities (subsonic and near subsonic) since their full-scale ranges are chosen for coverage of the low velocity flight region near impact. The temperature probes are deployed at a preset low axial g-level (6 g) to protect them from excessive heating during the higher speed portions of the entry.

All Probe data is transmitted to the spacecraft in the time period between exit from blackout and impact on the Mars surface. However, to increase reliability and simplicity, the Probe data handling, storage and telemetry system operate in a single mode throughout the entire entry. Thus the real-time data frame is played out all the time and the blackout data frame is always stored in a non-destructive readout memory and interleaved with the real-time data. During blackout, of course, even though the telemetry system is operating, the transmission is not received by the spacecraft. Nevertheless, the Probe storage can be sized and the frame readout sequence can be selected such that over the entire range of entry conditions and for all model atmospheres considered, this single playout mode guarantees that all blackout data will be played out at least once prior to impact.

## 4.0 PROBE SYSTEM DESIGN DESCRIPTION

This section contains a brief description of the total Probe System design together with some of the more important subsystem characteristics.

### 4.1 OVERALL PROBE SYSTEM DESCRIPTION

Figure 3 shows a layout of the entry Probe contained within the sterilization canister and Figure 4 shows a three-dimensional cutaway drawing of the Probe to allow better visualization of the physical arrangement of the components within it. The entry probe itself is a 55-degree half angle sphere-cone with a pulled-in afterbody. Its maximum diameter is 36 inches and its entry weight is about 50 pounds resulting in a ballistic coefficient,  $M/C_D A$ , of 0.167 slug/ft<sup>2</sup>. Table II presents a total weight breakdown for the complete Probe System.

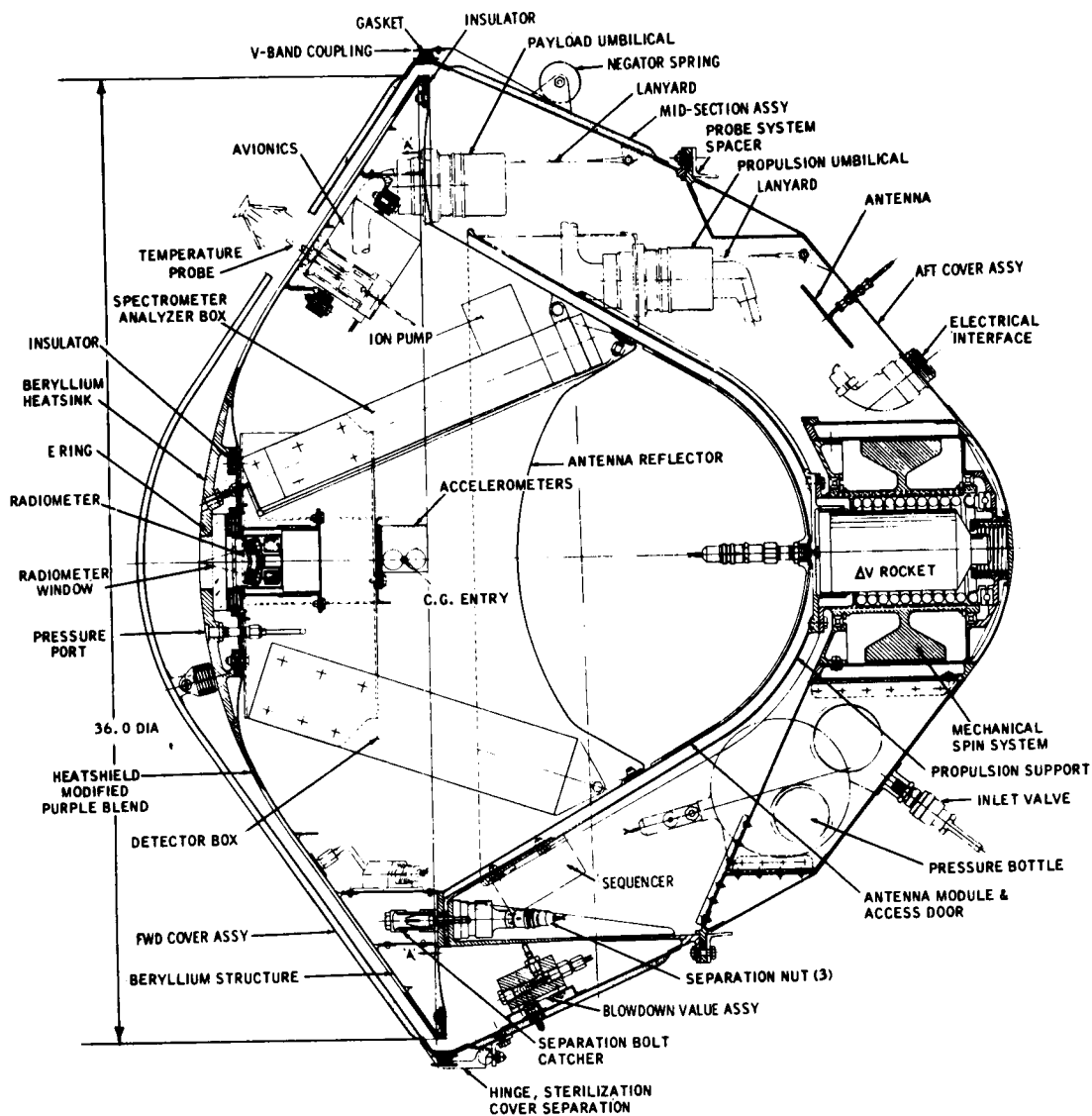
The complete Probe System consists of four major parts:

- a. The entry Probe itself which enters the Martian atmosphere, makes measurements on the atmospheric properties and telemeters this data back to the spacecraft.
- b. The sterilization canister (and the spacecraft adapter) which protects the probe from recontamination after sterilization and which also serves to provide some protection from micrometeoroid impacts.
- c. The probe separation, stabilization and propulsion equipment which is required to separate the Probe from the spacecraft and to alter the entry probe trajectory so as to result in a planetary impact trajectory with pre-selected and well controlled entry conditions.
- d. The communications equipment which is carried on board the spacecraft to complete the relay link between the entry Probe and the spacecraft. This equipment consists of the receiving antenna, the receiver with its associated bit detection and bit synchronization circuitry and finally the data storage equipment.

Each of these portions of the Probe System are briefly described below, together with their salient characteristics.

### 4.2 THE ENTRY PROBE

The entry Probe payload consists of the instrumentation payload and the necessary avionic equipment to process, store and transmit the data to the spacecraft. This total payload (consisting of the instrumentation plus the communications equipment) is housed in the vehicle shell and its heat protection system.



86-8652

Figure 3a. PROBE REFERENCE DESIGN

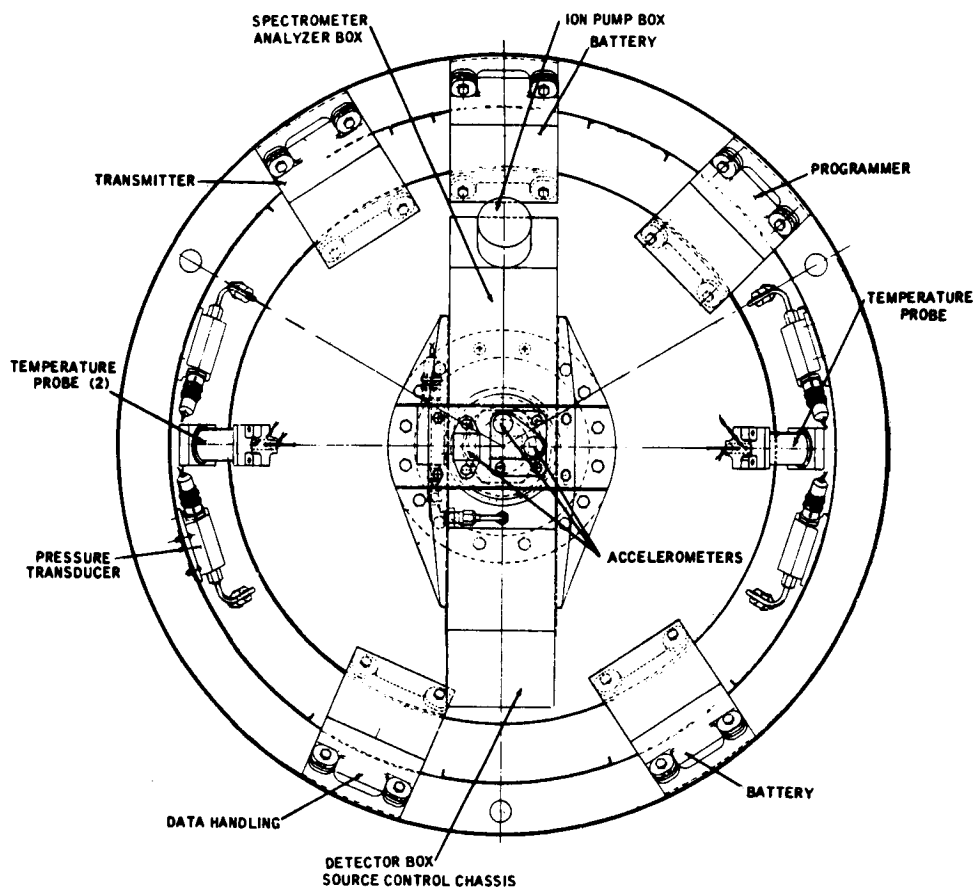


Figure 3b. PROBE REFERENCE DESIGN

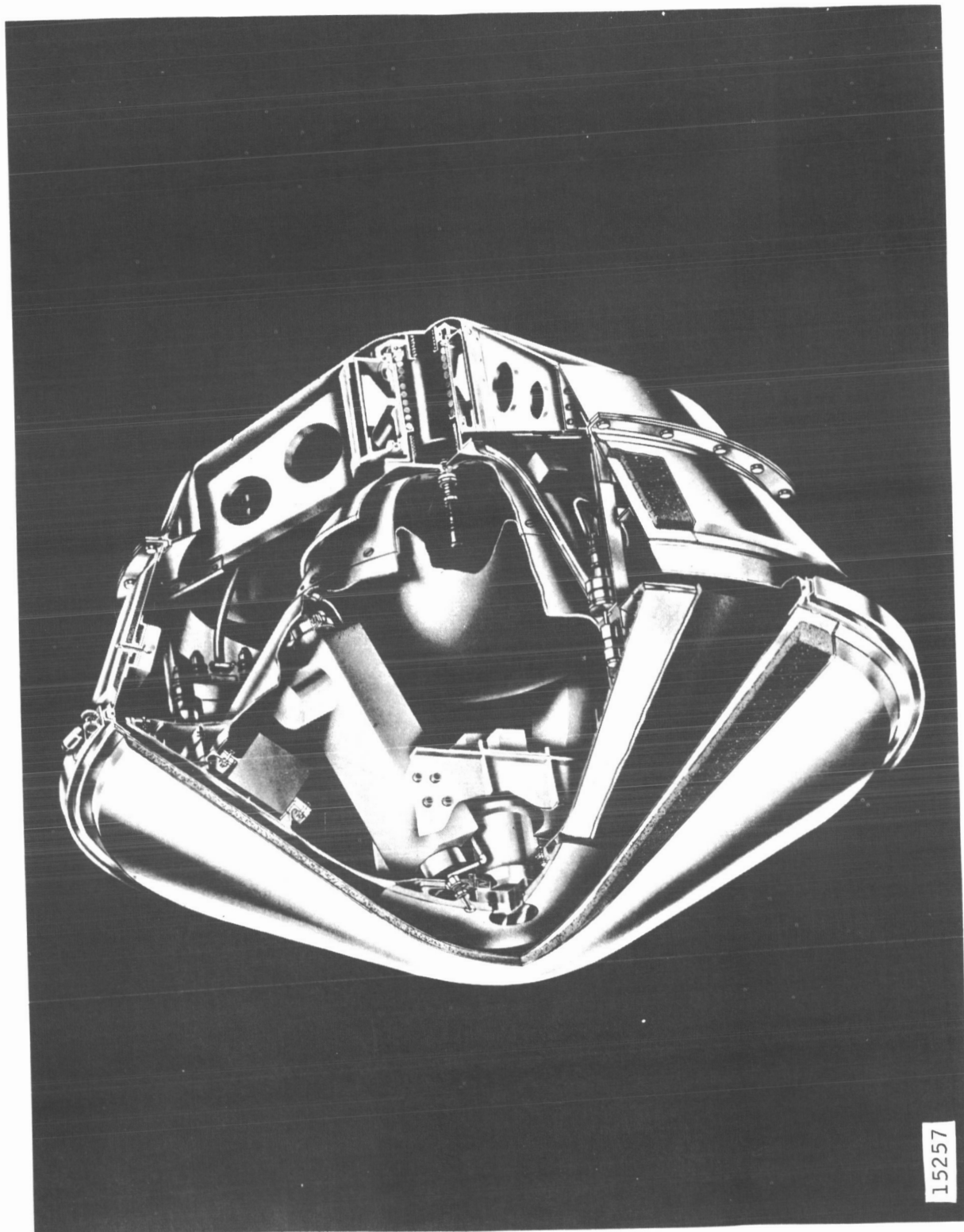


Figure 4 THREE-DIMENSIONAL PROBE CUT AWAY VIEW

15257

**TABLE II**  
**PROBE SYSTEM WEIGHT BREAKDOWN**

Diameter    36.0 inches  
M/C<sub>D</sub>A    =   0.167

	<u>Weight (pounds)</u>
<b>Instrumentation Subsystem</b>	
Accelerometers	1.8
Pressure Transducers and temperature probes	3.5
Radiometer	2.0
Mass spectrometer	9.0
Diagnostic instrumentation and cabling	0.9
Total	17.2
<b>Communication Subsystem</b>	
Transmitter & Battery	5.8
Data Handling	3.5
Programmer & Junction Box	1.5
Antenna & Cabling	1.5
Total	12.3
<b>Total Payload Weight</b>	29.5
<b>Empty Vehicle</b>	
Heat shield and coatings	5.6
Radiometer window assembly and heat sink	4.0
Ejection bolts and separation connector	1.0
Structure, supports and access door	10.1
Total	20.7
<b>Total Entry Weight</b>	50.2
<b>Propulsion System</b>	
Δ V Rocket	2.8
Support structure and torque thruster	6.0
Battery and sequencer	3.2
Total	12.0
<b>Total separated weight</b>	62.2
<b>Sterilization canister and spacecraft adapter</b>	
Cover assembly	12.0
Midsection assembly	16.5
Aft-section assembly	26.5
Spacecraft adapter	7.4
Total	62.4
<b>Total Launched Weight</b>	124.6

Passive thermal control coatings, on the outside and inside Probe surfaces and components, together with proper insulation, provide the necessary thermal control during the Probe cruise phase after separation and during the Probe entry phase.

#### 4.2.1 Probe Shell Structure

To achieve the lightest entry weight and hence lowest ballistic coefficient, the shell structure is fabricated out of beryllium. Beryllium is excellent for this application where high buckling strength is required since the design is governed by buckling under the dynamic pressure loadings and g-loadings experienced during vertical entry at 26,000 ft/sec into the worst atmosphere (for structural loading this is the VM-8 model atmosphere).

For the first 20 degrees from the stagnation point, the shell is thickened to serve as a heat sink so as to provide a flow field which is free of ablation products in the vicinity of the optical radiometer quartz window. Aft of the heat sink the shell structure is governed by minimum manufacturing gage limitations which imply a 0.035-inch shell thickness. Although chem-milling may possibly be successful in achieving still smaller gages, all weight calculations have been based on the 0.035-inch gage limit. The afterbody shell consists of a beryllium heat sink design (also with the shell gage) again limited by the manufacturing gage which results in more than adequate entry heat protection as well as structural strength. Crossed slots are cut into the shell and filled with a dielectric material to permit the antenna to radiate.

#### 4.2.2 Probe Heat Protection and Thermal Control

As mentioned previously, heat protection near the stagnation point is furnished by the beryllium heat sink whose thickness of 0.33 inch is sized by the shallowest (-50 degree) entry at 26,000 ft/sec into the maximum density atmosphere (the 25-millibar, Model 2 atmosphere). Beginning at 20 degrees from the stagnation point and extending up to the maximum Probe diameter, an elastomeric heat shield material (a modified version of the NASA Purple Blend) is used for heat protection. The heat shield thickness is approximately 0.15 inch thick except immediately at the corner at the maximum diameter where the thickness is about 0.30 inch to protect against increased corner heating.

The afterbody is a beryllium heat sink design and the antenna slots and the dielectric filling them are protected by a surface cover of Teflon. (Teflon is used to prevent charring over the antenna slots.)

Passive coatings and insulation techniques are used to provide thermal control during the Probe cruise phase and entry phase. While the Probe is attached to the spacecraft and located inside the sterilization container, a low emissivity surface finish on the container together with insulation and a small amount of spacecraft power are used to maintain the Probe Systems above their minimum

temperatures. After Probe separation, thermal control is provided by a coating (e.g., polished aluminum) on the forward portion of the Probe with an  $a/\epsilon$  of 4.0 ( $a = 0.18$ ,  $\epsilon = 0.045$ ) and a polished beryllium surface finish on the afterbody with an average  $a/\epsilon \approx 1.7$ . It is necessary to apply the coating on the forebody over the heat shield material. In addition, the inside of the Probe shell structure is finished to obtain a low emissivity and, if necessary, the individual black boxes have low emissivity coatings also. Insulation is used to isolate certain components (e.g., the battery) from the shell structure also.

#### 4.2.3 Probe Instrumentation Components

The Probe scientific instrumentation complement, together with the required instrument ranges, accuracies and individual instrument weights, are listed in Table III. In addition to the scientific data, a number of engineering and house-keeping measurements are made. These are listed in Table IV. It should be noted that despite the limited weight, the scientific instrumentation complement provides a reasonable level of redundancy. The axial accelerometer is duplicated and there are two lateral accelerometers. Only two of the five pressure gages are necessary for atmospheric reconstruction purposes and one of the two temperature probes suffices. In addition, atmospheric composition (and gas constant) is measured by two completely independent instruments and techniques; namely, the optical radiometer and the mass spectrometer.

The number of bits required per sampling for the total data complement is 276 as indicated in Table V. The encoding accuracy is governed by the accuracy (stated in Table III) desired for each measurement. The total data complement per sample is made up of a blackout frame and a real time frame and, as indicated in Table V, some measurements are contained in both frames (the accelerometer data) while others are read only into the blackout frame (the radiometer data) or the real-time frame (pressures, temperatures, mass spectrometer data). Engineering data is read into both frames.

The bit content is 158 bits for the real-time frame and 118 bits for the blackout frame. Atmospheric reconstruction analyses have indicated that a sampling rate of one frame-per-second is adequate for both the real-time and blackout data. However, it should be noted that even though the sampling interval is one second, the data for each sample is collected and recorded within 10 milliseconds. This ensures that the different data items in each sampling are obtained essentially simultaneously (no appreciable change in Probe motion or condition occurs over this small time interval). This is particularly important for the accelerometer data, since the combined readings of the axial and lateral accelerometers are required for angle of attack and atmospheric reconstruction and all three axes should be read simultaneously.

4.2.3.1 Accelerometers -- In addition to all standard environmental and functional requirements, the accelerometers must possess high accuracy (0.1 percent of full scale) and must retain this high accuracy and null stability after

TABLE III

## PROBE SCIENTIFIC DATA LIST

Item No.	Description of Data Required	Instrumentation To Be Used	Range	Accuracy (percent F. S.)	Quantity (each)
1	Drag deceleration	Force balance Servo accelerometers 3-axis Dual range each axis -- one single axis accelerometer as backup on x-axis	x-axis (Prime) 0 to + 210g 0 to + 15g y-axis ----- 0 to ± 50g 0 to ± 15g z-axis ----- 0 to ± 50g 0 to ± 15g x-axis (Backup) 0 to + 210g 0 to + 15g	± 0.1 high range ± 0.2 low range	1
2	Surface pressure	Capacitive type pressure transducer	0 to 0.5 psia	± 1 of reading	5
3	Total temperature	Resistance thermometer total temperature probe	0 to 1300° K	± 3	2
4	Atmospheric composition and Gas properties	Optical radiometer (4-channel)  Mass spectrometer (5-channel)	Atomic at 2478 Å NH at 3360 Å CN at 4197 Å C <sub>2</sub> (swan) at 5165 Å  H <sub>2</sub> O -- mass 18 N <sub>2</sub> -- mass 28 O <sub>2</sub> -- mass 32 A -- mass 40 CO <sub>2</sub> -- mass 44		1

F. S. = full scale

TABLE IV

## PROBE ENGINEERING DATA LIST

Item No.	Description of Measurement	Range	Accuracy (percent)	Sampling Rate (per sec)**
1	Battery temperature	0 to 175°F	± 5	1/5
2	Accelerometer temperature (x-Axis)	-40 to 100° F	↓	1/5
3	Accelerometer temperature (y-Axis)	-40 to 100° F		1/5
4	Accelerometer temperature (z-Axis)	-40 to 100° F		1/5
5	Antenna temperature	-40 to 500° F		1/2
6	Heat-sink temperature (backface)	-40 to 500° F		1/2
7	Mass spectrometer detector temperature	0 to 5vdc*		1/5
8	Spare			
9	Battery monitor	13 ± 3 vdc*		1/5
10	Mass spectrometer high voltage monitor	0 to 5 vdc*		1/2
11	Mass spectrometer B+ monitor	0 to 5 vdc*		1/2
12	Radiometer sensor bias monitor	0 to 5 vdc*		1/2
13	Battery current	0 to 11 amps		1/5
14	Transmitter dc current	0 to 8 amps		1/5
15	Temperature probe No. 1 deployment signal	1 vdc step		1
16	Temperature probe No. 2 deployment signal	1 vdc step		1
17	RF forward power	1.25:1	↓	1/2
18	RF reverse power	at 270 MHz		1/2

\*Mass spectrometer and radiometer provide these output levels to monitor functions described.

\*\*This is a subcommutation rate. Frame rate of subcommutator is set so that main frame commutator samples at rate of one sample per second

TABLE V

## DATA ACQUISITION SUMMARY

Instrument	Type of Data	Number of Outputs	Encoding Accuracy	Bits
Accelerometers	Real-Time	4	10 bits	40
Pressure transducers	Real-Time	5	7 bits	35
Mass spectrometer	Real-Time	5	7 bits	35
Temperature probes	Real-Time	2	6 bits	12
Engineering data	Real-Time	6	6 bits	36
Accelerometers	Blackout	4	10 bits	40
Radiometers	Blackout	4	6 bits	24
Engineering data	Blackout	6	6 bits	36
Sync code Frame count Sub comm ident.				18
Total				276

undergoing the sterilization environment and subsequent long storage life. Furthermore, this high accuracy must be obtained at full-scale ranges of up to 250 g. After careful evaluation of a number of candidates, two were found to be particularly desirable; namely, the Bell Aerosystems Model VII and the Autonetics Model A40. Both are force-balance servo accelerometers. The reference design utilizes three Bell accelerometers orthogonally oriented in one package and one additional axially mounted instrument (to serve as a redundant backup for the axial acceleration measurement). The accelerometer for each axis will provide two outputs, one each for the low and high range scales.

The Bell accelerometer is recommended for the reference design because of the extensive flight experience available for this type of instrument. However, since the Autonetics accelerometer offers a weight advantage and has been thoroughly tested in the laboratory, it should be considered as a backup to the Bell instrument despite the present lack of flight experience.

4.2.3.2 Pressure Transducer -- The critical requirement for this instrument is good accuracy (1 percent) over a low pressure range (0 to 0.5 psia) to be achieved with a compact and low weight transducer.

The prime selection is a transducer developed by NASA/Ames to measure pressures over the extremely wide range of  $10^{-5}$  to 200 torr Hg ( $\approx 10^{-7}$  to 4 psia). The accuracy of the unit is about one percent over a large portion of its range, including the range of interest for Mars.

The transducer is very compact and light and operates by sensing pressure through the damping effect of the gas on a thin, vibrating metallic diaphragm. A unique feature of the device is that it does not require a sealed reference pressure chamber; i. e., the output of the transducer is a measure of the absolute pressure. This is a significant advantage, since the maintenance of an accurate and stable reference pressure over the long storage life and range of environments would pose a serious problem.

As a backup to the reference design a modified version of a standard Lion Research Company instrument is recommended. The transducer employs a capacitance-type sensor with a prestressed diaphragm.

4.2.3.3 Total Temperature Probe -- The critical requirement for this instrument is a reasonably short response time (about 0.1 second) and good accuracy (about one degree) in the range of 300 to 1000° K. The probe must be compact and light and must be readily deployable.

No unusually great problems are anticipated for this instrument. The design chosen is characteristic of an instrument produced by the Rosemount Company and consists of a cylindrical probe two inches long and 1/2 inch in diameter containing a platinum resistance thermometer connected to a voltage divider network. The temperature is indicated by changes in the electrical resistance of the platinum element.

4.2.3.4 Optical Radiometer -- By observing the radiation in selected, fairly narrow-band wavelength regions corresponding to certain molecular bands, it is possible to determine the relative concentration of CO<sub>2</sub>, N<sub>2</sub> and Argon in the Mars atmosphere. This radiation is produced by the hot gas behind the probe bow shock at probe velocities above 18,000 ft/sec. Studies have indicated that the instrument should measure the radiation in four separate wavelength bands (see Table III) with a spectral resolution of 50 Å. The instrument must be compact, lightweight, mechanically rigged and compatible with the sterilization environment. An instrument dynamic range of 10<sup>3</sup> is required also.

The reference design consists of a four-channel radiometer utilizing interference filters for each channel. Radiation from the shock layer passes through the vehicle window. A separate instrument window is used to give protection to both the vehicle and the radiometer, should the vehicle window fail. This also permits the pressurization of the radiometer instrument. The radiation is chopped by a motor-driven chopper wheel, which is also used to provide an in-phase synchronizing signal from the solid-state emitter and sync detector. The radiation is passed through an optical filter selected for the center wavelength and bandwidth required for the specific molecular-band radiating system, and falls on the detector. An ac preamplifier amplifies the signal level to allow for synchronous demodulation to dc, after which the signal is compressed by a logarithmic amplifier and then conditioned to drive the telemetry or data storage system. The chopper-motor power is obtained from an inverter, and a means of regulation is provided to allow the motor to operate at minimum power input for the selected speed. A speed-error signal is derived from the sync detector and its amplifier.

It should be noted that by limiting the electrical band pass of the detector-preamplifier combination, a vastly improved signal-to-noise ratio compared with dc operation is obtained, allowing the detection of very low radiation levels. Individual channel ranges are adjusted with aperture rings or screen filters at each detector-filter combination.

4.2.3.5 Mass Spectrometer -- The optical radiometer can only operate during the high velocity (and thus high altitude) entry phase and it is therefore desirable to incorporate an instrument for composition measurements at lower altitudes. The dynamic range of the instrument should be 10<sup>4</sup> and the concentration measurement accuracy should be about 10 percent. At least several discrete species should be looked for and a total mass measurement should be included also.

A five channel, sterilizable, high-g mass spectrometer under development at NASA/Goddard appears quite suitable for this task. The instrument consists of a removable sampling plug in the Probe vehicle nose cap, a sample transfer tube, a calibrated gas leak, an ion source and accelerator, four rods forming the quadrupole electrodes and surrounded by a flight tube, a multiplier detector, an electrometer amplifier, a logarithmic amplifier, and an ion pump.

Sample gases enter the sample transfer tube, pass through the leak into the source, are ionized and accelerated in the source, and pass down the flight tube while undergoing mass discrimination. The selected masses pass into the detector and provide a high impedance electrical signal. This signal is amplified by the electrometer, and then logarithmically amplified.

Since the complete instrument is quite large and relatively heavy, it is advantageous for ease of Probe packaging and proper mass distribution to divide the instrument into two separate parts which are both mounted within the entry Probe.

#### 4.2.4 Probe Telecommunications Components

The telecommunications system for the Mars Probe experiment includes:

- a. The data handling system, which samples, stores and formats the instrument output data,
- b. The transmitter, which is modulated by the data handling system output and which provides a suitable RF signal,
- c. The Probe antenna, which radiates the RF signal, with essentially a hemi-omni pattern,
- d. The battery which provides all power after Probe/spacecraft separation,
- e. The spacecraft antenna, which receives the signal and has a directional pattern,
- f. The spacecraft receiver, which amplifies and envelope-detects the RF signal,
- g. The spacecraft data handling system, which includes a video matched filter, a bit synchronizer and a storage system to contain the detected data until the spacecraft can play it out to earth.

Finally, the cruise and entry sequencer forms a part of the Probe System also.

Each of the subsystems in this telecommunications system has been designed to meet the special requirements of the Mars Probe mission with a minimum of complexity. A wideband FSK modulation scheme was selected because it provided adequate performance while imposing a minimum of difficult and complicated requirements on the subsystem. The capsule data handling system was designed to provide a single mode of operation for a wide range of mission profiles, thereby avoiding the need to change modes during the mission. A body-fixed receiving antenna is used on the spacecraft to avoid the necessity for a complex tracking system and articulating RF connections. The spacecraft data

handling system provides bit detection capability but does not provide any further processing, as this can be accomplished more effectively and reliably on earth.

A block diagram of the probe telecommunications system is presented as Figure 5. The operation of the system is as follows:

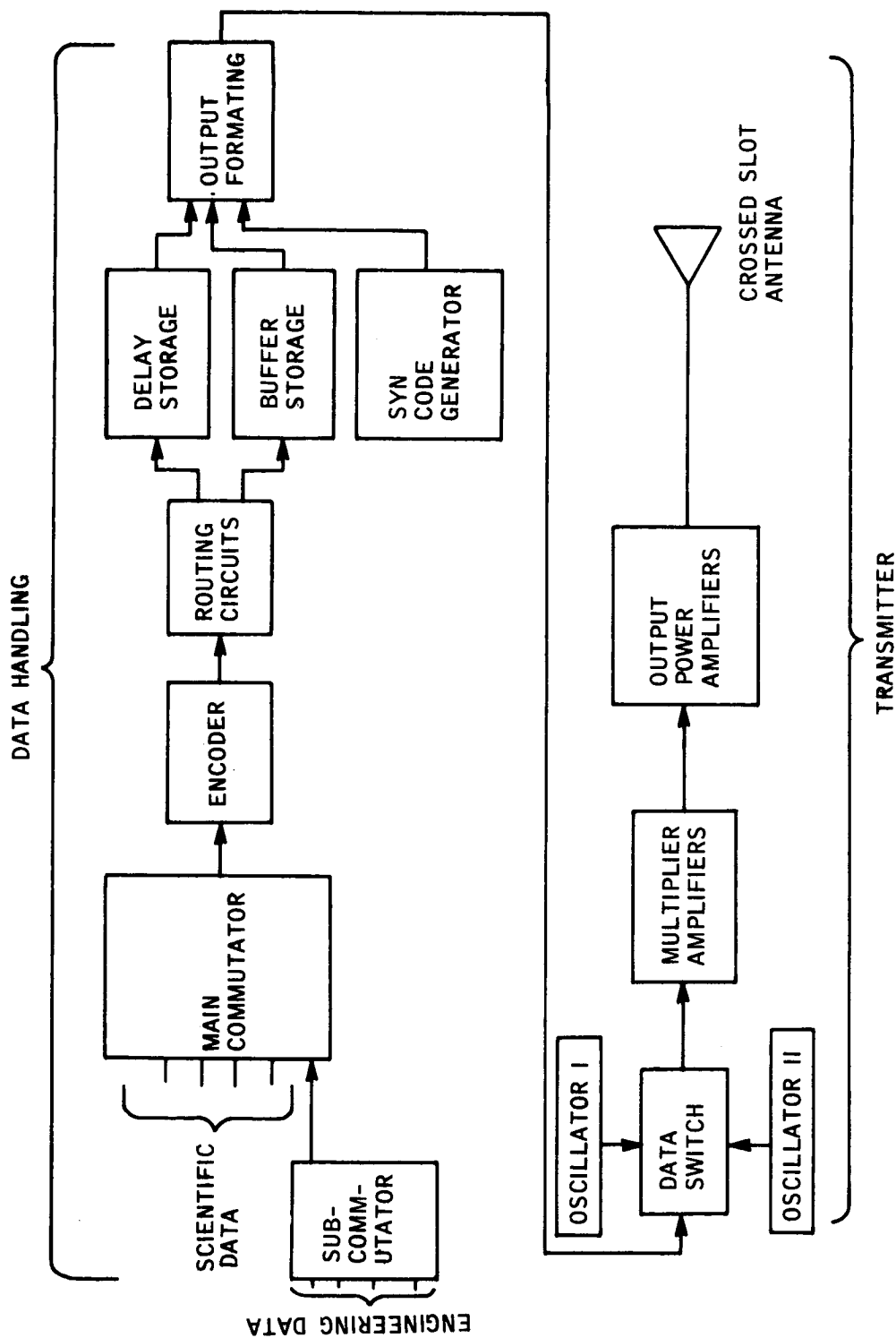
- a. The analog output of each of the scientific or engineering data sensors is sequentially sampled and encoded to form a serial binary nonreturn-to-zero (NRZ) waveform.
- b. The bits in this waveform are stored in either the blackout delay storage or the buffer storage unit, or both, depending upon whether the particular measurement is important during the blackout or post-blackout missions.

The outputs of both storage units are interleaved frame by frame at the data handling system output, resulting in an NRZ waveform containing alternating blackout and real-time data. The data then operates the data switch in the FSK transmitter. For transmission of a one, the data switch passes the higher frequency (mark) and for transmission of a zero, the lower frequency (space) is passed.

- c. The output of the data switch is a lower frequency (30 MHz), lower power replica of the FSK signal to be transmitted. This output is therefore multiplied and simplified to provide the desired 20-watt, 270 MHz signal to the probe antenna. The antenna consists of flush-mounted crossed slots at the aerodynamic rear of the Probe. The slots are fed so as to radiate a circularly polarized signal. The resulting pattern is essentially isotropic over the rear hemisphere.

Figure 6 presents a block diagram of the spacecraft receiving system required to support the Mars Atmospheric Probe. The system operation is detailed in the following paragraphs.

The receiving antenna is a helix and a half wavelength ground plane. It provides about 12 decibels of on-axis gain and has a 3-decibel beamwidth in excess of 40 degrees. The antenna is body-fixed to the spacecraft, and is oriented so as to be boresighted on the Probe at the time when the communications range is a maximum. The antenna is circularly polarized to match the Probe signal. The output of the antenna is fed to a low-noise transistor preamplifier and then to the double-conversion heterodyne receiver. The IF signal is passed through the mark or space filter (depending upon whether a one or zero is being transmitted), and then to the mark or space envelope detector. The outputs of the envelope detectors are combined resulting in a noise corrupted version of the desired NRZ signal. This signal is processed by the integrate and dump-matched filter detector which is keyed by the bit synchronizer which is locked



86-8653

Figure 5 PROBE TELECOMMUNICATIONS BLOCK DIAGRAM

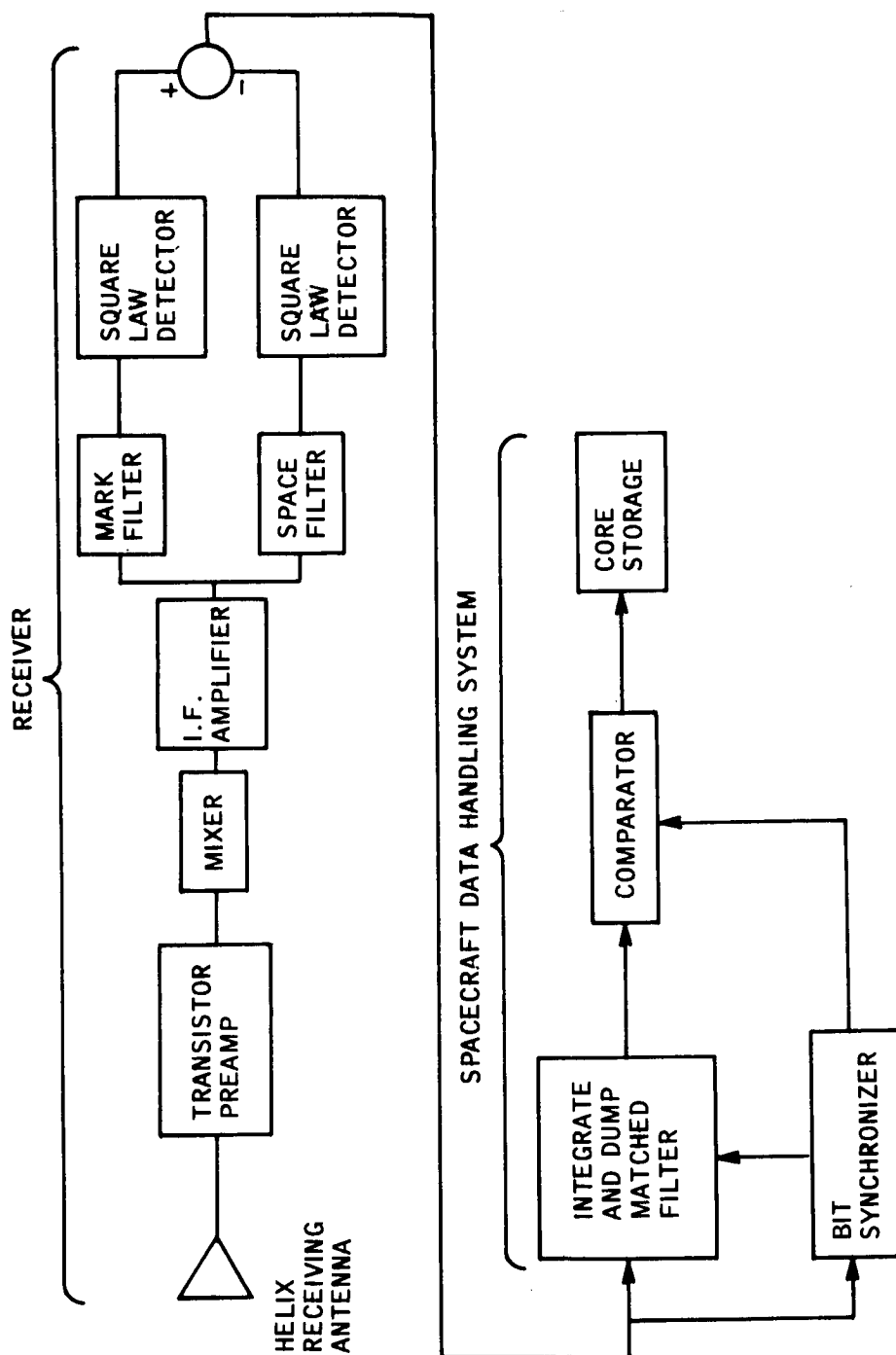


Figure 6 SPACECRAFT TELECOMMUNICATIONS (RECEIVING) BLOCK DIAGRAM

86-8654

to the noisy data signal. The matched filter output is processed by a decision-making comparator circuit which determines whether each bit is a one or a zero. The data is then placed in the storage system for subsequent transmission to earth via the existing spacecraft telemetry link. A description of each of the subsystems is presented in the following paragraphs.

4.2.4.1 Transmitting Antenna (Probe Vehicle) -- The probe antenna must be designed to provide near hemi-omni coverage at 270 MHz, and must be integrated into the Probe structure so as not to affect it aerodynamically. It is very desirable that the back-lobe radiation (radiation towards the aerodynamic front of the Probe) be kept as low as possible so as to minimize the radio power reflected to the receiving antenna from the Martian surface.

The present study has shown that the radiating structure selected for use as the Probe antenna has only a secondary effect on the radiated pattern compared with the effect of the Probe shape. The major factors in the selection of a radiating structure are appropriate bandwidth, light weight, ease of construction and ability to radiate a circularly polarized wave. Circular polarization is required in order to avoid the scalloped pattern and possible polarization mismatch that would result from linear polarization.

The requirements for the Probe antenna are summarized in Table VI. The approach selected for the Probe antenna radiating structure is a single pair of cavity-backed, orthogonal slots, fed in phase quadrature to produce circular polarization. The antenna is designed for operation at 270 MHz. The orthogonal slots, mounted on the afterbody of the Probe, will be approximately 22 inches long, backed by a bowl-shaped cavity 11 inches deep at its maximum dimension. Its on-peak gain will be comparable to a flush-mounted pair of planar crossed slots, modified by the curvature of the surface on which it is mounted. Its gain above an isotropic radiator, and its radiation pattern, is considerably modified by the shape of the Probe afterbody in a manner analogous to the effect generated by bending the arms of a turnstile antenna over a ground plane. This results in an essentially omni-directional antenna pattern in the forward hemisphere of the antenna field.

The antenna system produces circular polarization on axis and good circularity out to  $\pm 70$  degrees from the antenna boresight, at the center operating frequency of 270 MHz. This antenna system is a moderately narrow band device due to the nature of its feeding network. The 90 degree phasing cable is the band-limiting element in the input network, since its electrical length is essentially dependent on the center operating frequency; it is one-quarter wavelength long at 270 MHz. Its capability to produce circular polarization is determined by the electrical length of the cable, and its efficiency is limited primarily by the cavity depth. These are the major factors controlling the antenna operating bandwidth.

TABLE VI  
**PROBE TRANSMITTING ANTENNA DESIGN REQUIREMENTS**

Frequency	270 MHz
Polarization	Circular
Efficiency	62 percent
Input VSWR	1.50:1.00
Axial ratio	1 decibel on beam peak
Gain	-1.0 decibel below an isotropic radiator at $\pm 70$ degrees from antenna boresight
Temperature, shock and vibration	Shall be capable of performing reliably during and after exposure to the program prelaunch and flight environments.

The antenna design must be mechanically reliable. The coaxial cable and power dividers used in the input transmission must be capable of performing after exposure to a temperature of 300° F for 36 hours, for three cycles. The dielectric in the coaxial line must be carefully chosen to preclude swelling and splitting of the outer shield of the coaxial line.

4.2.4.2 Transmitter -- The transmitter is required to provide a 20-watt, FSK modulated signal to the probe antenna. Its input will be the scientific and engineering data from the data handling and storage system, in the form of a serial binary non-return-to-zero (NRZ) wave form.

Aside from the output source, the most critical transmitter parameter is its frequency stability. This is so because, for the wideband FSK receiver, the receiver bandwidth is determined by the total frequency uncertainty at the receiver. This frequency uncertainty is predominately the sum of the Doppler variation and the transmitter frequency variation. A transmitter stability of  $\pm 1 \times 10^{-5}$  has been selected as the goal, because it appears to be satisfactory and achievable.

The basic design requirements of the probe transmitter are indicated in Table VII.

TABLE VII  
PROBE TRANSMITTER DESIGN REQUIREMENTS

Frequency	267 to 273 MHz
Stability	±0.001 percent
Output power	20 watts minimum
Modulation technique	Non-coherent, wideband FSK
Input data rate	10 to 1000 bits/sec (NRZ)
Weight	less than 2 pounds

The FSK transmitter is a 20-watt, completely solid state unit. Its major sections are:

- Two Crystal Oscillators
- Two Buffer Amplifiers
- Two Diode Switches
- One Switch Driver
- One Frequency Tripler
- Transistorized Power Amplifiers.

The oscillators must meet the frequency stability requirement on one part in 10<sup>5</sup>. Since loading factors affect the frequency stability of an oscillator, a separate buffer amplifier will follow each oscillator to provide isolation. The buffer amplifiers will essentially be common emitter, class A amplifiers in which a certain amount of gain is sacrificed in order to obtain the required isolation. A diode switch, controlled by a switch driver, will follow each oscillator-buffer combination. When the input modulation signal is in the range of +1 to +2 volts, the driver will close the switch following the higher frequency oscillator (the mark channel), and will open the switch following the lower frequency oscillator (the space channel). When the input modulation signal is at ground

potential, the switch driver will close the space channel switch and open the higher frequency channel (the mark channel). With this method, switching rates of 10 to 1000 Hz can be accommodated. The input impedance of the switch driver will be greater than 100 kilohms.

The diode switches will each consist of one ED700 diode. The insertion loss of either switch, when closed, will not exceed three decibels. Isolation between ON-channel and OFF-channel will be 16 decibels, minimum. A single, class A, common emitter amplifier will be used immediately after the diode switches. This amplifier will simplify the RF power to a level high enough for efficient operation of a frequency tripler. This tripler, and the next amplifier stage, will consist of common emitter class AB stages. The driver and parallel output stages will be modified class C common emitter stages. Parallel transistors will be used in the output stage to provide the required output power, with adequate derating for power dissipation, including the effects of variations in the load-voltage standing wave ratio (VSWR). Stability and equal division of the load will be achieved.

The use of separate base drive circuits and separate emitter resistors for the output transistors will assure stability as well as an equal distribution of load. Excluding the time when the Probe is in blackout, the output power will vary less than 0.2 decibels over the entire operating temperature range. For a VSWR (load) of 1.2, maximum output power variance will be 1.0 decibel. During entry into the Martian atmosphere, high VSWR will exist, due to poor matching of the antenna to the ionized atmosphere.

If the output of the power stage is operating in a high VSWR, the effective output power is reduced and power dissipation in the output stage is increased. To withstand the increase in power dissipation, four transistors are used in the output stage so that the total power out may be reflected into (and hence dissipated in) the transistors without exceeding the rated dissipation, including a 2:1 safety factor for each transistor.

4.2.4.3 Data Handling Subsystem -- The data handling subsystem provides the means for collecting and storing the Probe data and converting it into a form compatible with transmission via the relay link. The Data Handling Subsystem consists of:

- a. The Telemetry Subsystem, which includes all equipment required to sample the Probe instrumentation, to encode the samples, and to format the data for presentation to the FSK transmitter
- b. The Data Storage Subsystem, which buffers the real-time data and stores the sampled blackout data during radio communications blackout for subsequent transmission via the RF link.

Soon after initial atmospheric contact, the ionization of the atmosphere due to entry heating will cause radio communication blackout. Some of the data received during this time is critical, and must be stored for playout after emergence from the blackout.

The data handling subsystem is designed to operate in a single data collection and transmission mode, from entry (when the Probe first senses 0.1g as it enters the Martian atmosphere) to impact. This feature isolates the data frame format from all acceleration, altitude or timed events, and therefore minimizes the possible loss of data. This single-mode operation is made possible by a unique scanning-storage-readout system.

Two types of data will be alternately sequenced from the telemetry subsystem, real-time data and delayed (blackout) data.

The real-time data is described in Tables III and V. Included in this list is the experiment sampling rate, accuracy, and number of outputs. All instruments will be operating from Probe entry to impact, and will be sampled continuously during this interval. It is required that data samples from different instruments be correlated in time. This can be accomplished by sampling all instruments at nearly the same time. In this system, all of the instruments will be scanned and sampled in bursts of approximately 10 milliseconds during any one sampling interval.

The delayed (blackout) data is stored during radio communication blackout and retransmitted after emergence from blackout. Because communications blackout may last anywhere from 8 to 30 seconds, and the time between emergence from blackout and impact may vary from 8 to 270 seconds, the playout format must be designed to satisfy this wide range of times in-blackout and out-of-blackout. The values of playout and blackout times depend upon the atmospheric structure (density and scale height) and the Probe entry trajectory. An important quantity is the ratio of the blackout duration to the playout duration. This quantity can vary from 1 to 1/9. The following constitute the major performance specifications which must be imposed on the data handling system:

- a. Accept analog input signals in the range of 0 to 5 volts. A total of 37 input signals must be accommodated.
- b. Perform analog-to-digital conversion of the input signals with an accuracy of up to one part in 1000. This dictates a 10 binary bit conversion.
- c. Encode inputs into data words at a rate of up to 20,000 bit/sec.

- d. Provide data frame forming and synchronization patterns.
- e. Provide non-return-to-zero (NRZ) outputs suitable for frequency shift modulation of a VHF transmitter.
- f. Provide bit storage and non-destructive readout of stored data of up to 3000 bits.

The above performance requirements must be met with a minimum expenditure of size, weight and power consumption. Additionally, the system must be capable of meeting these requirements after both chemical and thermal sterilization cycles and long-term storage.

A block diagram of the data handling subsystem is shown in Figure 7.

As discussed previously, all data is sampled at a rate of one sample per second, but each frame is completely sampled in 10 milliseconds. In addition, the blackout data is sampled one-half second out of phase from the real-time data. This procedure allows the possibility of an effective sampling rate increase for some of the accelerometer data. This increase is possible because, for a portion of the time in some atmospheres, real-time and delayed-time data sampled at the same instant can both be played out.

Because of the variation in accuracies required of the different measurements, and because of the desire to minimize the required data rate (thereby maximizing the communications margin possible), ten, seven, and six-bit word lengths are used.

The sampling format is such that 276-data bits are accumulated every second, in order to satisfy the experiment data requirements. These 276 bits, consisting of real-time data, blackout data, sync and timing bits, constitute the one-second data frame.

Each transmitted data frame will consist of both real-time and blackout data frames interleaved. However, to account for varying blackout and playout durations, the blackout frames of the data are not read out in the order taken,

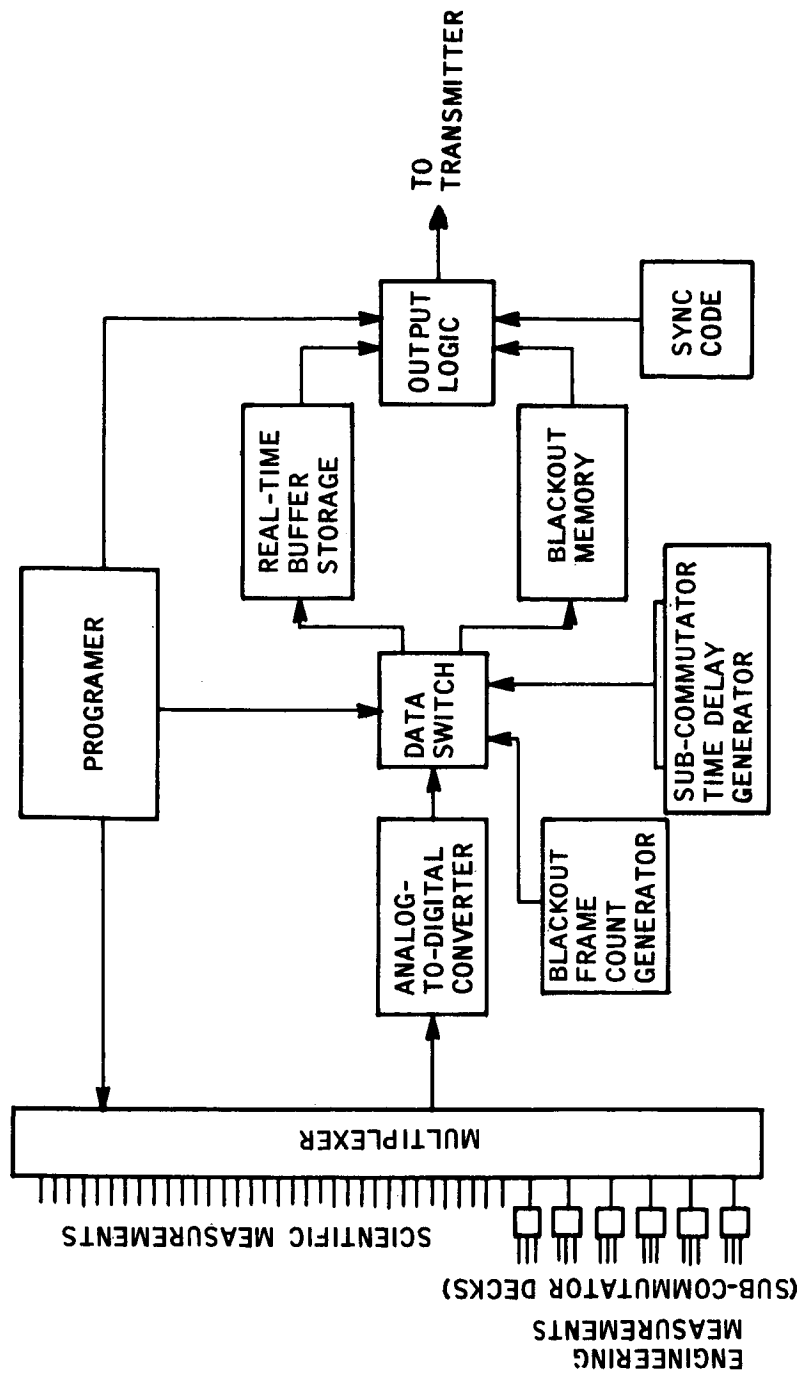


Figure 7 PROBE DATA HANDLING BLOCK DIAGRAM

86-8655

but are read out in cycles of increasing size. Since the time in blackout is unknown because of the uncertainty of the atmospheric density, it is desirable to have a nonadaptive playout scheme to guarantee a recovery of all the blackout data. Although there are methods to determine the end of radio communications blackout, the complexity and added instrumentation associated with these schemes negates their advantage.

The frame playout sequence proposed here is designed to allow playout of all data acquired during blackout during the time between the end of blackout and impact, independently of the duration of blackout or playout. This scheme works because the shortest possible playout period occurs for the same trajectory and model atmosphere as the shortest blackout time, and as the blackout duration increases for different trajectories and atmospheres the time available for playout generally increases more rapidly.

The format is therefore based upon playing out the blackout data once during the available playout time for the case of the VM-8 atmosphere (shortest playout time). This requires the first eight frames of blackout data to be played out between the 8th and 16th second of the mission. To allow for a slightly denser atmosphere which would result in a slight increase in blackout time but an increasingly longer playout time, the 9th and 10th second of blackout data are played out during the 17th and 18th second of the mission. The memory then cycles back to the beginning, and the first 20 frames of blackout data are played out, followed by the first 30 frames. The playout and the sampling formats are shown graphically in Figure 8.

The played-out blackout data is interleaved frame-by-frame with the data taken and played out in real-time as shown in Figure 8. The resulting frame, consisting of the blackout data, the real-time data and frame sync and identification codes, is shown in Figure 9. By comparing the times in and out of blackout with the playout format, it can be shown that all of the blackout data is played out at least once before impact. In addition, there will be some redundant data in each case. The playout format for the stored data in the first eight seconds of the mission (when the probe is almost certainly blacked out) is chosen arbitrarily. Small modifications to the format (changing cycle size or increment) will allow this scheme to accommodate any reasonable set of entry conditions or even a range of entry conditions if required.

CODE: SF- Sampled Frame  
 PF- Playout Frame  
 RT - Real-Time Data  
 D - Delayed (Blackout) Data  
 MT- Mission Time After Entry

SF	RT 1	D 1	RT 2	D 2	RT 3	D 3	RT 4	D 4	RT 5	D 5	RT 6	D 6	RT 7	D 7	RT 8	D 8
PF																
MT	1		2		3		4		5		6		7		8	

SF	RT 9	D 9	RT 10	D 10	RT 11	D 11	RT 12	D 12	RT 15	D 15	RT 16	D 16	RT 17	D 17	RT 18	D 18
PF																
MT	9		10		11		12		15		16		17		18	

SF	RT 19	D 19	RT 20	D 20	RT 21	D 21	RT 22	D 22	RT 35	D 35	RT 36	D 36	RT 37	D 37	RT 38	D 38
PF																
MT	19		20		21		22		35		36		37		38	

SF	RT 39	D 39	RT 40	D 40	RT 41	D 41	RT 42	D 42	RT 65	D 65	RT 66	D 66	RT 67	D 67	RT 68	D 68
PF																
MT	39		40		41		42		65		66		67		68	

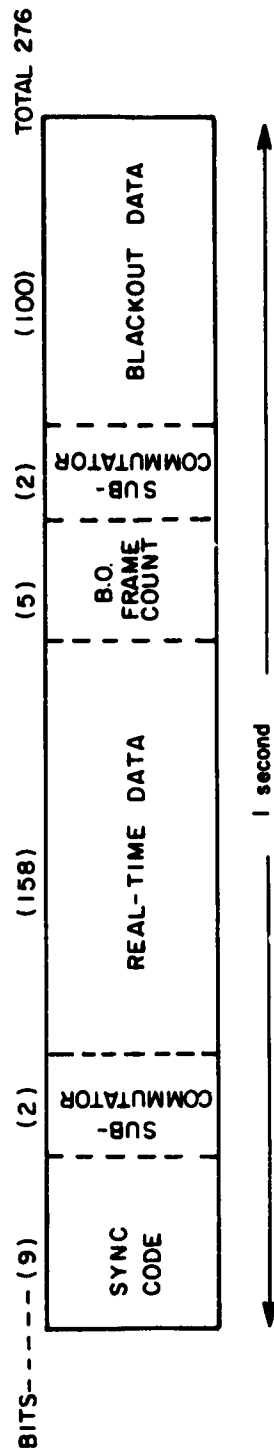
  

SF	RT 69	D 69	RT 70	D 70	RT 71	D 71	RT 72	D 72	RT 95	D 95	RT 96	D 96	RT 97	D 97	RT 98	D 98
PF																
MT	69		70		71		72		95		96		97		98	

\*All subscripts refer to time after entry in seconds.

86-8656

Figure 8 DATA PLAYOUT AND SAMPLING FORMAT



86-8657

Figure 9 DATA FRAME SEQUENCE

4.2.4.4 Power Subsystem (Battery) -- The power subsystem for the total Probe System consists of two nickel-cadmium batteries, a charge regulator and power switches. The charge regulator is located on the flight spacecraft and is disconnected from the Probe at separation. The power switches are controlled by the safing, sequencing and initiation (SS&I) system.

Power is supplied to all users directly without voltage regulation and where necessary, individual users will provide their own regulator. In the case of the transmitter it is necessary to up-convert the 10 volts minimum provided to 25 volts and a converter is supplied. For all other users the 10 to 12 volts provided is the preferred level and no conversion is necessary.

Table VIII shows salient characteristics of the power subsystem. It should be noted that one of the batteries is located on the outside of the Probe and attached to the propulsion cone. This battery provides the power for the timer which initiates the rocket and also ignites the rocket itself. Power for pyrotechnics initiated prior to this is provided by a capacitor or non-heat sterilizable battery located in the spacer.

The batteries consist of hermetically sealed nickel-cadmium cells connected in series to produce the desired voltage levels. For the battery inside the Probe which provides power until impact, twelve cells are used. Battery No. 2 on the propulsion cone consists of six cells. The cells used are the same rating and size for both batteries in order to cut down development time and costs. For the sake of convenience in mounting, both groups of cells are fastened inside rectangular shaped containers which are not, however, hermetically sealed. Provision is made for shorting out each cell individually through the connector (for heat sterilization purposes) and monitoring of current, voltage and temperature.

Both batteries have to be kept warm (above 40° F) in order to operate efficiently. Heat for this will be provided by the flight spacecraft prior to separation. Afterwards, the batteries are kept warm by insulation and thermal control design. Charging is by trickle at the C/100 (100 hour) rate or at the full-charge rate of C/10 as required by the mode of operation.

Nickel cadmium batteries have been extensively tested at Avco under the sterilization environment and have been found to operate satisfactorily after sterilization and long storage life.

4.2.4.5 Spacecraft Receiving Antenna -- The function of the spacecraft antenna system is to provide an efficient RF transition between the Probe and the flight spacecraft. It must be designed to receive a predominantly circularly polarized wave of a single sense with minimum polarization loss. Its requirements are summarized in Table IX.

TABLE VIII

## PROBE POWER SUBSYSTEM CHARACTERISTICS

Item	Location	Weight	Description
Battery No. 1	Inside Probe	5.1	Output Volts: 10.5 to 16 vdc 17.0 volts-open circuit Capacity: 42 watt-hrs 3 amp-hrs Type: Sealed Ni-Cad
Battery No. 2	Attached to propulsion cone	3.0	Output Volts: 7.2 to 8.2 vdc 8.5 volts open circuit Capacity: 21 watt-hrs 3 amp-hrs Type: Sealed Ni-Cad
Charge regulator (2 Required)	Flight Spacecraft	2	Charge rates 1 to 3 amps Trickle charge 20 to 400 ma Voltage ref. by zener Coulometer high rate control
Power switching	Inside probe part of CC&S		Transistor switches, SCR Blocking diodes and fuses

TABLE IX

SPACECRAFT RECEIVING ANTENNA DESIGN REQUIREMENTS

Gain	12 db above an isotropic radiator
Beamwidth	50 degrees at the one-half power points
Efficiency	$\geq 62$ percent
Input VSWR	$\leq 1.25:1.00$
Center operating frequency	272 MHz
Polarization	Circular
Axial ratio	$\leq 6.0$ db $\pm 45$ degrees from antenna boresight
Weight	5.0 pounds
Temperature	-250° F to +250° F

A helix configuration is recommended which will radiate in the end-fire or axial mode. It is a fundamental form of antenna of which loops and straight wires are limiting cases. When the helix is small compared to the wavelength, radiation is maximum normal to the helix axis. Depending on the helix geometry, the radiation, in theory, may be elliptically, linearly or circularly polarized. When the helix circumference is about a wavelength, radiation may be maximum in the direction of the helix axis and circularly polarized or nearly so. This mode of radiation, called the axial mode, is generated in practice with great ease and may be dominant over a wide frequency range with desirable pattern, impedance and polarization characteristics. The radiation pattern is maintained in the axial mode over wide frequency ranges because of a natural adjustment of the phase velocity of wave propagation in the helix. The terminal impedance is relatively constant over the same frequency range because of the large initial attenuation of wave on the helix.<sup>8</sup>

Its outstanding characteristics are the relative ease with which it may be fabricated and tested and the ease with which a near-circularly polarized wave may be generated. The helix will be nearly circularly polarized out to  $\pm 50$  degrees from antenna boresight (axial ratio less than 6.0 decibels) and will provide an inherently broadband radiating antenna, eliminating the possibility of its becoming desensitized when exposed to the environments of outer space.

Some difficulty may arise in packaging this antenna on the spacecraft since it is in excess of four-feet long. One possibility which suggests itself is to compress the helix into a spring which will be unloaded prior to use. An advantage for the helix is that a second helix, oppositely wound, may be incorporated within the volume occupied by the first helix if polarization diversity is desired.

4.2.4.6 Spacecraft Receiving Subsystem -- The functional requirements of the flight spacecraft receiving subsystem will be to receive the transmitted signals appearing at the output of the receiving antenna and to provide suitable amplification, detection and signal conditioning such that the receiver output signal is in a form suitable for direct insertion into the Flight Spacecraft Data Handling Subsystem.

As explained earlier, the use of the wideband PCM/FSK system requires that pre-detection bandwidth be considerably in excess of the information bandwidth, due to several frequency uncertainties such as transmitter instability, local oscillator instabilities and Doppler shift. To achieve optimum detection efficiency, post detection filtering will be employed in the form of a linear periodically-dumped integrator following the envelope detectors. This method results in a requirement for very accurate bit timing which will be satisfied by the use of a bit synchronizer located on-board the spacecraft. Due to the interrelationship between the receiver and the bit synchronizer, the following discussion will consider these two units as part of the receiver subsystem. A summary of the receiver subsystem characteristics is shown in Table X.

A block diagram of the flight spacecraft receiver is shown in Figure 10. The input RF section contains a circulator followed by a limiter and a low-noise preamplifier. The limiter is required to protect the receiving subsystem, and in particular, the sensitive RF preamplifier, from excessive power levels. The limiter will utilize silicon diodes in a simple shunt configuration. Typically, they will limit at approximately + 10 to + 15 dbm and will provide no more than 0.3 decibels small signal insertion loss.

The diode limiter will not interfere with reception when the received signal level is below the limiting level. When the input signal level is above the limiting level, the excess power is reflected back to the input. These reflections will generally result in extreme variations in the flight spacecraft antenna characteristics unless the antenna output can be adequately isolated from the limiter input. This can be accomplished with the addition of a loaded circulator as shown in Figure 10. The circulator will provide an isolation of 20 decibels minimum and will present an insertion loss of 0.5 decibels maximum.

The limiter is followed by an RF preamplifier which is required to present a low input noise figure and provide adequate RF gain to sufficiently isolate the noise figure of the succeeding mixer-IF combination.

TABLE X

SPACECRAFT RECEIVER CHARACTERISTICS

Frequency	272 MHz
Type	Double Conversion Superheterodyne
Noise figure	< 4 decibels
Image rejection	60-decibels minimum
IF rejection	80-decibels minimum
Threshold signal level at antenna terminal	-130 dbm
Receiver limiting level	+10 dbm
Operating range	140 decibel
Local oscillator stability	±0.0001 percent
<u>1<sup>st</sup> IF</u>	
Center frequency	30 MHz
Bandwidth	1 MHz
<u>2<sup>nd</sup> IF</u>	
Center frequency	10 MHz
Bandwidth	50 kHz
Mark/space	
Frequency separation	20 kHz
Mark/space	
Filter bandwidths	8 kHz
Detector type	Square law envelope detector
AGC response	Adjustable
AGC output	Linear with respect to input signal level in dbm
Weight	3.5 pounds
Power	4 watts

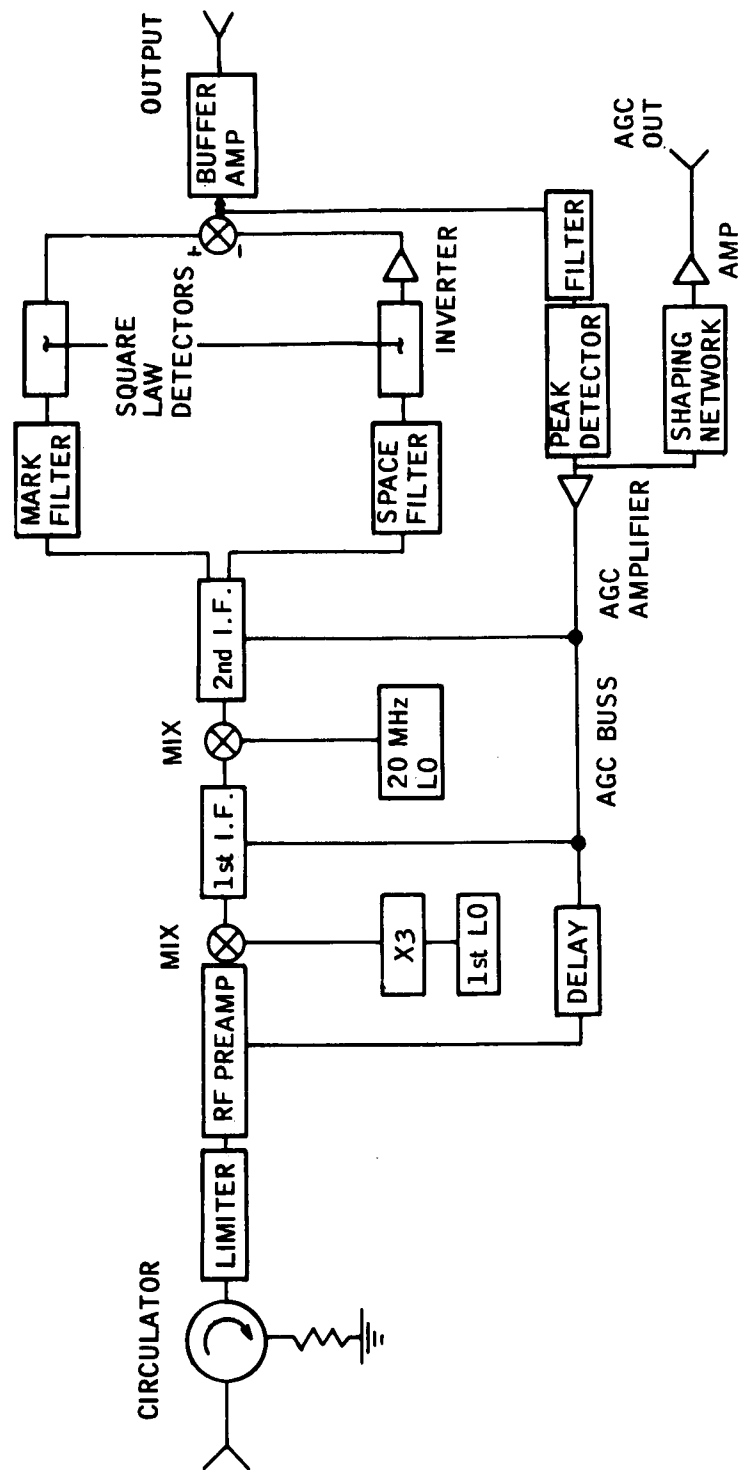


Figure 10 SPACECRAFT RECEIVING BLOCK DIAGRAM

86-8658

The limiter preceding the RF preamplifier helps to limit the maximum applied RF power, however, there is a practical limit to the lowest limiting level that can be obtained with state-of-the-art devices. The RF preamplifier will provide an operating range corresponding to the range from receiver threshold to the lowest limiting level obtainable with the limiter. Receiver threshold will be defined as the input signal level which causes the resultant bit-error rate to exceed  $1 \times 10^{-3}$ .

The block diagram of the proposed flight spacecraft receiver indicates a double conversion receiver. This choice was arrived at on the basis of gain distribution, image rejection and filter fabrication considerations. The mark/space filters are required to pass the modulated signal without distortion in the presence of relatively large uncertainties due to Doppler and equipment drift. The 3 decibel bandwidth  $b_o$  of the mark/space filters are determined from the expression

$$b_o = 3 \dot{B} + f_T + f_R + f_d$$

where:

$\dot{B}$  = bit rate (300 bit/sec)

$f_T$  = Transmitter frequency instability ( $\pm 0.001$  percent)

$f_R$  = Receiver instability ( $\pm 0.0001$  percent)

$f_d$  = Doppler shift

The example below has been constructed to illustrate the determination of the required bandwidths for an assumed carrier frequency of 272 MHz

$$3 \dot{B} = 900 \text{ Hz,}$$

$$f_T (\pm 0.001 \text{ percent}) = 5400 \text{ Hz,}$$

$$f_R (\pm 0.0001 \text{ percent}) = 544 \text{ Hz,}$$

$$\underline{f_d (v = 10,000 \text{ ft/sec}) = 2760 \text{ Hz,}}$$

$$b_o = 8204 \text{ Hz}$$

This indicates that for a bit rate of 300 bit/sec the required mark/space filter bandwidths will be approximately 8 kHz. A second IF frequency of 10 MHz allows convenient use of crystal filters for the mark/space channel filters. A conservative choice of 4:1 shape factor simplifies the temperature compensation problem and avoids violent phase characteristics near band edge. The minimum required 10 MHz IF bandwidth is then found from the mark/space filter separation.

If we require that the 60 decibel point of the mark filter fall at the 4 decibel point of the space filter and vice versa, the mark/space filter separation will be found to be approximately 20 kHz. The required 2<sup>nd</sup> IF bandwidth will be approximately 50 kHz. This is a typical telemetry receiver bandwidth at 10 MHz. The first IF will be located at 30 MHz and provide approximately 100 kHz bandwidth. A choice of 30 MHz 1<sup>st</sup> IF eases the RF preamplifier image rejection problem somewhat. The first LO injection will be derived from the X3 multiplier output of a fifth-overtone crystal oscillator operating in the 80 to 90 MHz range. This approach offers a compromise between stability and system complexity. The second LO will be a 20 MHz fundamental mode crystal oscillator.

The outputs of the mark/space channel filters are square-law envelope detected and subtracted. This difference signal is filtered and peak detected to provide the agc signal. The peak detector output is heavily filtered in accord with the required AGE time constant, and then amplified to provide the agc control.

The agc signal is made accessible through a buffer at the receiver output. This output will be shaped to provide an agc output which is linear with respect to the input signal level in decibels minimum. This output will provide useful engineering and diagnostic data on the performance of the spacecraft telecommunications system. Suitable delay in the agc to the front end is also provided. The agc bandwidth will be adjusted to respond to the slow signal fades typical of vehicle dynamics effects when these fades occur at rates considerably below the data rate. The suitably buffered square-law envelope detected and differenced outputs of the mark and space channels are provided at the receiver output terminals.

All bit decisions will be made in the bit detector, consisting of a periodically dumped integrator and suitable decision and signal conditioning circuitry. The bit timing is provided by the bit synchronizer which accepts the noisy NRZ output from the receiver and provides appropriate synchronization signals to the integrate-and-dump bit detector. The output of the bit detector will then be a clean binary sequence representing the data transmitted from the entry Probe. This output is fed directly into the buffer storage in the spacecraft data handling subsystem. The stored data is then retimed and the output of the data handling subsystem applied to the spacecraft transmitter for transmission to the earth receiving site.

4.2.4.7 Spacecraft Data Handling Subsystem -- The spacecraft data handling subsystem will consist of the equipment to collect and store the received data from the Probe. The data received by the spacecraft will consist of the real time and blackout data transmitted from the Probe data handling subsystem.

Two methods are proposed for processing the data on-board the spacecraft. One method would demodulate and detect the received data on the spacecraft and store the data for retransmission to earth; the alternate method would simply sample and encode the output from the envelope detector and store the digitized data for transmission to earth. The sampling and encoding technique has the advantage of not requiring a bit synchronizer since data detection is not performed by the spacecraft. However, this scheme leads to increased data storage requirements since each relay-link bit must be represented by at least 15 spacecraft-earth link bits. Both data processing methods are discussed below.

a. Sample and Encode Technique -- The spacecraft Data Handling Subsystem will sample and quantitize the low-pass filtered, envelope detected, signal from the spacecraft receiver. The sampling rate required to reconstruct the output waveform is at least three times the relay-link-data rate. This sampling rate is the Nyquist rate for the third harmonic of the highest square wave frequency present in the data. Each sample will be quantitized into 32 levels (5-bit word) and will be stored in a tape recorder for subsequent play-out. The storage capacity of the tape recorder, to be consistent with storing all the Probe data from entry to impact would have to be about  $5 \times 10^5$  bits or the equivalent of one TV picture. A summary of the design characteristics is described in Table XI.

TABLE XI  
SPACECRAFT DATA HANDLING CHARACTERISTICS  
(Sample and Encode Technique)

Received Probe data rate	300 bit/sec
Spacecraft sampling rate	300 x 3 sps (minimum)
Quantization levels	32
Total spacecraft bps	4500 bit/sec
Operational time (entry to impact)	100 seconds (Mod 3 atmosphere)
Data storage Type	Tape recorder
Storage capacity	$5 \times 10^5$ bits

b. Synchronous Detection Technique -- The synchronous detection technique of processing the data received by the Probe provides for detection of the data on-board the spacecraft.

The major elements in this data processor include a video-matched filter, bit synchronizer, detector, and storage memory. The video-matched filter is an integrate and dump circuit which is synchronized to the incoming data by the bit synchronizer.

The bit synchronizer uses transitions in the data itself (changes from a one to a zero or vice versa) to determine and synchronize to the beginning and end of each bit. The input to the synchronizer is a filtered version of the envelope detected video data waveform. Because the data format is NRZ, the rate of transitions is a random process and (particularly when the noise level is significant) the synchronizer could take appreciable time to lock up (one or more frame lengths).

Several techniques are available to avoid the loss of these data. One is to use the sample and encode technique to acquire data before the synchronizer has locked. With some synchronizer designs a signal could be made available which would be proportional to the probability that correct synchronization is achieved at the moment. This could be used to key in and out the sample encode system. The result would be the availability of the sample encode back-up technique without the penalty of having to store the data from the total mission. Another possibility is the use of coding to enhance system performance and also to guarantee a regular transition rate.

The data storage required will be consistent with storing all the received digitized data from Probe entry to Probe impact which corresponds to a time of 300 seconds (maximum) for 25 millibar atmosphere. The memory read-out will be nondestructive. A summary of the design characteristics for the synchronous detection technique is described in Table XII.

TABLE XII

SPACECRAFT DATA HANDLING DESIGN CHARACTERISTICS

(Synchronous Detection Technique)

Input data rates	300 bit/sec
Sync acquisition time	5-10 bit periods
Operational time (entry to impact)	100 seconds (max)
Data storage	
Type	Ferrite core
Storage capacity	30,000 bits (minimum)

The block diagram of the spacecraft data handling subsystem is shown in Figure 11 for both alternatives.

Both data handling schemes, the sample and encode and the synchronous detection technique, will be incorporated into the nominal design for the spacecraft receiver to serve as redundant back-ups to each other. If the spacecraft data storage capability is limited, then the sample and encode technique could be used only during bit synchronizer "out of lock" conditions, otherwise the two schemes could operate continuously for the duration of the mission.

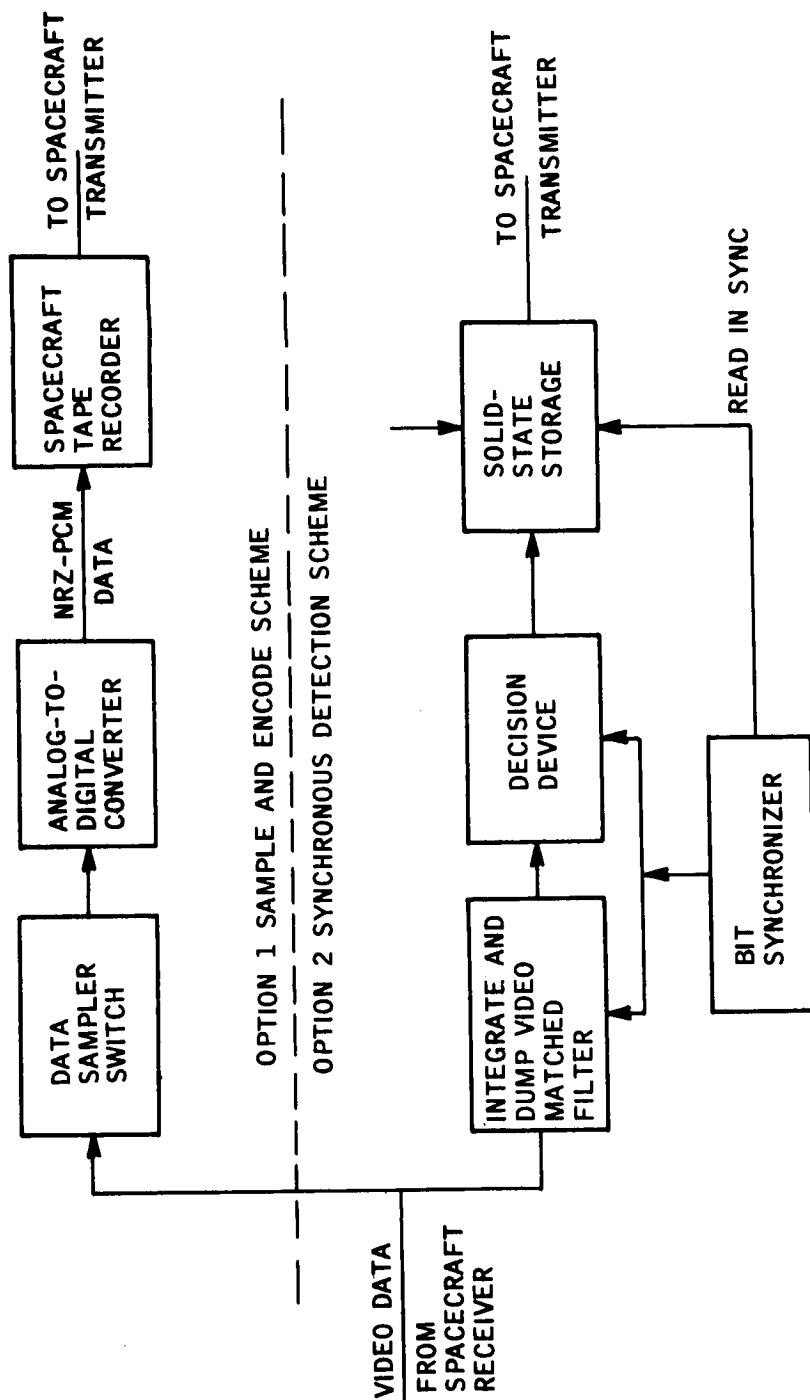
4.2.4.9 Cruise and Entry Sequencer -- The Probe cruise and entry sequencer is a single unit containing all of the devices required to operate the Probe Subsystems from separation from the flight spacecraft through planetary entry and impact. It will also incorporate the means of controlling the internal subsystems at all other times after the Probe is completely assembled. This will be accomplished by a power control switch which will allow turn-on of Probe Subsystems using either internal or external power, and according to a programmed sequence or utilizing external control.

The functions which must be performed by the sequencer during the mission are described as follows:

a. Long Duration Timer -- This timer is required to initiate all probe functions from separation up to planetary atmospheric entry. The events which must be initiated are:

- 1) Turn on and turn off all avionics for 30 second checkouts at 4 fixed times during the flight.
- 2) Separation of propulsion cone assembly.
- 3) Turn on accelerometers and transmitter (at reduced power) for warmup.

The time from separation to entry may not be fixed before the approach trajectory of the spacecraft is known. In fact, the presently favored separation procedure is to vary this time to keep the entry angle fixed and to compensate for varying actual spacecraft periapsis altitude. Since the timer must provide a signal to initiate warmup just prior to entry, the running time of the timer must be adjustable, by command from earth, prior to probe/spacecraft separation. For the mission parameters selected as nominal, the timer would have a nominal running time of 3.5 days and would be adjustable by  $\pm 20$  hours. All functions except the initiation of warmup will occur at fixed times after separation and therefore will require no adjustment capability.



96-8659

Figure 11 SPACECRAFT DATA HANDLING BLOCK DIAGRAM

b. Temperature Probe Deployment Initiator -- The two temperature probes must be deployed when the Probe velocity is about Mach 2. It has been found that for the given  $M/C_D A$ , Mach 2 is always attained at very nearly the same time as 6.0 g, independent of the atmosphere and entry conditions. Thus by sensing 6.0 g descending, a signal suitable for initiating the temperature probe deployment can be obtained from the accelerometers. The Probe is deployed by explosively cutting a tiedown cable or wire. Since pyrotechnics are involved, a safing device must be employed to prevent premature ignition. This could take the form of a set of contacts on the separation sensing switch. The firing current itself will be armed by a high g level (100 g) which will occur after entry. The circuit will fire when the deceleration decreases to about 6 g. The circuits will operate from the output signals of one of the two axial accelerometers which are part of the science payload.

c. Power Distribution -- The sequencer will include the necessary circuitry to control the distribution of battery power to each user. The total power to be handled will be less than 125 watts, up to 85 watts of which are required by the transmitter. The design will be based on the use of solid-state switches to actually handle the power.

As is the case for all subsystems located on the Probe, the sequencer must be designed to minimize total system weight. In this regard, it is found that the weight of the sequencer itself is not so important as the power consumption of the long duration timer. Because this timer will be on for over three days in the nominal case (separation to entry times of up to 20 days have received consideration) the total electrical energy consumed by the timer can be a substantial portion of the total energy required for the mission. In fact, the weight of the battery required to operate the timer could be several times the weight of the timer itself. Thus, in addition to requiring the usual lightweight, rugged, sterilizable design, the power consumption must be kept to an absolute minimum.

After a thorough investigation of the various types of electronic, electromagnetic and electromechanical timers which have been used in aerospace applications and which might satisfy the Probe System functional requirements, it was found that one type had clearly outstanding advantages for this application. This type utilizes incrementally saturable magnetic cores to perform counting and frequency division functions. The oscillator to drive the counting circuits will be an all solid-state transistor oscillator. The principle advantages of this type of timer are:

a. Very Low Power Consumption -- The magnetic core counting circuits consume power only when the count is being changed. Thus only a few cores at most consume power at any instant of time and the power consumption is a linear function of the driving frequency. In any case, it is much lower than, for example, a transistorized counting chain where each stage continuously requires bias power. The transistor oscillator is selected because

it not only can be designed to consume less power than a crystal or tuning fork oscillator, but it also can be designed to provide much lower frequencies without countdown stages. The accuracy of a transistor oscillator is poorer than for any of the alternatives. However, under the conditions of the mission an accuracy of better than  $\pm 1 \times 10^{-3}$  can be achieved. For a four-day separation-to-entry time this instability will result in an uncertainty of about  $\pm 5$  minutes which is acceptable. Studies by several prospective vendors of this equipment have shown that the total average power consumption of the long duration time will be between 10 and 20 milliwatts.

b. No Standby Power Requirements -- The final timing duration is set into this type of timer by reading in a number corresponding to that portion of the maximum time which will not be used. Thus, in effect, the timer starts counting from a time other than time zero. Reading in the number changes the magnetic state of some of the cores by a specific amount. The cores will retain the new state until properly sized pulses cause them to change state in the counting process. Once the number has been set in, no power is required to keep the cores in the desired state.

c. Low Number of Parts Required -- Each incrementally saturable magnetic core stage will have the capability of counting up to at least eight. (Higher counts are possible but require more stringent regulation and control conditions.) The total number of stages required in the timer will thus be a factor of three less than the number required by an equivalent all electric timer.

#### 4.3 THE PROBE SEPARATION, STABILIZATION, AND PROPULSION SUB-SYSTEM

This subsystem consists of the Probe separation and stabilization equipment, the Probe propulsion components and the safing, sequencing and initiation equipment required to accomplish the total separation and propulsion sequence.

##### 4.3.1 Probe Separation and Stabilization

The Probe separation and stabilization system must meet two major requirements, namely:

a. Stabilize the Probe very well so that the velocity increment can be imparted to the Probe in a well known and controlled direction (the errors in thrust application angle should not exceed a three sigma value of three degrees).

b. The entire separation and stabilization process must be performed with minimum perturbation to the spacecraft. In particular, all forces and torques acting on the spacecraft should be minimized and impingement of

any exhaust gases on the spacecraft should be minimized (or eliminated altogether).

High reliability of the system is also an important requirement since failure of the separation and stabilization system leads to total Probe Mission failure.

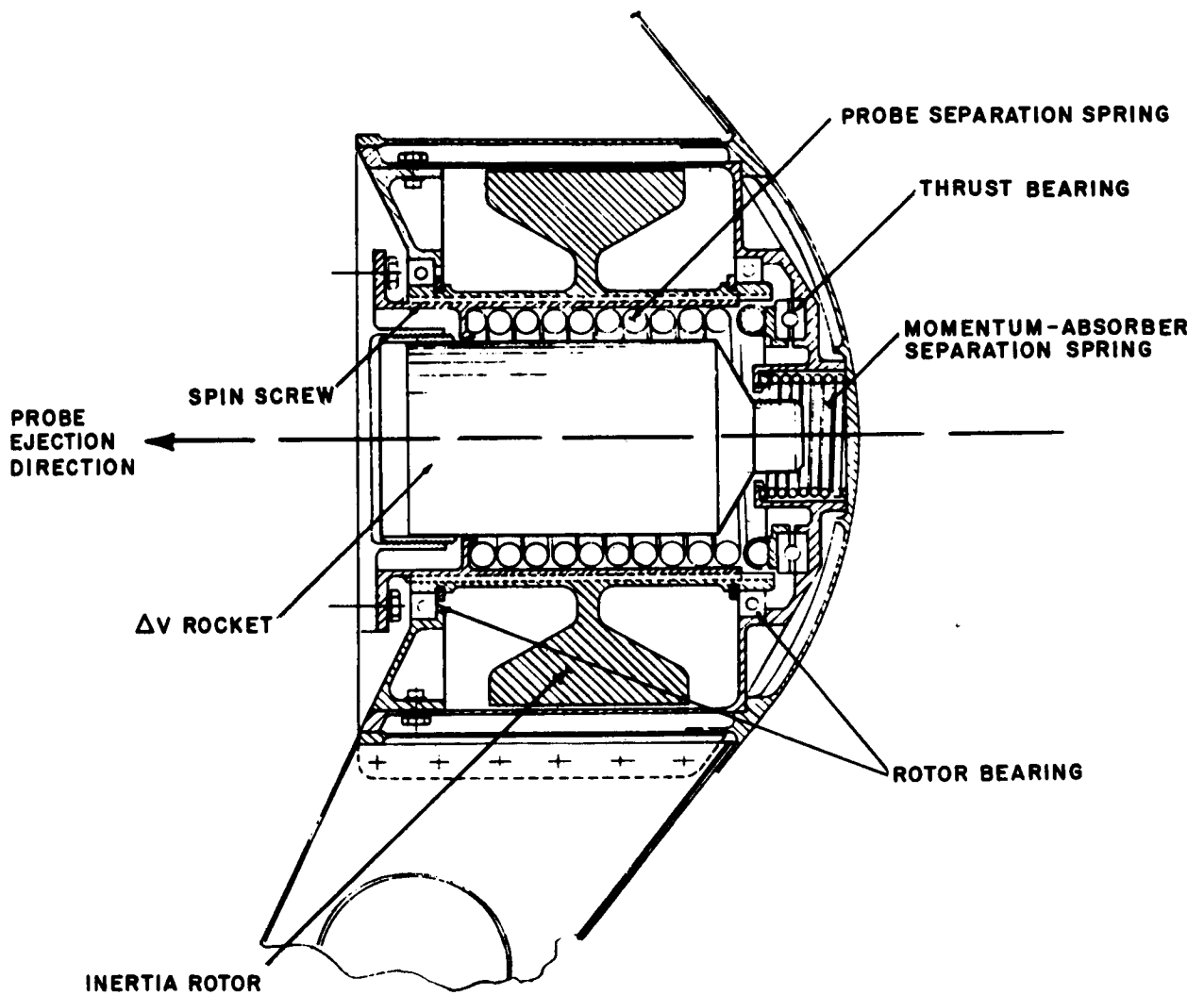
In view of the above factors, it was decided to select a type of system which accomplishes separation and stabilization concurrently so that successful separation guarantees accurate stabilization.

Probe separation and stabilization are achieved concurrently by spring ejecting the Probe through a rifled tube so as to provide both linear and angular acceleration to the Probe. The linear separation velocity is about 3 ft/sec and the imparted spin rate is about 30 rpm. As mentioned previously, the spacecraft is oriented prior to separation so as to properly position the Probe for ejection, stabilization and propulsion. Such a spacecraft maneuver eases the mechanical integration of the Probe on the spacecraft since no specific clock and cone mounting angles are required. For a large spacecraft such as Voyager, however, there may be sufficient latitude in mounting a small Probe so that by selecting the proper cone and clock angles the necessity for a spacecraft maneuver could be avoided.

A schematic of the Probe separation and stabilization assembly is shown in Figure 12. Probe separation is initiated by the activation of three inflight separation bolts (not shown in Figure 12). These are double-squib, double-bridge wire, hi-shear bolts equipped with bolt catchers. Bolt retraction allows the Probe separation spring to accelerate the Probe. As the Probe accelerates forward, it is also spun to 30 rpm due to the axially spiraled gear torque thruster. The torque thruster reacts against the mating teeth of the inertia rotor shown in Figure 12 which counter rotates, absorbing the angular momentum required for probe spinup. The rotor weight is about 10 pounds.

This is a passive system in which the momentum absorber rotor assumes whatever rotational speed is required to match the rotational inertia of the Probe. For a 30 rpm Probe-spin rate the rotor achieves a spin rate of about 1100 rpm. The final rotational speed of both masses is a function of the stored energy in the Probe-separation spring and the final axial velocity of the Probe is a function of the thread pitch of the spiral gear. The only torque transmitted to the spacecraft is due to bearing friction. As the Probe separates, the axial reaction transmitted to the momentum absorber housing falls to zero, the stored energy in the momentum absorber separation spring is released, and the momentum absorber is ejected with a forward velocity which is small (1 ft/sec) as compared to the velocity of the separated Probe (3 ft/sec). This design possesses the following advantages:

- a. Immediate Probe spinup minimizes separation tipoff errors.



86-8660

Figure 12 PROBE SEPARATION ASSEMBLY

- b. No torque reaction is transmitted to the spacecraft since the reactive torsional momentum is absorbed by the momentum absorber which is then ejected from the spacecraft.
- c. After initiation of the separation bolt squibs, all other Probe separation events are passive in order to upgrade reliability.
- d. No hot or cold gas jets are fired near the spacecraft, minimizing possible interference with the spacecraft operation, as well as removing the possibility that the jet exhaust gases could dislodge microorganisms from the spacecraft some of which could settle on the Probe.

During the course of the study a number of different systems were considered which utilized spin rockets (or cold gas jets) to spin stabilize the Probe after separation. Thus the Probe separation system was required to provide only a linear separation velocity. Such systems, however, possess two disadvantages. First, since very low Probe misalignments (relative to the separation velocity vector) are required, it is necessary to achieve very low tipoff rates and spinup has to be achieved very soon (within at most a very few seconds) after separation so as to prevent Probe misalignment due to integration of the tipoff rates. Second, to achieve a rapid stabilization, the spin rockets (or cold gas jets) must be fired very near the spacecraft (within a few feet) thus potentially interfering with the spacecraft operation.

#### 4.3.2 Probe Propulsion

After the separation and stabilization process, the Probe is allowed to coast away from the spacecraft until the separation distance is large enough (of the order of 3000 feet) so that the Probe  $\Delta V$  rocket can be safely fired without interfering with the spacecraft. The purpose of this rocket is to impart to the Probe a well defined velocity increment which puts the Probe on the desired planet impact trajectory. To minimize entry angle dispersion, it is necessary to control both the direction and the magnitude of the applied velocity increment.

The magnitude of the velocity increment is controlled by requiring that the total impulse of the rocket be accurate to within a 3-sigma value of 3 percent. The direction of the velocity increment (the thrust application angle) is controlled by the spin stabilized attitude of the Probe. However, there will always be some misalignment (due to manufacturing tolerances, etc.) between the rocket thrust vector and the direction along which the Probe is stabilized. To minimize the effects of such misalignments, it is desirable to operate with long motor burning times (as well as high Probe-spin rates). With long motor burning times the error due to the thrust vector misalignment tends to be averaged and so reduced. As discussed later, burning times of about 15 seconds are desirable. The total  $\Delta V$  requirements depend upon the desired Probe-spacecraft lead time and the selected approach trajectories. For the 1969 Type I trajectories a  $\Delta V$

of about 75 ft/sec is typical, while for the 1969 Type II and the 1971 Type I trajectories  $\Delta V$ 's of 190 and 150 ft/sec are required, respectively.

An Atlantic Research Corp. end burner, solid propellant rocket motor was selected. The advantages of a solid propellant motor are the expected high reliability and minimum interface problems. The use of an end-burning configuration is necessary to achieve the desired long burning times. The characteristics and performance of this motor are shown in Table XIII.

#### 4.3.3 Probe Safing, Sequencing, and Initiation

The SS&I subsystem safes and sequences the probe and sterilization canister pyrotechnics and thus controls the separation sequence events. The sequence of primary events is shown in Table XIV and the block diagram of the SS&I subsystem is shown in Figure 13. There are six primary initiation signals which originate from the flight spacecraft, namely:

- Vent Sterilization Canister
- Deploy Sterilization Canister Cover
- Initiate Separation (start timers)
- Separate Entry Probe-Spacecraft Umbilical
- Separate Propulsion Module Umbilical
- Separate Probe from Spacecraft Mechanically.

These signals are numbered and shown in Figure 13 to identify the initiation circuits. The major components of the SS&I subsystem are listed below together with their functions.

- a. Timer -- To sequence the impulse rocket firing at the proper time after Probe separation from the canister.
- b. Separation Connectors -- To electrically connect the Probe propulsion cone assembly with the canister, and to disconnect when mechanical separation occurs.
- c. Barometric Lockout Switches -- To open electrical circuits to pyrotechnic devices before the space vehicle is launched from earth.
- d. Probe Pressure Switch -- To safe impulse rocket prior to and during launch.

TABLE XIII

## PROBE ROCKET MOTOR CHARACTERISTICS

I. GRAIN	
Propellant	Arcite 377A
Grain type	End-burner
Grain length	4.00 inches
Grain diameter	2.542 inches
Grain weight	1.235 pounds
Propellant density	0.059 lb/in. <sup>3</sup>
Burning surface	5.06 in. <sup>2</sup>
Ratio of specific heats	1.237
Flame temperature	2316° K
Delivered specific impulse (vac., $\epsilon = 8.5$ )	226 lb-sec/lb
Discharge coefficient	0.0072 sec <sup>-1</sup>
II. NOZZLE	
Type	Conical
Half angle	15 degrees
Throat area	0.019 in. <sup>2</sup>
Throat diameter	0.149 inch
Exit area	0.436 in. <sup>2</sup>
Expansion ratio	8.5

TABLE XIII (Cont'd)

III. IGNITER		
Type		Film
Bridgewires		Pyrofuze
Conductor		Laminated Copper
Ignition material		B-KCL0 <sub>4</sub>
Film Support material		Polycarbonate
IV. MOTOR DESIGN		
Length		6.500 inches
Diameter		3.000 inches
Weight		
Loaded		2.67 pounds
Fired		1.23 pounds
Mass fraction		0.54 pounds
Temperature limits		
Operational & storage		-65° to 165° F
Sterilization limit		100hours at 300° F
Operating altitude		Vacuum
Exterior finish		Cadmium plate

TABLE XIII (Concl'd)

V. PERFORMANCE	
Burn time	15.0 seconds
Average thrust	18.7 pounds
Average pressure	600 lb/in. <sup>2</sup>
Total impulse	281 lb-sec
Specific impulse	226 seconds
Burn rate	0.267 in/sec
Total impulse accuracy	3 percent (3 $\sigma$ )

TABLE XIV

SEQUENCE OF PRIMARY EVENTS DURING PROBE SEPARATION AND PROPULSION

Event	Time	Source of Initiating Signal
1. Vent sterilization canister	in parking orbit (or later, if so desired)	Spacecraft CC&S
2. Initiate cruise mode configuration		Spacecraft CC&S
3. Initiate 30-sec Probe checkout		Spacecraft CC&S
4. Initiate final warmup (canister battery)	$T_o - 10$ minutes	Spacecraft CC&S
5. Deploy canister cover	$T_o - 5$ minutes	Spacecraft CC&S
6. Initiate separation (start timers)	$T_o$	Spacecraft CC&S
7. Separate entry probe umbilical	$T_o + 1$ second	Pyrotechnic delay
8. Separate propulsion module umbilical	$T_o + 2$ seconds	Pyrotechnic delay
9. Separate probe mechanically	$T_o + 3$ and $T_o + 4$ seconds	Pyrotechnic delay
10. Start 30-sec checkout	$T_o + 999$ seconds	Long-duration timer
11. Ignite rocket	$T_o + 1000$ seconds	SS&I sequencer timer
12. Jettison propulsion cone	$T_o + 1025$ seconds	Long-duration timer

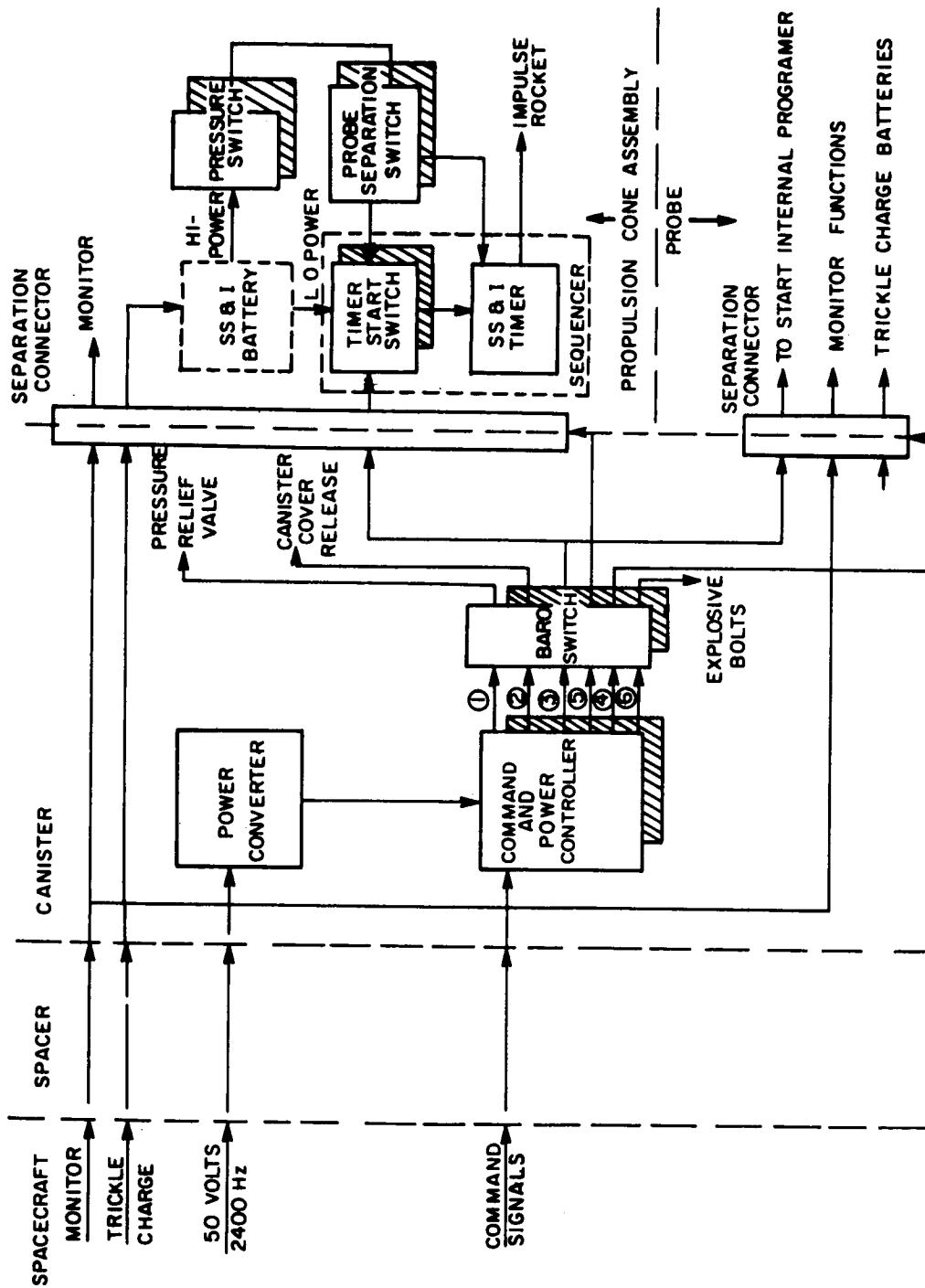


Figure 13 PROBE SAFING, SEQUENCING, AND INITIATION BLOCK DIAGRAM

86-8661

- e. Probe Separation Switch -- To close electrical circuits which must be used only after mechanical separation.
- f. Timer Start Switch -- To initiate the timer.
- g. Command and Power Controller -- To distinguish between discrete command signals and random transients and to distribute power to initiate pyrotechnics.
- h. Power Converter and Storage Unit -- To rectify Probe ac power and dc power for use within the canister and Probe, and to store electrical energy until distributed by the command and power controller.

From assembly of the Probe until after launch from earth, the system is safed from externally generated random signals by means of a baro-lockout switch which interrupts the electrical circuits from the spacecraft. A similar pressure lockout switch, (which senses canister pressure) electrically separates the impulse rocket from the SS&I battery. Above 50,000 feet altitude after launch, the baroswitch in the canister closes, thus arming the separation circuits. After injection into the interplanetary transfer trajectory, a discrete (signal 1) from the spacecraft initiates the canister-venting function.

The power to fire the squibs located in the pressure relief valve for canister venting is delivered from the power converter and storage unit. This unit, located in the canister, converts 50-volt 2400 Hz from the spacecraft to 50-volt dc. The dc energy charges a capacitor in the power converter designed to store sufficient electrical energy for firing three bridgewires in parallel. After the capacitor is discharged, it is recharged and the energy is stored for use later in the flight for mechanically separating the Probe from the canister.

The reduction of internal pressure by venting permits the Probe pressure switch in the propulsion cone assembly to arm the battery circuits to the SS&I timer in the propulsion cone assembly.

The energy for firing squibs is safed by electrical circuits in the command and power controller and is distributed when discrete signals are received from the spacecraft. The discretes are measured and compared with design command pulse signals.

For planning purposes, it was assumed that these discretes are 28 volts with 100 millisecond pulse widths. Signals coming into the command and power controller which do not match the pre-programmed discrete image will not permit energy from the power converter to be transmitted to subsystems in the canister or Probe.

Several days prior to entry into the Martian atmosphere, the sequence begins for separating the Probe from the canister. A spacecraft command (signal 2) discrete enables the voltage discriminator to release energy for separating the cover from the canister. Following this event, spacecraft command (signal 3) is energized to initiate the SS&I timer and Probe internal timer. One second later, command (signal 4) causes separation of the electrical disconnect, severing the electrical circuits between the Probe Assembly and canister. Immediately after this event (one second), another command (signal 5) results in the electrical disconnection between the propulsion cone assembly and canister. When the electrical circuits are open, the Probe with the propulsion cone assembly is then mechanically separated from the canister. Power to activate the explosive bolts is also obtained from the power converter through the command and power controller command from the spacecraft (signal 6).

At separation, a backup timer "start" signal for the SS&I timer and internal programmer is generated by the Probe separation sensors located both on the propulsion cone assembly and also within the Probe. These sensors also arm circuits in both the propulsion cone and the Probe. On the cone assembly, the impulse rocket motor igniter circuit is armed, while within the Probe the circuits to the temperature sensing Probes and the explosive bolt holding the propulsion cone assembly to the Probe are armed. The impulse rocket is fired 17 minutes after separation by 100 millisecond-long discrete signals provided separately to each of the two bridgewires in the rocket initiators. This particular sequence of rocket firing signals minimizes the voltage requirements of the SS&I battery. Distribution of the battery power is controlled by the SS&I timer.

#### 4.4 THE PROBE STERILIZATION CANISTER

The sterilization canister serves to protect the entry Probe and its associated propulsion subsystem from recontamination with microorganisms subsequent to the terminal sterilization process. In addition, the canister provides (by virtue of its double wall construction) some micrometeoroid impact protection and is designed to facilitate the thermal control of the Probe during its cruise on the spacecraft.

The sterilization canister design chosen is a double-walled aluminum container with a forward ejectable cover to provide Probe egress, an aluminum midsection, an afterbody which serves as the main structural load carrying member, and a pressurization and blowdown system.

The cover assembly is made up of the forward sphere-cone portion of the canister. It consists of two aluminum spinings separated by a foam layer, a toroidal entry probe vibration dampener, an ejection spring assembly, a rotation spring which releases after a 70 degree cover rotation and a separation flange equipped with a metallic "O" ring seal. The canister cover weighs 12 pounds. This assembly is sealed to the canister mid-section by a V-band coupling equipped with two

double-bridged power cartridges located 180 degrees apart at either end of the coupling halves. The successful operation of either separator will cause coupling ejection.

The coupling halves are pulled back and stowed on the canister mid section shell. The canister must be hermetically sealed prior to the terminal sterilization cycle and remain so sealed until it is desired to relieve the canister pressure (typically after the spacecraft is injected into the transfer trajectory). Just prior to Probe separation, the canister cover must be jettisoned.

A number of reliable cover sealing and separation schemes were investigated including some where sealing is accomplished by welding the cover to the midsection and separation is achieved by cutting the cover along its circumference by a flexible linear-shaped charge (FLSC). The V-band coupling described above has been tentatively chosen in preference to the FLSC so as to remove the possibility of debris created by the FLSC cutting action from interfering with the spacecraft and/or entry Probe systems. In addition, the V-band coupling allows disassembly and subsequent assembly of the sealed canister without destroying the canister itself. Of course, reesterilization of the Probe would be required in such a case, unless such disassembly and assembly occurred in a bioclean assembly area. The sealing capability of such a V-band coupling has been extensively investigated experimentally under NASA contract NAS 8-20502 and has been found to seal quite satisfactorily.

The midsection is made up of a forward separation flange; separation coupling retractors consisting of four negator constant force springs which stow the V-band coupling after cover ejection; two foam-separated aluminum shells which provide a barrier for internal pressure, for thermal control and also for micro-meteoroid protection; and an after mounting bolted and sealed flange. The titanium entry Probe support is attached to the mid section aft flange. The use of titanium reduces conductive heat losses from the entry Probe during cruise by about a factor of 18 over aluminum.

The afterbody is made up of its mounting flange, an aft aluminum shell and the thrust-spin system supporting structure. The thrust-spin supporting structure is designed to prevent deflection and to maintain alignment during the thrust-spin separation event. It consists of an inner cylinder with closely machined forward and aft lands to position the housing, three radial struts welded to and strengthened by the aft canister shell, and an outboard thin-walled triangular tube, one corner of which is the main canister structural flange.

The pressurization and blowdown system is made up of a fill port, a pressure blowdown assembly and an internal pressure tank assembly. The fill port is used to fill the sterilization canister prior to sterilization and is sealed by welding. The blowdown system consists of a tee-shaped blowdown nozzle to prevent spacecraft torque perturbation during blowdown, dual blowdown valves provided with metallic diaphragms which are ruptured by squib-actuated pistons at blowdown

and dual capillary internal-valve inlet tubes sized to regulate the residual canister pressure to levels ranging from 0.001 torr after blowdown to  $> 0.00001$  torr during cruise. This is desirable in order to achieve a low enough pressure to reduce Probe heat loss during cruise due to heat conduction through the gas and yet not expose the Probe Systems to completely hard vacuum.

#### 4.5 PROBE/SPACECRAFT INTEGRATION

An attempt has been made to keep both the mechanical and electrical interfaces between the Probe and the spacecraft as simple as possible so as to reduce interference with the spacecraft to a minimum. The electrical and mechanical interfaces are described in the following sections.

##### 4.5.1 Probe/Spacecraft Electrical Interface

The electrical interface between the Probe Assembly and spacecraft provides the following functions:

- Pass initiation signals from spacecraft-to-Probe
- Pass diagnostic hard-line data from Probe-to-spacecraft
- Provide support function from spacecraft-to-Probe (battery charging, heater power)
- Provide RF link for checkout and operation purposes.

In addition, it may be required to route the ground handling electrical connections from the Probe through the spacecraft to allow convenient launch pad checkout operations.

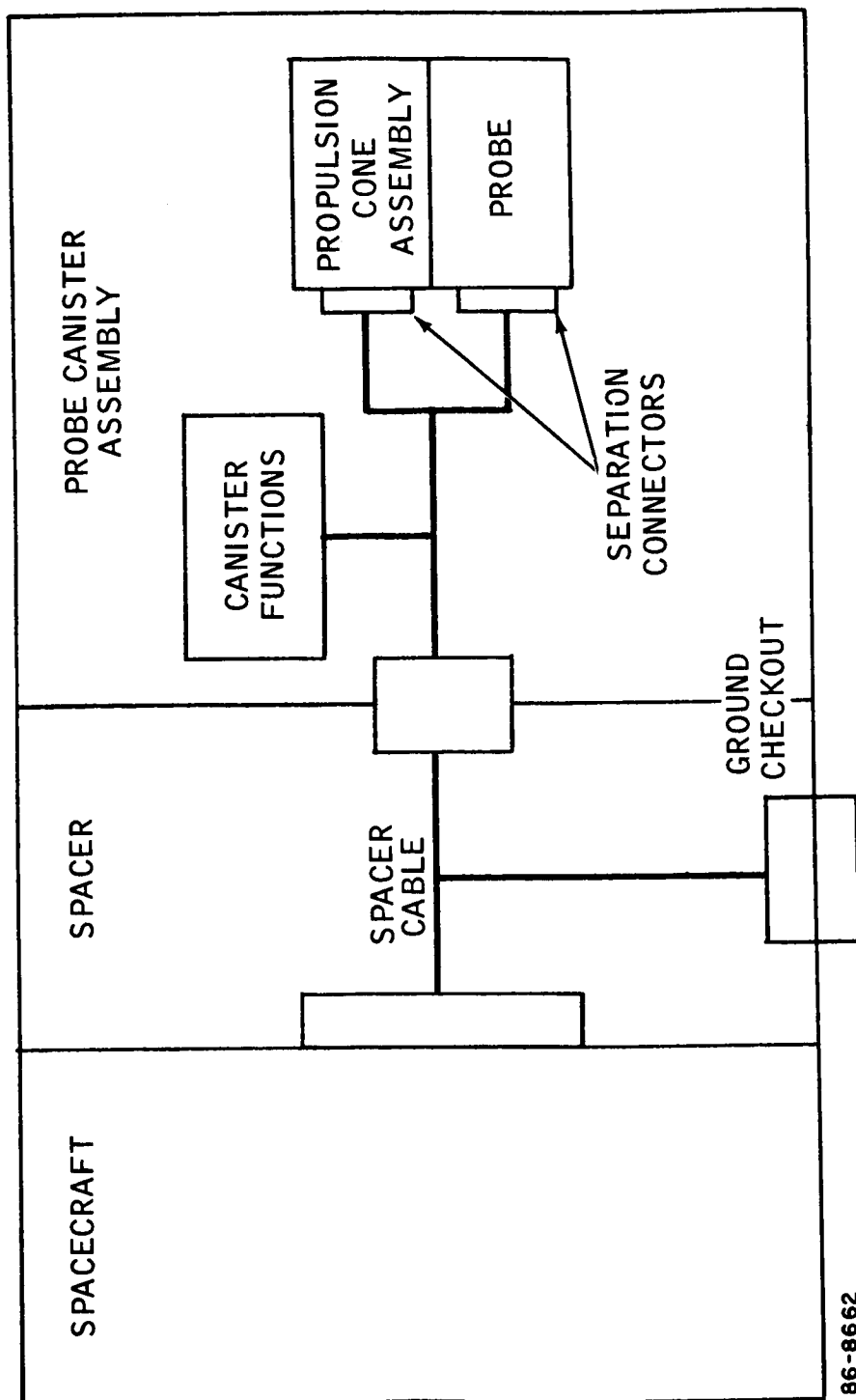
The interface is carried through a permanent connector routed through the sterilization canister and to the spacecraft. About 50 pins are required in the connector.

The RF test link is completed using the spacecraft relay receiving antenna and receiving signal. The signal from the Probe is passed through the canister by using a parasitic antenna fixed to the inside of the canister. The signal is hard wired through the canister to a stub radiator on the outside.

A schematic of the electrical interface is shown in Figure 14.

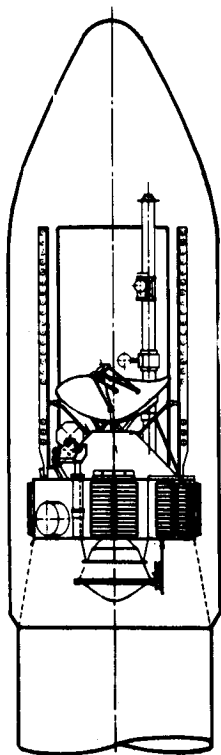
##### 4.5.2 Probe/Spacecraft Mechanical Integration

The mechanical interface arrangement for mounting the Mars Atmospheric Probe with the Mariner IV and Atlas/Agena is shown in Figure 15 a, b, and c. Figure 15 c shows an arrangement of the Mariner IV with the Probe and its receiving

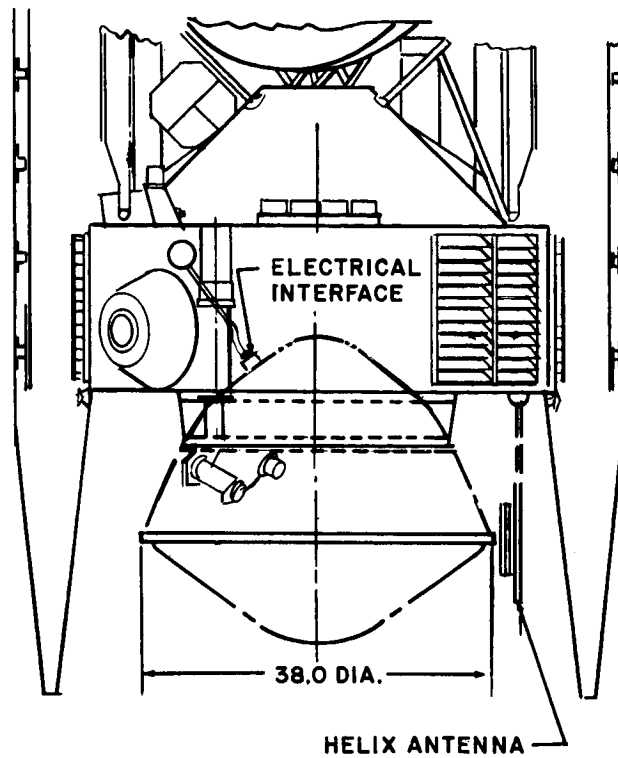


86-8662

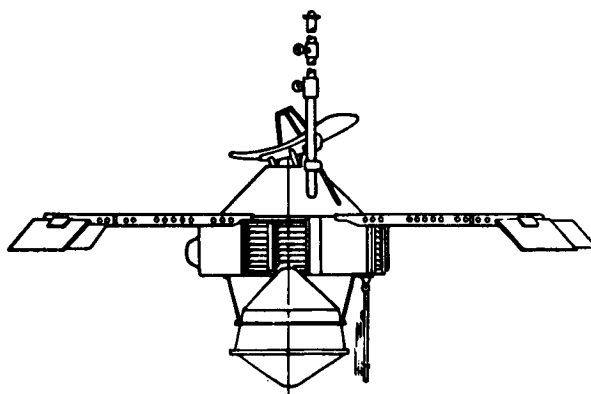
Figure 14 ELECTRICAL INTERFACE SCHEMATIC



A



B



C

86-8663

Figure 15 PROBE-SPACECRAFT AGENA MATING AND INTEGRATION

antenna mounted within the Atlas/Agena ascent shroud. Figure 15b has the mounting arrangement in more detail including the location of the probe-to-spacecraft interface umbilical. Figure 15c shows the Probe mounted to the deployed Mariner spacecraft. The Probe, including its sterilization container, is 38 inches in diameter, 33 inches in length and has a launch weight of 125 pounds with its interface spacer.

Interface flexibility is accomplished by providing a Probe-interface spacer bolted to the aft-probe flange and tailored to the Mariner spacecraft as required. The typical arrangement depicted in Figure 15b shows the Probe mounted to the dark side of the Mariner via a 6-1/2 inch-deep spacer bolted to the lower ring of the spacecraft octagonal structure. The attachment points would be the eight corners of the inner spacecraft octagonal structure at approximately a 46-inch diameter. This provides direct attachment to the main Mariner structure without interfering with the Mariner Agena V-band separation joint located at the 55-inch diameter outer octagonal structural mounting points.

Since the Probe is mounted along the axial spacecraft center line, the planetary science platform is relocated as shown in Figure 15b and the Canopus sensor has a clear view. The Probe receiving antenna is mounted to the spacecraft as shown in Figure 15. It consists of a 16-inch diameter helix mounted to a 35-inch diameter ground plane and is shown in the stowed position. At the time of Probe separation from the spacecraft, the helix antenna is deployed by squib actuation and rotated into position such that its helix centerline is directed toward Mars.

Mounting of the Probe beneath the Mariner requires an additional 33 inches of axial length. An approach for acquiring this space is as follows: The Probe can be so mounted that its aft position penetrates the Mariner spacecraft by four or more inches. The remaining space can be provided by an increased height of the Agena-to-spacecraft adapter and by similarly increasing the height of the ascent shroud-to-Agena adapter. In this manner the required space for the Probe is achieved without modification to the Agena-ascent shroud.

## 5.0 PROBE SYSTEM SELECTION AND PERFORMANCE

The previous sections have described the Probe System design. This section briefly summarizes the reasons for selecting the specific design and operating characteristics of the Probe as well as describing the typical Probe performance which is achieved with these characteristics.

There are five major factors which require careful consideration in order to arrive at satisfactory Probe design and performance.

- a. The selection of the scientific instrumentation payload.
- b. The selection of the launch window, the planetary approach trajectory, and the Probe/spacecraft separation conditions.
- c. The selection and performance of the Probe/spacecraft separation system.
- d. The selection of the Probe entry trajectory and the Probe ballistic coefficient ( $M/C_{DA}$ ).
- e. The selection and performance of the Probe-to-spacecraft relay communications system.

All of these factors must, of course, be considered in the light of existing or projected spacecraft and mission constraints as mentioned in Section 2.0.

### 5.1 PROBE INSTRUMENTATION PAYLOAD SELECTION

The selection of the scientific instrumentation complement is based primarily upon the extensive atmosphere reconstruction analyses conducted by the Ames Research Center. In addition, the desire to provide redundant measurements influenced the number and type of sensors selected. Finally, specific instruments were selected on the basis of compactness and low weight as well as their expected performance under the launch, space, entry and sterilization environments.

The basic types of instrumentation and their performance requirements have been defined in References 1 thru 6. At flight velocities above 1000 ft/sec reconstruction of the density profile is best accomplished with three-axis acceleration measurements. To minimize errors, an accelerometer accuracy of 0.1 percent of full scale is desired. Furthermore, to perform the measurements as accurately as possible in all deceleration regimes, it is desirable to utilize dual-range instruments with scale factors of typically 10:1. Finally, to provide redundancy two separate axial accelerometers are provided, in addition

to the two lateral accelerometers. Since induced errors due to vehicle motions are minimized by locating the accelerometers near the center of gravity of the entry Probe, compact instruments are very desirable. The required maximum accelerometer ranges are determined by the shortest scale height model atmosphere (VM-8), the steepest entry angle (90 degrees) and the largest entry velocity (26,000 ft/sec). These conditions generally result in peak decelerations of about 200 earth g.

At Probe velocities below 1000 ft/sec (which are encountered at lower altitudes for denser model atmospheres and/or shallower entry angles) the prolonged integration of accelerometer bias errors can result in appreciable errors in altitude and hence in the density-altitude profile. Therefore, an alternate method for obtaining vehicle velocity, altitude and density is required for this flight regime. This information can be obtained by measuring the ambient temperature and pressure. These quantities can in turn be deduced from pressure measurements of the Probe surface pressure and the total temperature as measured by extending temperature probes ahead of the Probe surface.

The accuracy with which the ambient pressure can be determined is a function of the free-stream Mach number and the orientation of the pressure port (which depends on the Probe angle of attack) relative to the free stream velocity vector. The Probe angle of attack can be determined from the accelerometer measurements with good accuracy (typically 1 to 3 degrees) and the Mach number can be computed from simultaneous measurements of two pressures located at two different vehicle stations. Thus at least two simultaneous pressure measurements are required. To provide redundancy and several different pressure-gage locations, a total of five pressure gages are actually carried on board the Probe. The temperature measurements are also a function of the Mach number but are less sensitive to the Probe angle of attack (up to angles of attack of 30 to 40 degrees). A single temperature measurement location is adequate, but two separate temperature readings are taken at two opposite locations for redundancy and to guard against the possibility of extremely large angles of attack. The instrument ranges are selected to maximize the accuracy of the measurements during the subsonic flight regime since that is where the accelerometer reconstruction loses accuracy. For very low density atmospheres the Probe may not decelerate to subsonic speeds, but there the accelerometers provide an accurate density profile.

In addition to the density profile (and the low altitude pressure and temperature data), it is highly desirable to obtain measurements on the composition of the Martian atmosphere. This can be accomplished using optical radiometry and measuring the relative intensity of several molecular bands (and certain strong atomic lines) during the high speed entry regime. The radiation is produced by the shock-heated gas behind the Probe bow shock and is observed by the instrument located at the stagnation point. It is estimated that in the vicinity of peak heating this technique can yield the concentrations of  $N_2$ ,  $CO_2$ , and Argon to within 10 percent.

At entry velocities below 18,000 ft/sec, however, the radiant intensities decrease to marginal values and an alternate measurement method is required. The use of a mass spectrometer is then attractive because in addition to the major constituents, it can also search for important trace constituents (water). Therefore, such an instrument is included in the payload. It should be pointed out that mass spectrometer measurements at high velocities are difficult (carbon deposits can form and plug the small sampling port, mass ambiguities exist between different species such as  $N_2$  and  $CO_2$ , etc.). Thus the mass spectrometer measurements are expected to be most valuable at low altitudes (low velocities) while the radiometer measurements provide the high altitude (high velocity) data. To accommodate as wide an entry regime as possible, both instruments should possess large dynamic ranges ( $10^3$  to  $10^4$ ).

The requirements common to all instruments are low weight and compactness, long storage life and calibration stability, compatibility with high g-level operation, and compatibility with the space environment and the terminal sterilization environment.

## 5.2 LAUNCH WINDOW, APPROACH TRAJECTORY AND PROBE/SPACECRAFT SEPARATION CONDITIONS SELECTION

The selection of these parameters not only determines the payload capability for a given launch vehicle and other parameters such as the flight time, the communications distance to earth, the ZAP angle, etc., but also determines the initial entry conditions of the Probe and the dispersion in these initial conditions.

### 5.2.1 Launch Window Selection

Both the 1969 and 1971 launch opportunities were considered during the course of the study. For 1969 two launch windows were examined, corresponding to Type I and Type II trajectories (corresponding to heliocentric transfer angles of less than or greater than 180 degrees, respectively). For 1971 only Type I trajectories were considered.

Figure 16 presents a summary of the three launch windows and their associated parameters. The 1969 Type I window is selected around the minimum launch energy (departure velocity). It results in short flight times (174 to 144 days) and Mars-to-earth communications distances (about  $100 \times 10^6$  kilometers). The Mars arrival velocity is constant over the window and is 6.5 km/sec. This results in Probe entry velocities of 26,000 ft/sec. The 1969 Type II window, on the other hand, results in earlier launch dates, considerably longer times of flight and earth communications distances and lower approach velocities resulting in Probe entry velocities of about 22,000 ft/sec. The shorter flight times and communications distances favor the selection of the Type I window for the 1969 launch opportunity.

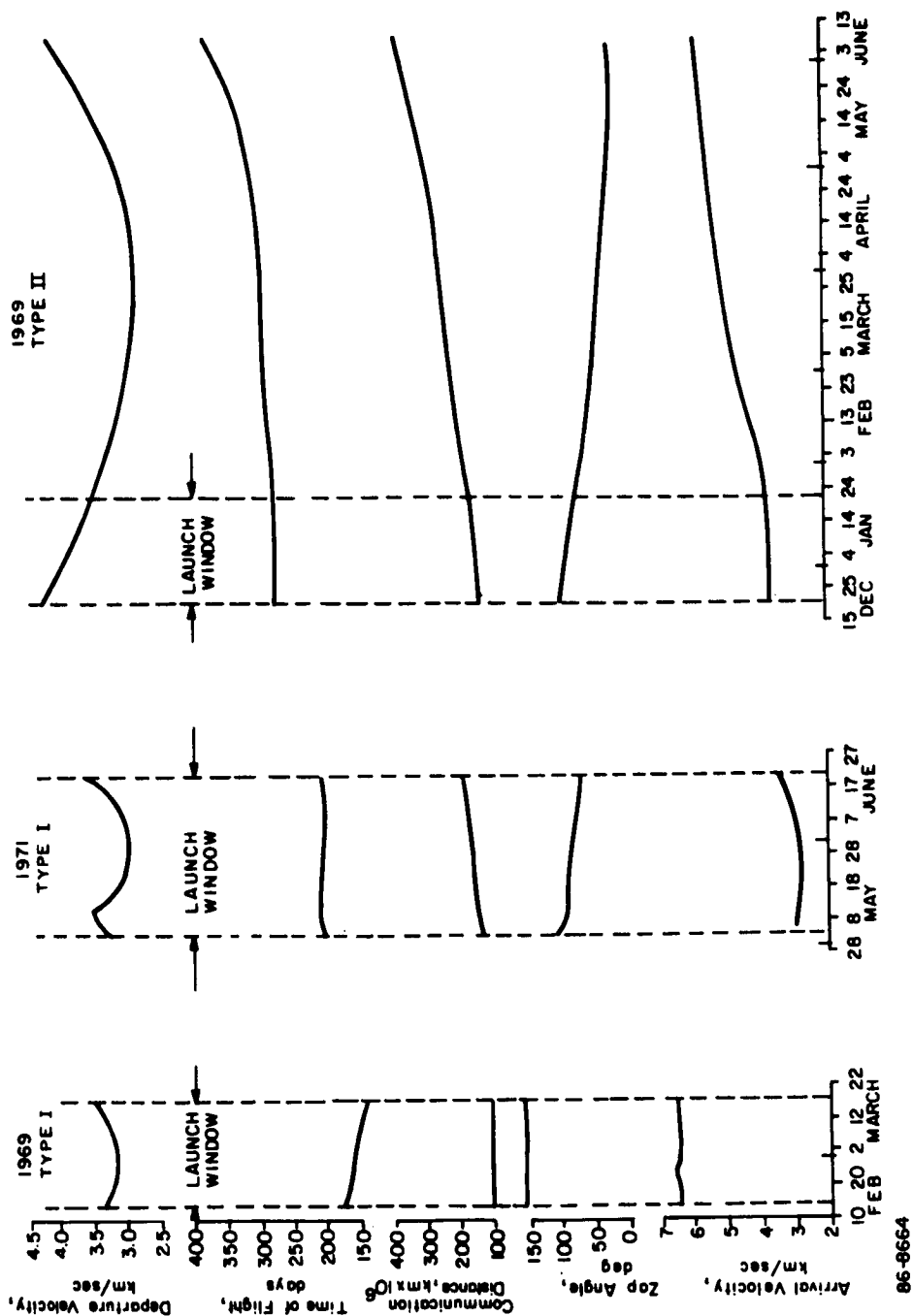


Figure 16 INTERPLANETARY TRAJECTORY CHARACTERISTICS SUMMARY

It should be noted that for the Atlas/Centaur launch vehicle with a Mariner-class spacecraft and Probe there is enough excess launch energy available to achieve still shorter flight times. However, the approach velocities (and hence the Probe-entry velocity) increase sharply and only relatively small gains in communications range result. Consequently, only approach velocities of up to 6.5 km/sec have been considered.

The 1971 launch window is characterized by longer flight times and communications ranges together with quite low arrival velocities (corresponding to entry velocities of 18,000 to 20,000 ft/sec).

It is usually assumed that the Probe entry should take place on the sunlit side of the planet (since this may be the most likely subsequent large Probe targeting). For this to occur, it is necessary to approach the planet along a trajectory whose ZAP angle is greater than 90 degrees. A schematic of the trajectory geometry, together with the definition of commonly used terminology, is presented in Figure 17. The launch windows discussed previously all meet this condition. Somewhat greater latitude in the choice of launch window is possible if the Probe entry is not limited to the sunlit side.

#### 5.2.2 Effects of Approach Velocity and Probe Separation Conditions

Several days prior to planetary encounter, the Probe is separated from the spacecraft and a velocity increment is added to the Probe so as to change the Probe trajectory to a planetary-impact trajectory. The magnitude and direction of the velocity increment, together with the separation range from the planet, determine uniquely the Probe entry angle, the Probe angle of attack at entry and the geometry (e.g., range and look-angles) at entry between the Probe and the spacecraft. The first two items are of particular interest for the atmospheric reconstruction, while the Probe-spacecraft geometry is of crucial importance for the relay-communications system. Furthermore, the accuracy with which the desired  $\Delta V$  magnitude and direction are achieved determine the dispersion in the initial entry conditions (primarily the entry angle). Dispersions in the initial entry angle lead to errors in atmospheric reconstruction and should therefore be minimized.

Figure 18 shows the separation geometry and the resulting entry geometry associated with the Probe velocity increment. A velocity increment of magnitude  $\Delta V$  is applied to the Probe at an angle,  $\theta_{op}$  (called the thrust application angle) relative to the spacecraft velocity vector. For a given separation range from the planet, the entry angle can be controlled by selecting suitable values of  $\Delta V$  and  $\theta_{op}$ . There is an infinite set of pairs of  $\Delta V$  and  $\theta_{op}$  values which all result in the same entry angle since large  $\Delta V$  at small  $\theta_{op}$  are equivalent to small  $\Delta V$  at large  $\theta_{op}$  angles. However, although the same entry angle is achieved for a variety of separation conditions, the Probe-spacecraft geometry at entry (the range and look-angles) is different for each set of  $\Delta V$  and  $\theta_{op}$ .

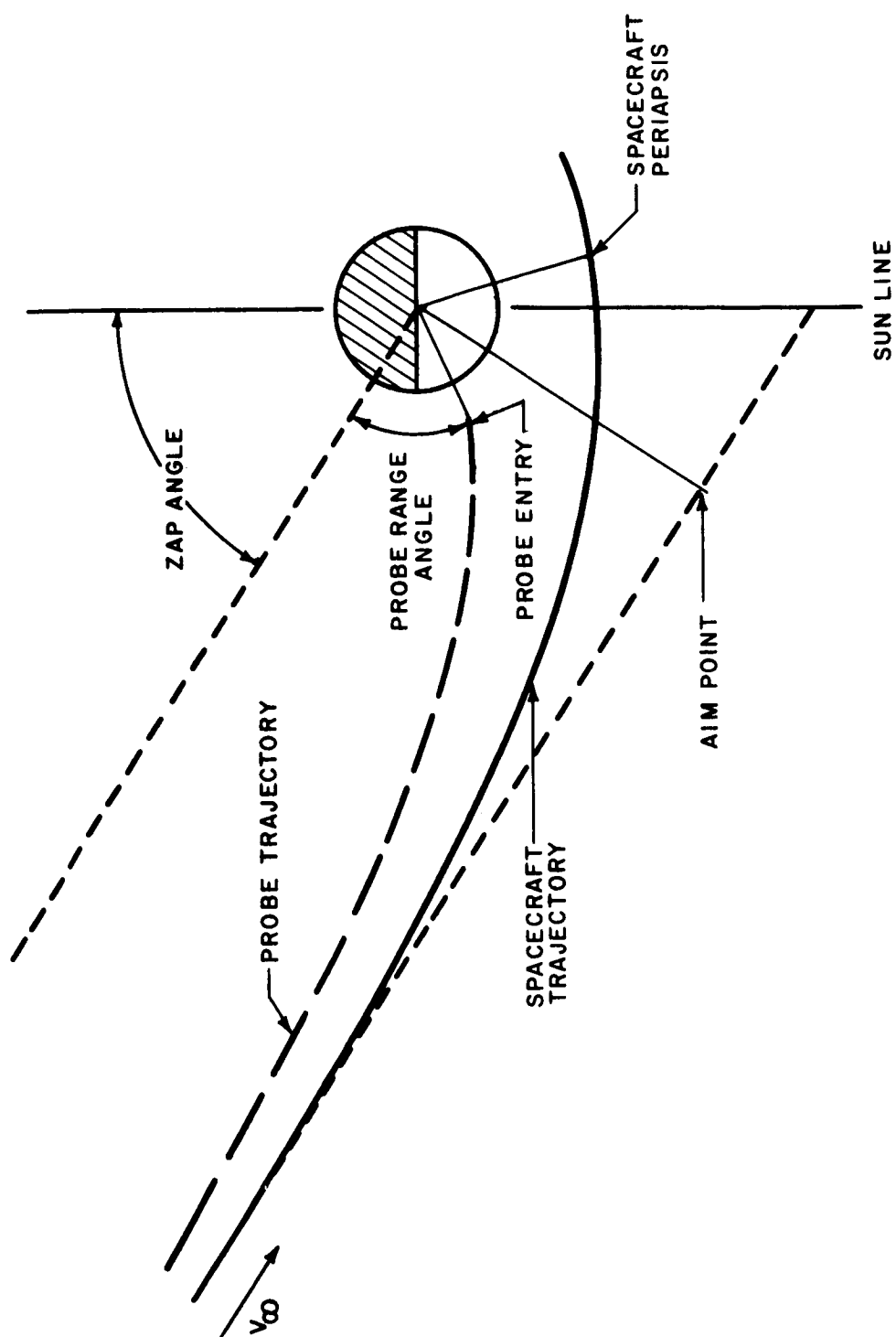


Figure 17 PLANETARY APPROACH GEOMETRY

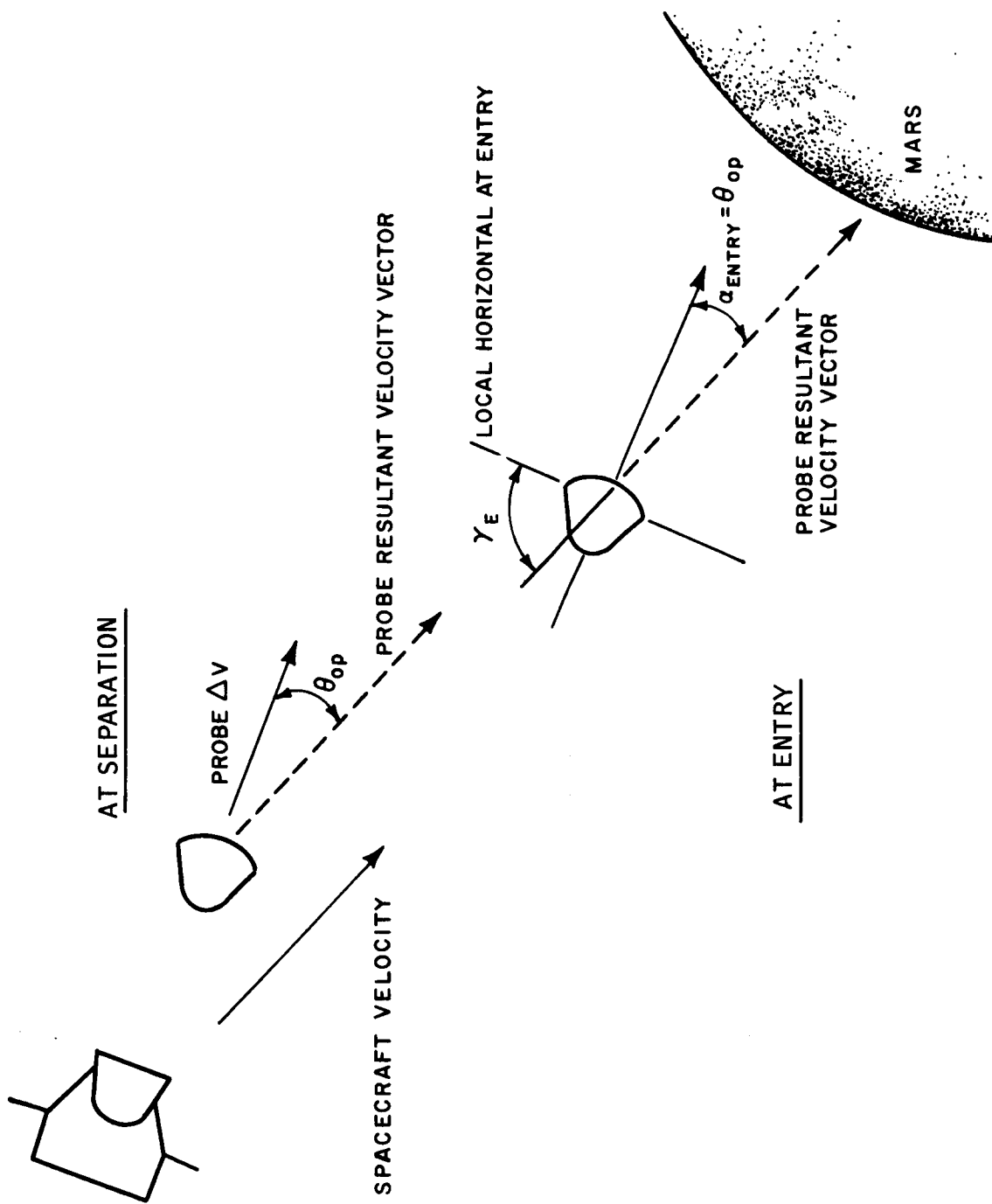


Figure 18 PROBE SEPARATION AND PLANETARY ENTRY GEOMETRY

values. Similarly, the angle of attack at entry is different since it is equal to  $\theta_{op}$  (for a Probe which remains spin stabilized in the  $\theta_{op}$  direction after separation).

Furthermore, the dispersion in the entry angle associated with the different sets of  $\Delta V$  and  $\theta_{op}$  values are quite different (primarily because a fixed magnitude error in  $\theta_{op}$  is much more effective in producing errors in entry angle at small values of  $\theta_{op}$  as compared to large  $\theta_{op}$ . In addition, the large  $\Delta V$  required to achieve a given entry angle at low  $\theta_{op}$  aggravate and contribute to the entry-angle dispersion). Thus, the separation conditions should be chosen so as to result in short Probe-spacecraft communications distances and low dispersions in entry angle. This can be achieved with low  $\Delta V$  applied at a relatively large  $\theta_{op}$ . The specific values are dependent upon the approach trajectories and separation points. For the 1969 Type I trajectories, for example, a  $\Delta V$  of 75 ft/sec applied at a  $\theta_{op}$  of 70 degrees at a range from the planet of  $1 \times 10^6$  kilometers results in an entry angle of 66 degrees.

At entry the Probe is ahead of the spacecraft, the amount of lead time depending upon the separation conditions. The effects of different lead times are shown in Figure 19 where the Probe-spacecraft communications range is shown as a function of approach velocity for different lead times. As expected, long lead times correspond to large communications ranges. In addition, however, high approach velocities and long lead times result in very large penalties in increased communications ranges. It is, therefore, desirable to select short lead times.

The importance of selecting short lead times is further illustrated by Figure 20 which shows the 3-sigma dispersion in entry angle as a function of approach velocity for different lead times and entry angles. Large increases in dispersion occur at long lead times and high approach velocities. This again emphasizes the desirability of short lead times.

The dispersions shown in Figure 20 are due to three error sources, namely:

- a. The error in thrust application angle,  $\Delta \theta_{op}$ . A 3-sigma value of 3 degrees has been used in the calculations.
- b. The error in the magnitude of the velocity increment,  $\Delta(\Delta V)$ . A 3-sigma value of 3 percent has been used in the calculations.
- c. The error in location of the spacecraft,  $\Delta R$ . A 3-sigma value of 450 kilometers has been used in the calculations.

The chosen values for these errors represent the best estimate of what could be achieved at this time. The most important error by far is the error in the thrust application angle. The bulk of the entry angle dispersion is due to this error source. Since the magnitude of this error is largely a function of the

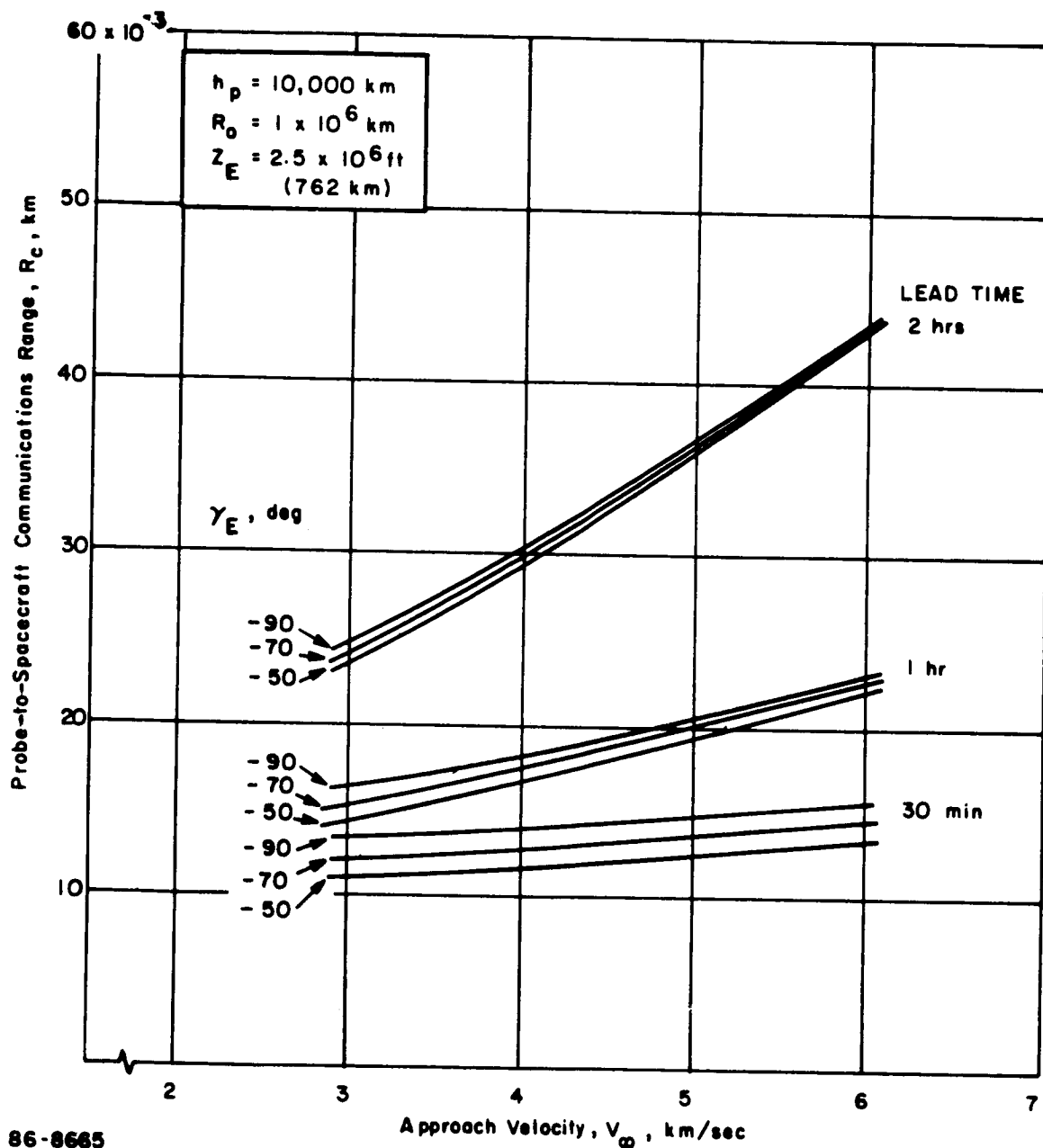


Figure 19 EFFECT OF PROBE-TO-SPACECRAFT LEAD TIME AND PLANETARY APPROACH VELOCITY ON RELAY COMMUNICATIONS RANGE

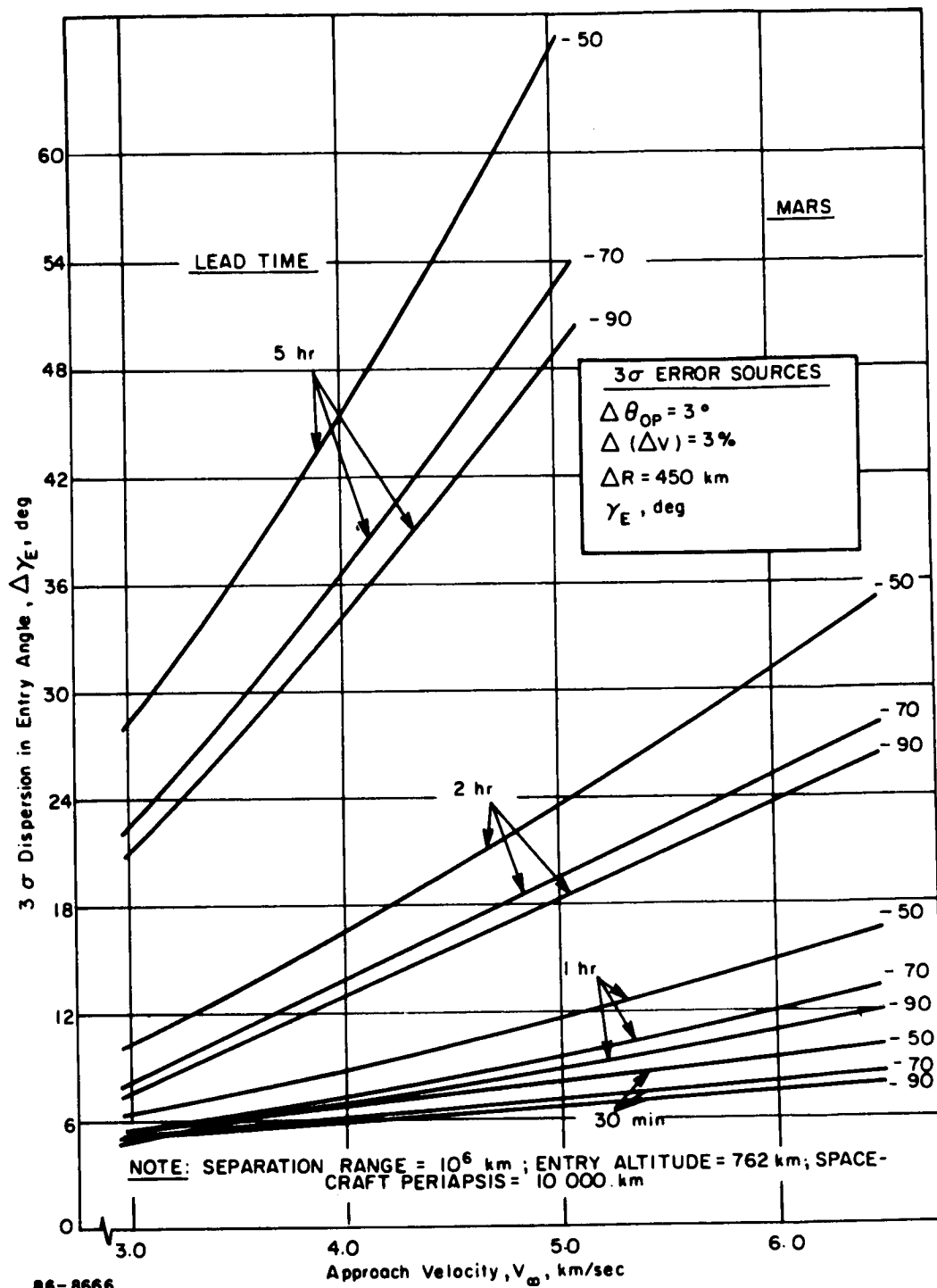


Figure 20 EFFECT OF LEAD TIME AND APPROACH VELOCITY ON THE PROBE ENTRY ANGLE DISPERSION

Probe/spacecraft separation and stabilization system performance, it is important to select a separation and stabilization scheme which minimizes this error.

In summary, a low  $\Delta V$  applied at large  $\theta_{op}$  angles results in low Probe-to-spacecraft communications ranges and low entry angle dispersions even for large approach velocities. As discussed in Volumes II and III of this report, the time at which the Probe is separated from the spacecraft can be used as a variable to accommodate deviations from the nominal spacecraft trajectory. Thus, it is possible to use both a fixed  $\Delta V$  and a fixed  $\theta_{op}$  to achieve a preselected entry angle for a given mission.

### 5.3 PROBE SEPARATION SYSTEM SELECTION AND PERFORMANCE

As illustrated above, it is essential to achieve accurate control over the thrust application angle in order to be able to accurately achieve the desired entry angle. Consequently, an accurate separation and spin stabilization system is required. (Active three-axis attitude control systems were not considered during this study.) It must be understood, however, that there are major interactions between the stabilization system and the propulsion requirements. Also, since various misalignments and the Probe mass properties affect the stabilization accuracy, the entry Probe design itself plays a major role in the stabilization system performance.

To minimize the error in  $\theta_{op}$ , it is necessary to minimize the following error sources:

- a. Tipoff Rates: Tipoff rates during Probe separation, but prior to Probe spinup, can result in substantial errors if allowed to persist for even short intervals of time. Therefore, it is desirable to achieve Probe spinup immediately after separation or concurrently with it.
- b. Thrust Misalignment: Misalignments between the rocket thrust vector and the Probe center of gravity and the spin axis are caused by manufacturing and alignment tolerances, but can also be influenced by thermal distortions during the sterilization cycle. The effects of thrust misalignment can be reduced by minimizing the distance between the rocket and the Probe center of gravity.
- c. Initial Misalignments: The Probe alignment accuracy just prior to separation is a function of the dead band of the spacecraft limit cycle, the mounting accuracy of alignment of the Probe to the spacecraft and the launch tube clearances.

In addition to minimizing the above error sources wherever possible, it is also desirable to achieve a large ratio of spin moment-of-inertia to transverse moment of inertia so as to facilitate spin stabilization.

The two parameters which are at the disposal of the separation and stabilization system designer are the spin rate and the thrust-rocket motor-burning time. High spin rates can be used for better stabilization. The long burning times reduce the effects of thrust misalignment by averaging the errors. However, there are practical limitations on both of these parameters. Very high spin rates inhibit the convergence of the Probe angle of attack during entry, a situation which is undesirable. Despinning the Probe to moderate spin rates prior to entry is possible but adds an additional element of complexity and unreliability to the Probe System. Thus only moderate spin rates (20 to 50 rpm) are desirable. Similarly, the rocket burn time cannot be increased indefinitely because solid, end-burning rockets used to achieve extended burn time are very long. This aggravates the thrust misalignments and causes additional Probe/spacecraft mechanical integration problems. Thus, burning times are limited to 15 to 20 seconds.

The above considerations, plus minimum spacecraft interference requirements, led to selection of the previously described separation, stabilization and propulsion subsystem where separation and spin stabilization are obtained concurrently by ejecting the Probe through a rifled tube. This minimizes tipoff errors and does not require the firing of spin rockets or cold gas jets near the spacecraft.

The performance of the stabilization system is illustrated in Figure 21 where the 1-sigma value of the thrust application error,  $\theta_{op}$ , is shown as a function of the spin rate (for a fixed 15-second burning time) for different values of  $\Delta V$ . A spin rate of 30 rpm and a rocket burning time of 15 seconds result in  $\theta_{op}$  control of better than 3 degrees, 3-sigma. It is also evident that higher spin rates result in only modest improvement since the spacecraft dead band limit cycle itself contributes an error of about 1.5 degrees, 3-sigma.

The effect of moderate spin rates on the angle-of-attack convergence is shown in Figure 22 for different initial angles of attack. As can be seen, for initial angles of attack of up to 60 degrees, satisfactory convergence to less than 15 degrees is achieved below peak heating.

#### 5.4 PROBE BALLISTIC COEFFICIENT, PROBE CONFIGURATION, AND ENTRY TRAJECTORY SELECTION

With the possibility of very low surface pressures on Mars (lower limits ranging from 4 to 7 millibars are under consideration) the choice of ballistic coefficient and Probe configuration becomes quite critical for the Probe design. There are essentially three considerations which influence the choice of ballistic coefficient, namely:

- a. The availability of adequate communication time after emergence from blackout and before impact so that all blackout data, together with the real-time data, can be transmitted to the spacecraft without resorting to extremely high data transmission rates.

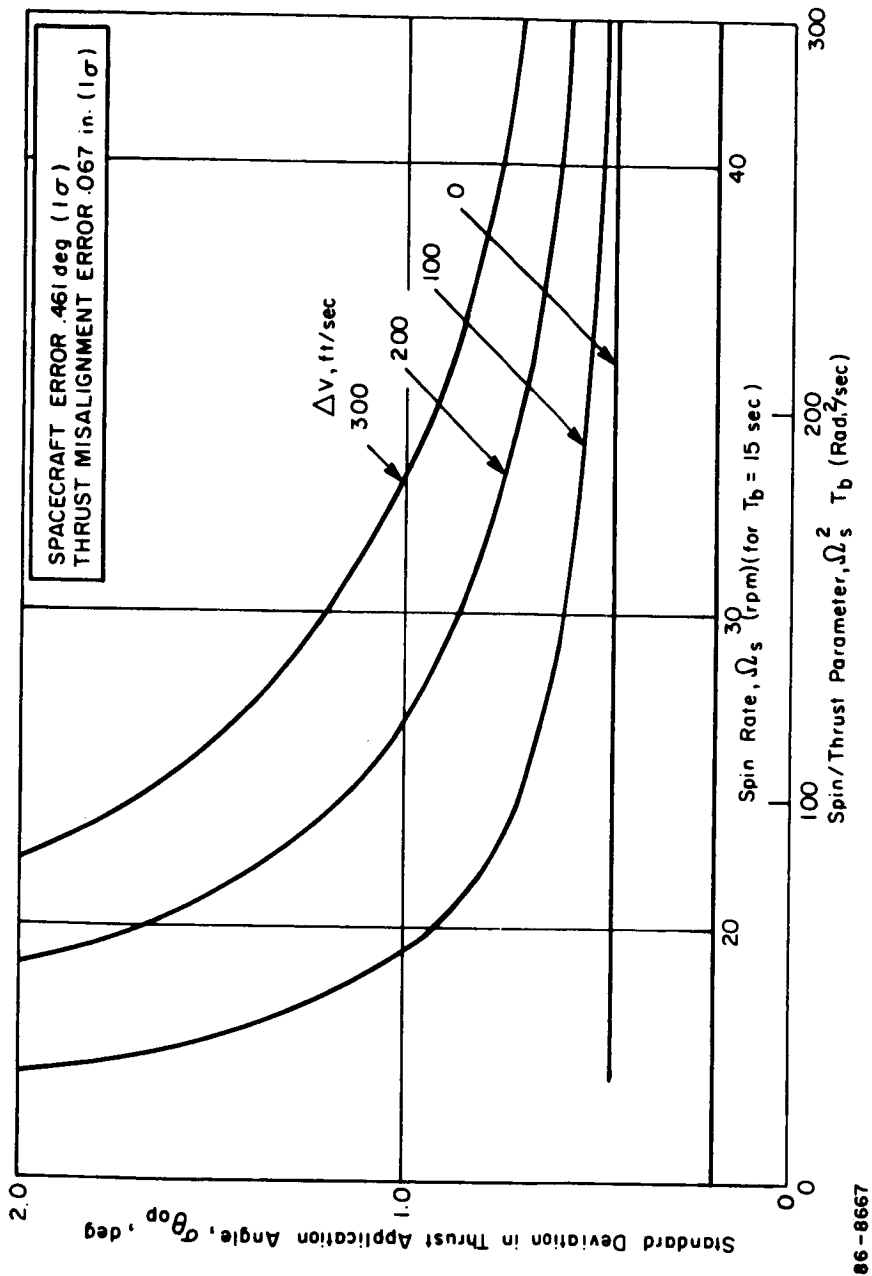
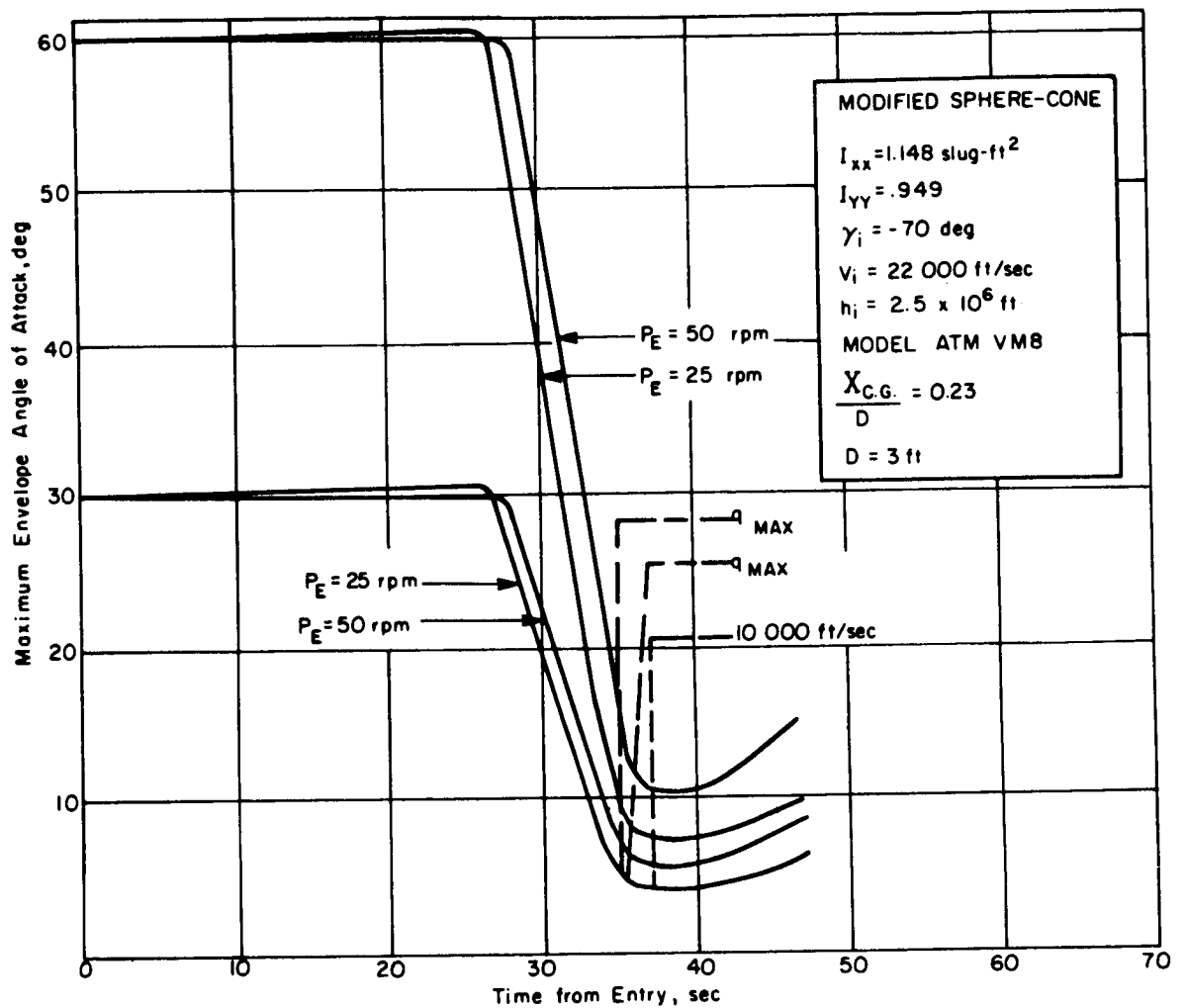


Figure 21 EFFECT OF SPIN/THRUST PARAMETER ON THRUST APPLICATION ANGLE ERROR



86-8668

Figure 22 EFFECT OF PROBE SPIN RATE AND INITIAL ENTRY ANGLE OF ATTACK ON ANGLE OF ATTACK CONVERGENCE

b. The availability of adequate low velocity (preferably subsonic) flight time so that accurate ambient pressure and temperature measurements can be performed with the Probe pressure and temperature instrumentation.

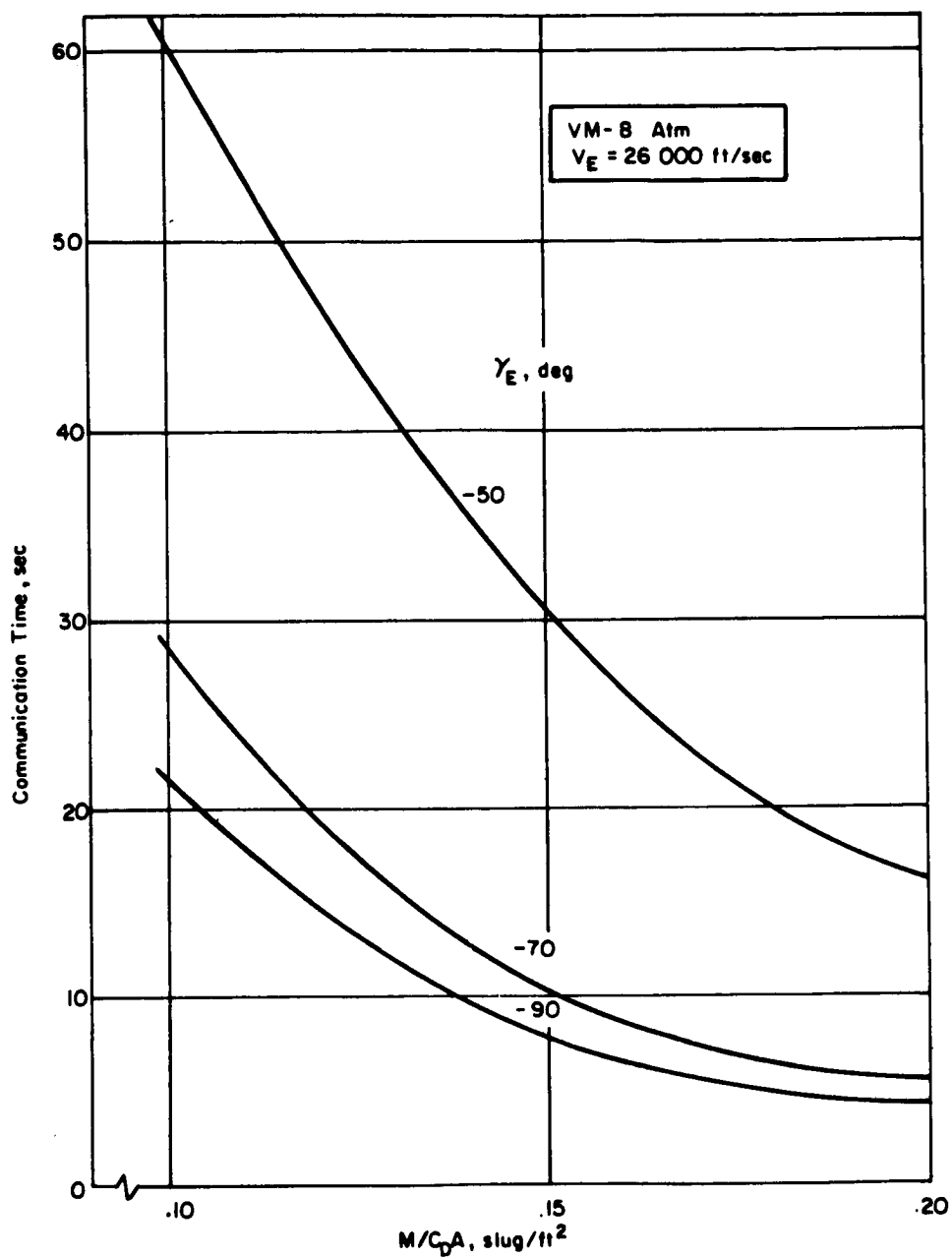
c. The desirability of designing the smallest and lightest vehicle (which still contains the full payload weight) so as to minimize the impact of the Probe on the spacecraft size and weight requirements and to facilitate earth-entry tests of the full-scale Mars Probe vehicle.

Certain tradeoffs are possible in each of these areas. For example, entry at shallower angles is equivalent to lowering the Probe  $M/C_{DA}$ . Communications time can be traded off against higher communications data rates. The degradation in subsonic pressure and temperature data accuracy with increasing Mach number (higher  $M/C_{DA}$ ) can be traded off against the improvement in the accelerometer data accuracy as the Probe velocity at low altitudes increases. It is, therefore, necessary to consider all of the above factors in order to arrive at an optimum choice of ballistic coefficient.

#### 5.4.1 Effect of Ballistic Coefficient and Entry Angle on Communications Time

The shortest communications time occurs for entry into the VM-8 model atmosphere at the highest velocity (26,000 ft/sec). Figure 23 presents the effect of ballistic coefficient and entry angle on the available communications time. As can be seen, the communications time decreases rapidly with increasing  $M/C_{DA}$ . A communications time of 10 seconds necessitates a playout data rate of about 300 bit/sec to transmit all of the real-time data as well as the stored blackout data once before impact. Since it has been found that the blackout time (for a given model atmosphere and entry angle) is quite independent of  $M/C_{DA}$ , reductions in the communications time have a serious effect on required data rate since all the blackout data must now be transmitted in a shorter period of time. For example, reducing the communications time from 10 seconds to 5 seconds increases the required data rate from about 300 bit/sec to about 450 bit/sec for the 70-degree entry angle case. Since such decreases in communications time are associated with increases in  $M/C_{DA}$  from 0.15 to 0.20 slug/ft<sup>2</sup>, it is quite desirable to constrain the Probe ballistic coefficient to less than 0.20 and to strive for a value near 0.15.

Figure 23 also shows the large increases in communications time which can be achieved by entering at shallower entry angles. It is to be noted, however, that substantial benefits can be attained only for entry angles less than 70 degrees. Since the dispersion in entry angle increases for shallower entries, the increased communications time is obtained at the penalty of somewhat greater dispersions. For example, the 3-sigma dispersion at an entry angle of 66 degrees is about 6 degrees, whereas at an entry angle of 50 degrees it is about 8 degrees (for an approach velocity of 6.5 km/sec which corresponds to 26,000 ft/sec



86-8669

Figure 23 AVAILABLE COMMUNICATIONS TIME (TIME FROM 10,000 FT/SEC VELOCITY TO IMPACT)

entry velocity). Thus at the low entry angles, the increased dispersion would lead to somewhat less accurate atmospheric reconstructions. Therefore, the most desirable procedure appears to be to design to the lowest feasible  $M/C_{DA}$  (consistent with Probe diameter constraints for spacecraft/booster integration, etc.) and then target for the highest entry angle which is consistent with obtaining adequate communications times. For Probe  $M/C_{DA}$  of around 0.15 slug/ft<sup>2</sup>, it is then possible to target for entry angles of around 60 to 70 degrees.

#### 5.4.2 Effect of Ballistic Coefficient on Ambient Pressure and Temperature Measurements

The accuracy with which these quantities can be deduced from the onboard measurements is primarily a function of the free-stream Mach number and the uncertainty in free-stream Mach number. In general, the accuracy of the measurement improves with decreasing Mach number. Thus, it is desirable to attain low subsonic velocities in order to maximize the accuracy of the pressure measurements.

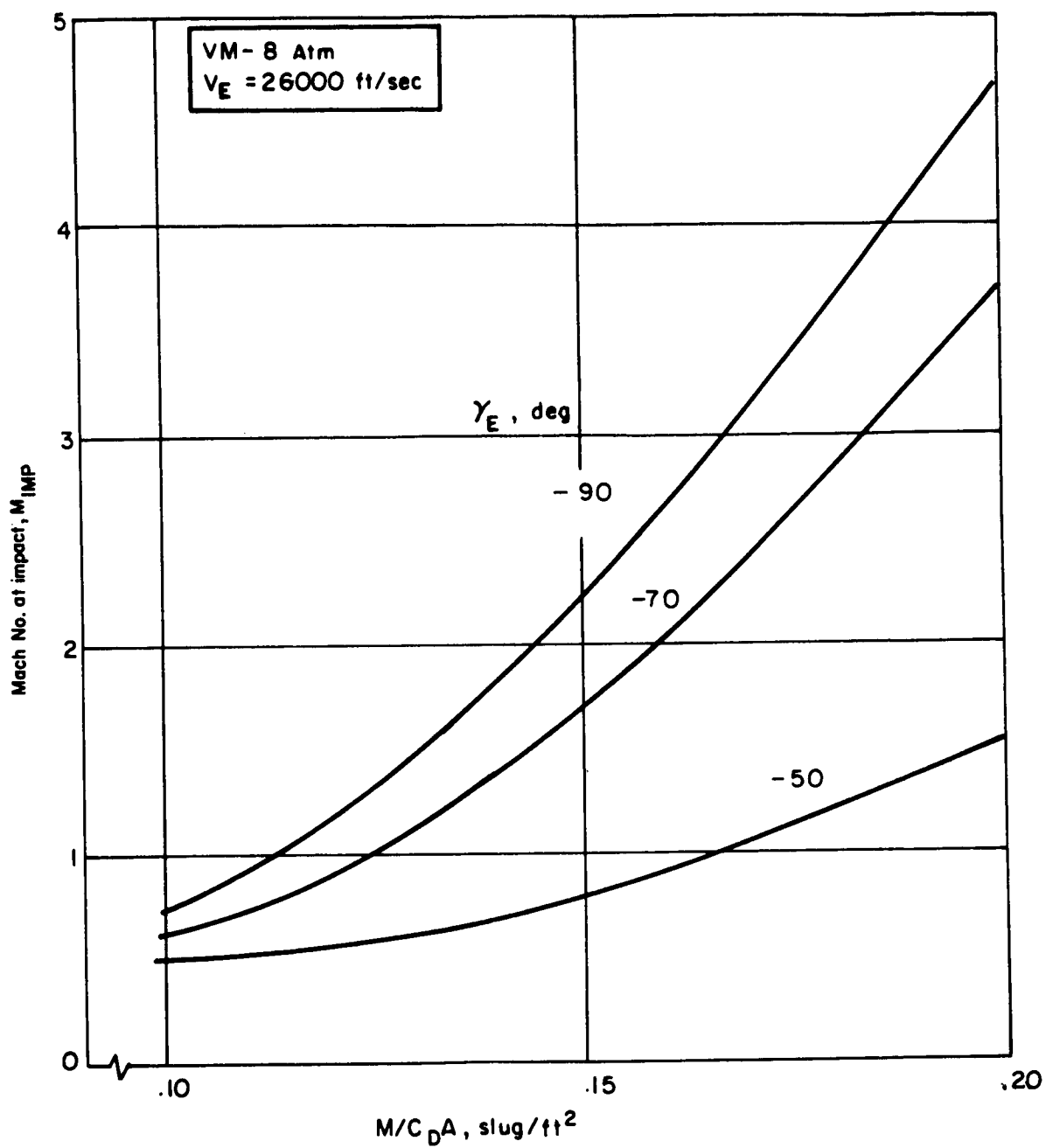
Similarly, the ambient temperature measurement accuracy depends upon Mach number. Although the accuracy is still a function of free-stream Mach number (and the uncertainties in Mach number), the temperature measurement is less sensitive to these parameters than the pressure measurement.

Figure 24 indicates that very low ballistic coefficients are required to achieve subsonic impact velocities in the worst model atmosphere (VM-8) unless very shallow entry angles are selected. However, it should be noted that the results are presented for the worst model atmosphere which not only has a low surface pressure (5 millibars) but also an extremely small scale height (about 5 kilometers). For atmospheres with somewhat greater scale heights (even if the surface pressure is still held low), the situation improves quite rapidly. Thus for a seven millibar, 8.5-kilometer scale height, a subsonic flight time of 8 seconds and an impact Mach number of 0.6 are achieved even for vertical entry for an  $M/C_{DA}$  of 0.15 slug/ft<sup>2</sup>.

Consequently, the selection of the worst atmosphere model plays a major role in the selection of the Probe entry angle. In all cases, however, a low Probe ballistic coefficient around 0.15 slug/ft<sup>2</sup> (or less) is quite desirable.

#### 5.4.3 Probe Configuration Selection

Since it appears desirable to achieve ballistic coefficients around 0.15 slug/ft<sup>2</sup>, it is important to select a Probe configuration which allows such low  $M/C_{DA}$  for reasonably small vehicle sizes. For this program two configurations, a pure sphere and a blunt, 55-degree sphere-cone have been studied. The higher drag coefficient of the sphere-cone leads to a clear-cut  $M/C_{DA}$  versus size advantage relative to the sphere.



86-8670

Figure 24 PROBE MACH NUMBER AT IMPACT

This is illustrated in Figure 25 which shows Probe payload as a function of Probe diameter for the two configurations at an  $M/C_{DA}$  of 0.15 and 0.25 slug/ft<sup>2</sup>. Since the present reference mission requires payload weights of 26 to 29 pounds, it can be seen that the spherical configuration cannot achieve an  $M/C_{DA}$  of about 0.15 for small vehicle sizes, whereas the sphere cone can achieve such an  $M/C_{DA}$  with a vehicle size of about 36 inches in diameter.

Figure 25 was constructed on the basis of parametric information. Figure 26 illustrates what can be achieved in the way of detailed and fully analyzed Probe designs. The figure is a plot of Probe  $M/C_{DA}$  versus Probe diameter. The curves are calculated variations while the symbols are actual design. Again it can be seen that for the sphere cone, an  $M/C_{DA}$  of approximately 0.15 slug/ft<sup>2</sup> can be obtained with vehicle diameters of about 36 inches, whereas much larger diameters are required for the sphere.

The requirement for a low ballistic coefficient also has a significant impact upon the choice of the structural and heat shield materials of the Probe. The emphasis placed on low weight results in the selection of an efficient, charring ablator as the heat shield material. Similarly, beryllium is selected for the shell structure of the Probe because of the excellent resistance to buckling loads which can be obtained with very low shell gages (about 0.030 inch) and consequently very low weights.

## 5.5 TELECOMMUNICATIONS SYSTEM SELECTION AND PERFORMANCE

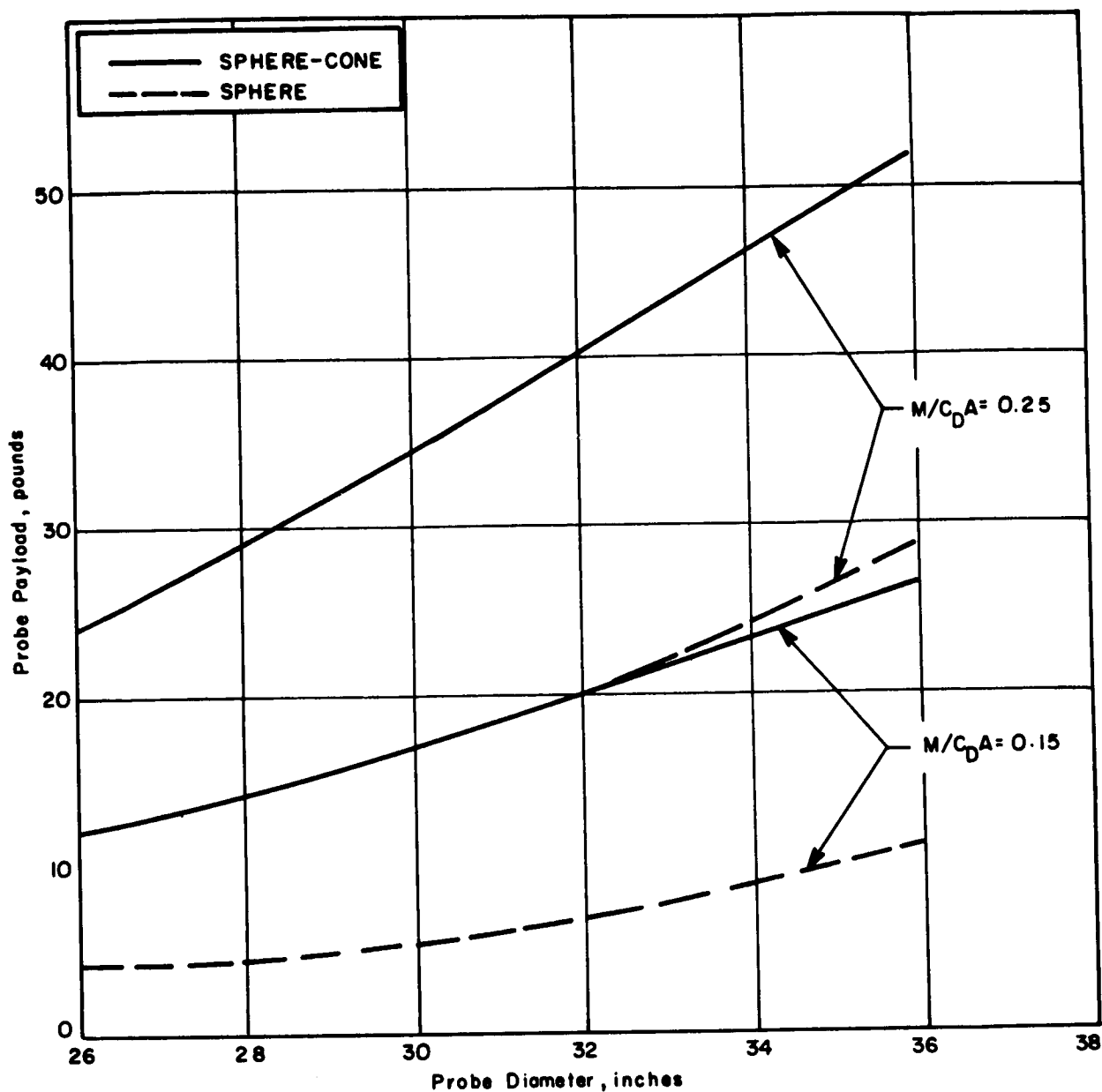
A large number of factors must be considered in the selection and performance of the communications system. All are discussed in detail in Volume III of this report. The most important considerations are briefly summarized below.

### 5.5.1 Telecommunications System Selection

In the design of the relay link telecommunications system, selections must be made for the following system characteristics:

- Frequency of Transmission
- Transmitter Power
- Antenna Characteristics
- Modulation Techniques.

In general, all other system parameters are determined by the geometry (range and look-angle) of the relay link. The geometry also affects the performance of the transmitting and receiving antennas.



86-8671

Figure 25 PROBE PAYLOAD COMPARISON FOR DIFFERENT PROBE CONFIGURATIONS

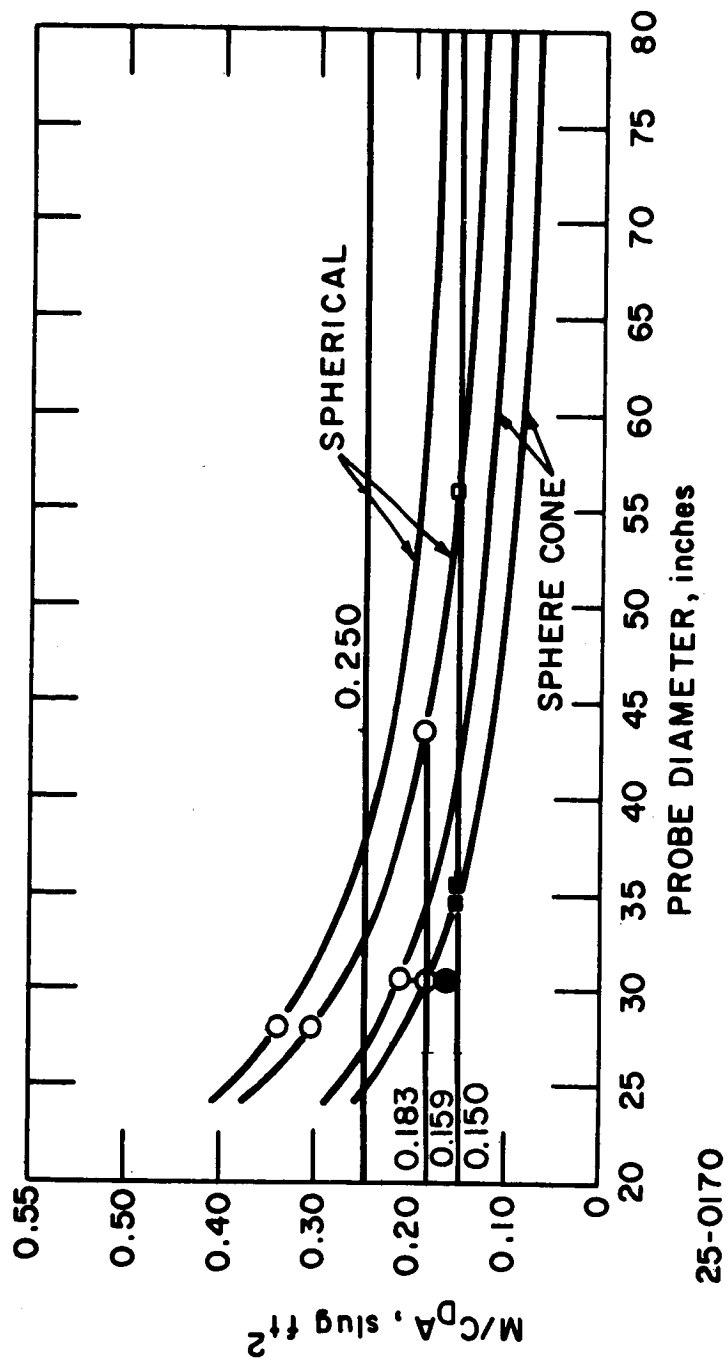


Figure 26 EFFECT OF PROBE DIAMETER ON ACHIEVABLE PROBE BALLISTIC COEFFICIENT

The following discussion summarizes the factors which were considered in the selection of the Mars Probe telecommunications system characteristics.

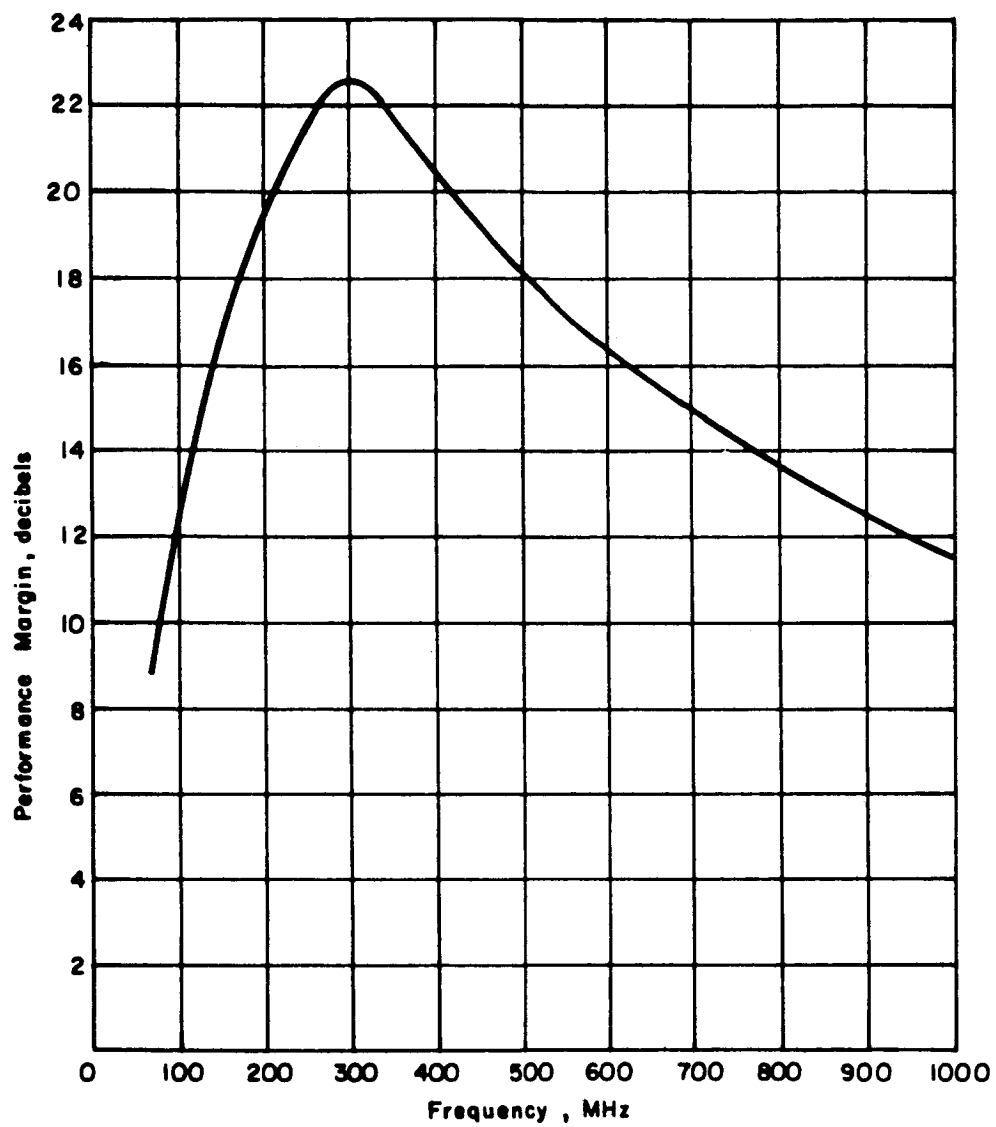
a. Frequency of Transmission -- During the study, all of the factors which determine performance capability and which depend on frequency were evaluated to determine the overall effect of frequency on system performance. The factors of importance were: transmitting antenna gain, multipath effects, system noise and the pre-detection bandwidth. The net effect of frequency on system performance is illustrated in Figure 27. An available band in the vicinity of 272 MHz was selected for the reference design.

b. Transmitter Power -- A number of factors enter into the selection of transmitter power for the Mars Probe. Clearly, it will be desirable to utilize the maximum available power. However, this goal must be consistent with the desire to utilize a solid-state transmitter design and by the efficiency obtained as the output power is increased. Since the gain bandwidth product of power transistors is limited, the number of stages and the number of parallel output transistors increases as the output power is increased. This causes the transmitter weight to go up and the efficiency to decrease with increasing transmitter power.

The limit to the usable transmitter power is reached when there is danger of antenna breakdown in the rarified Martian atmosphere. In Figure 28 the power at which antenna breakdown occurs is shown as a function of the ambient gas pressure. Experimental results are shown for two gases, air and Argon. As can be seen, breakdown can be expected for a transmitter power above 30 watts. Based on the previous considerations and the need to remain safely below the breakdown power limitation, a transmitter power of 20 watts has been selected for the Mars Probe reference design.

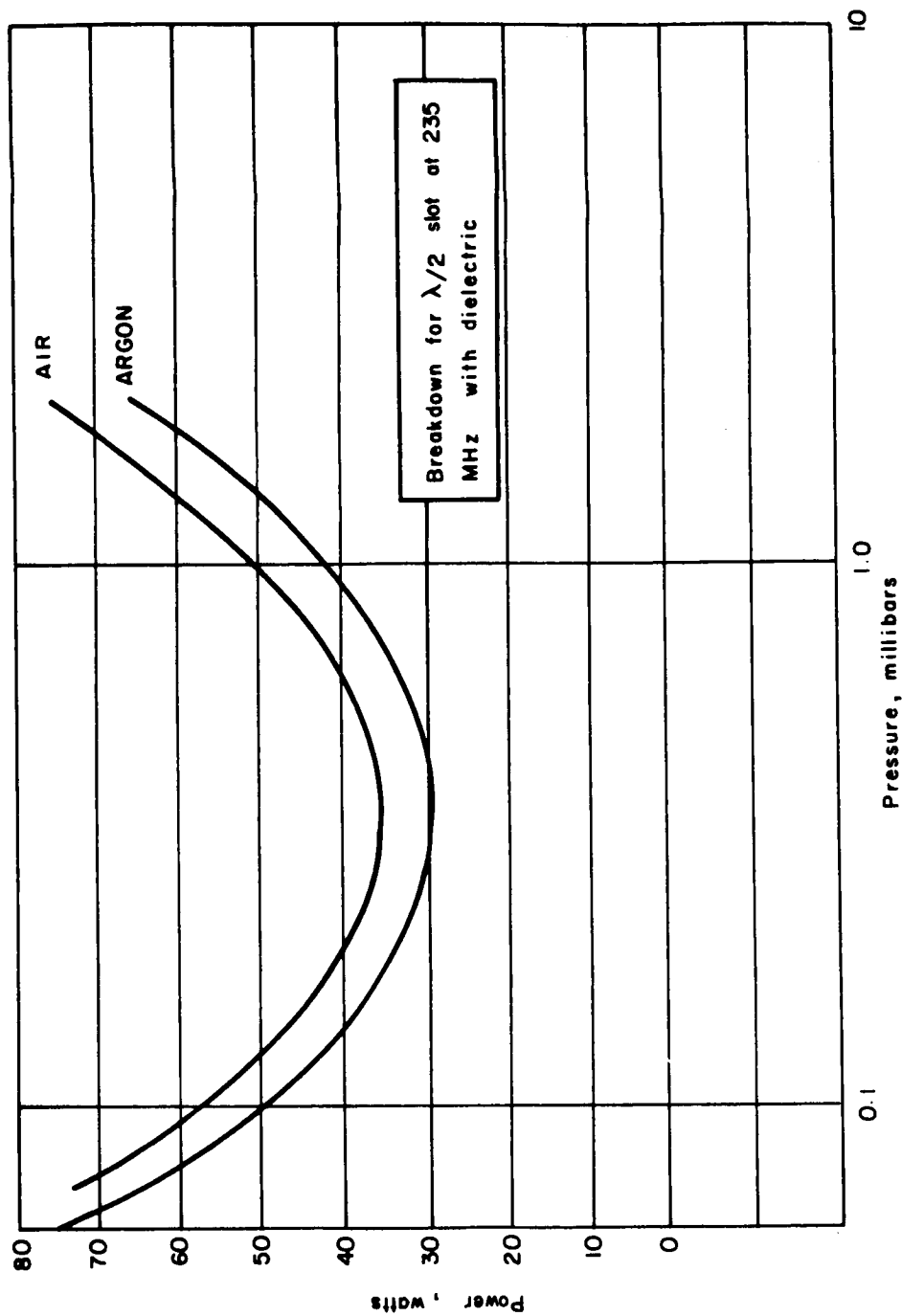
c. Antenna Characteristics -- Because of the small size and oscillatory motion of the Probe during entry, a near hemi-omni antenna pattern is the best that can be achieved and utilized. For the spacecraft receiving antenna, however, there are no obvious limitations on the antenna gain other than the physical size of the antenna. The study has shown that for realistically sized antennas (about 12 decibels), the resultant beamwidth is large enough to illuminate the Probe over the full range of possible entry positions without the necessity for pointing. It was therefore concluded that a spacecraft body-fixed antenna design was most suitable.

d. Modulation Selection -- During the study a thorough investigation was made of the possible modulation techniques for the Mars Probe telecommunications system. The results of this investigation are summarized in Table XV. As can be seen, the results in terms of achievable performance margin are substantially the same for all types of systems. As a result,



86-8673

Figure 27 COMMUNICATIONS PERFORMANCE MARGIN AS A FUNCTION OF FREQUENCY



86-8674

Figure 28 ANTENNA BREAKDOWN CORRELATION

**TABLE XV**  
**MODULATION TECHNIQUE COMPARISON**

System	*Ta = 0.1 sec	*Ta = 1.0 sec	Remarks
<b>I. Coherent</b>			
a. PCM/PSK/PM	12.7 db	17.0 db	**Acquisition cannot be initiated until deceleration has decreased sufficiently. This only allows approximately 2 sec. communications time.
b. PCM/PSK/PM	12.4 db	16.2 db	
<b>II. Noncoherent Tracking</b>			
a. PCM/MFS	19.3 db	19.3 db	** The noncoherent tracking schemes cannot acquire and track in high deceleration regimes. The allowable communications time is considerably less than the total mission time.
b. PCM/FM	17.5 db	17.5 db	
c. PCM/FSK	17.0 db	17.0 db	
d. PCM/AM	17.2 db	17.2 db	
<b><u>Non-Tracking</u></b>			
a. PCM/MFS	18.2 db	18.2 db	The wideband systems are able to initiate communications at exit from blackout and hence provide maximum communications time.
b. PCM/FSK	15.2 db	15.2 db	
c. PCM/AM	16.0 db	16.0 db	

\* The acquisition time (Ta) is the time allowed for signal acquisition for the coherent system. A shorter time allotted requires more carrier power which results in a lowered margin.

\*\* Before the coherent systems can acquire a signal the rate of change of signal frequency (primarily due to doppler rate) must be below a threshold value related to the tracking bandwidth. Thus acquisition cannot occur until the Probe deceleration has decreased to low values.

non-coherent, non-tracking, wideband PCM/FSK was chosen for the reference design since this system provides the simplest mechanization for both the Probe and spacecraft systems. The resulting reference design telecommunications system characteristics are:

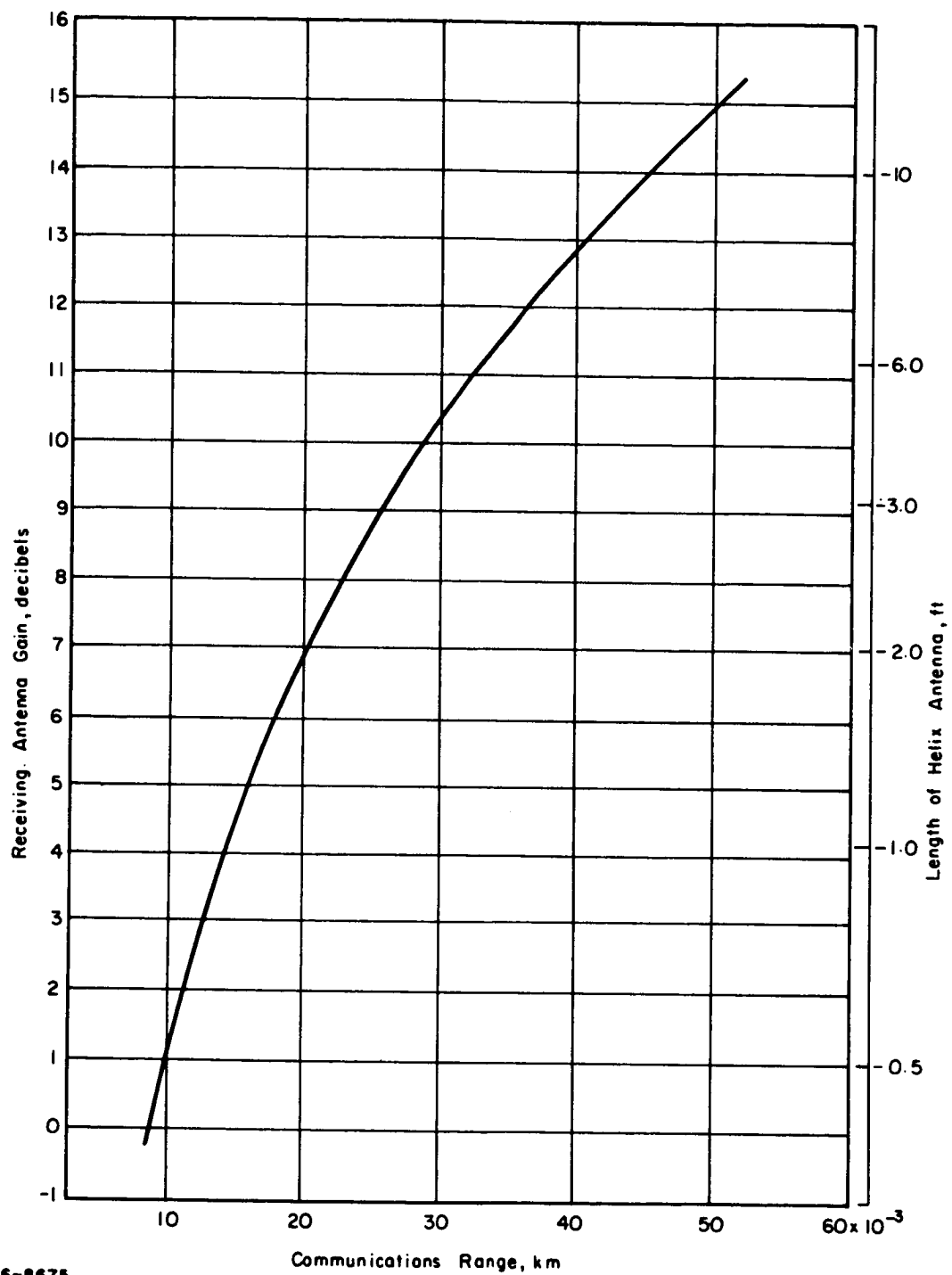
- Modulation -- Wideband PCM/FSK
- Transmission Frequency -- 272 MHz
- Transmitter Power -- 20 watts
- Receiving Antenna -- 12 decibel gain, body fixed

#### 5.5.2 System Performance

For the reference design telecommunications system, the system performance (performance margin obtainable for the 276 bit/sec mission-data rate) is determined by the communications geometry at Probe entry. The primary geometric factor is the communications range. Its effect is shown in Figure 29 which plots the range against the receiving antenna gain for a 10 decibel performance margin. The study has shown that a 12-decibel antenna is about the largest that can be accommodated on a Mariner-class spacecraft. For such an antenna a 10-decibel margin can be obtained at ranges of up to about  $35 \times 10^3$  kilometers.

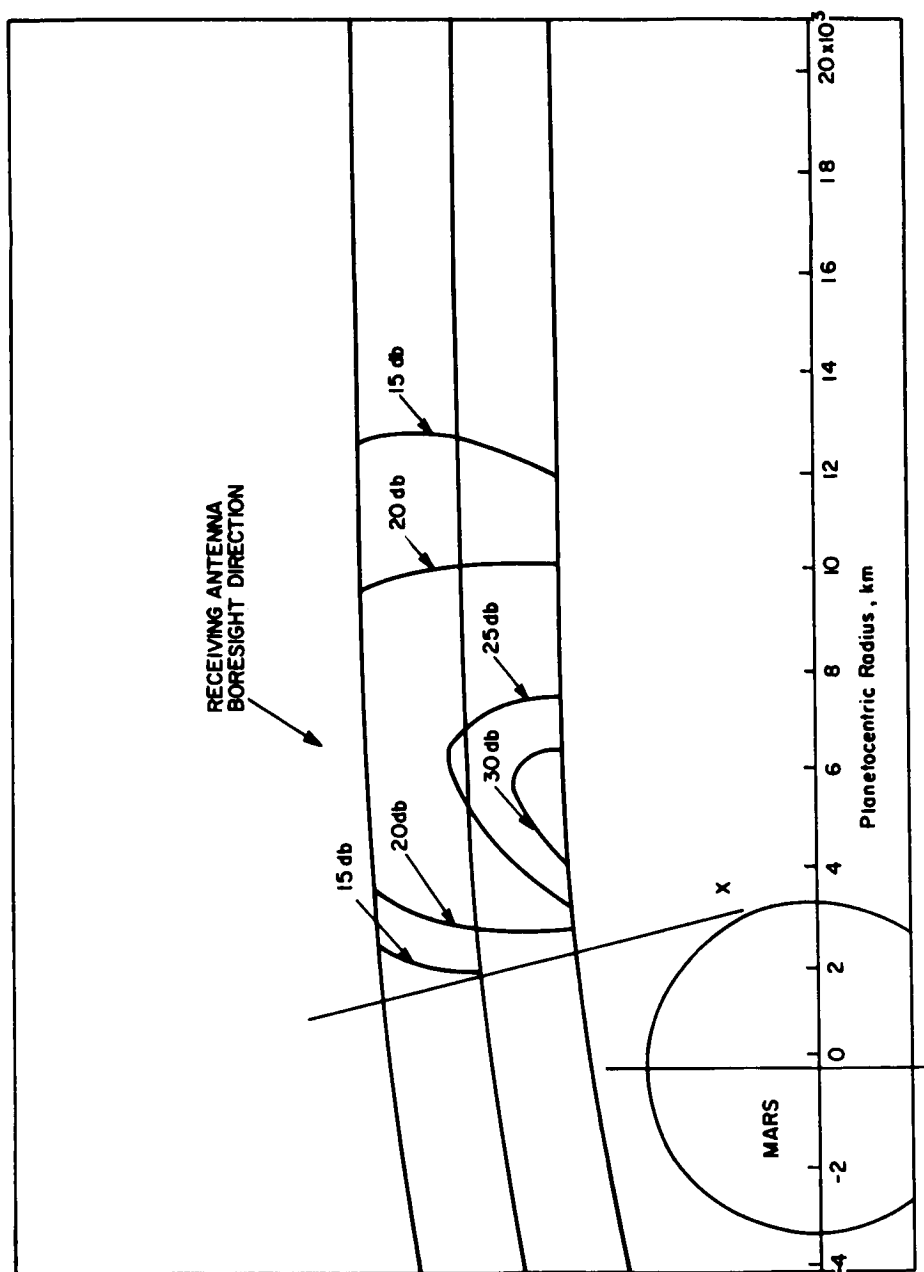
When the other geometric factors such as antenna look-angles are taken into account, the performance margin can be determined for any possible Probe and spacecraft position. This performance determination is summarized in Figure 30 which shows the margin contours for the possible spacecraft position based on a normal entry from the approach trajectory.

The indicated trajectories show the nominal case as well as the  $\pm 3$ -sigma trajectories. Therefore, the spacecraft will be found to lie within these limiting trajectories. As can be seen, margins in excess of 10 decibels can be obtained for spacecraft ranges from periapsis of less than 15,000 kilometers.



86-8675

Figure 29 EFFECT OF RECEIVING ANTENNA GAIN AND RELAY COMMUNICATIONS RANGE ON ACHIEVING 10-DB COMMUNICATIONS MARGIN



86-8676

Figure 30 CONSTANT MARGIN CONTOURS

## 6.0 PROBE STERILIZATION ANALYSIS

NASA has placed a biological quarantine on the planet Mars which requires that any probe used to enter the planet's atmosphere have a probability of biological contamination less than one in ten thousand. The method of sterilization has been specified to be exposure of the probe, after assembly, to a dry-heat thermal cycle\* with a stated biological kill effectivity of a factor of  $10^{12}$ . This divides the steps necessary to satisfy the quarantine requirement into three clear groupings.

- a. The biological burden on the Probe prior to application of dry-heat must be demonstrated to be  $\leq 10^8$  microorganisms if the specified terminal cycle is to provide the required probability of sterility (i. e.,  $10^{-4}$ ).
- b. The terminal heat cycle must be applied and verified that it was applied adequately.
- c. The Probe must not be recontaminated, and demonstrated as not recontaminated, during subsequent events, from the time of application of terminal sterilization heating until planet surface impact.

Study efforts have therefore been oriented - (1) to provide a comprehensive understanding of all factors affecting the establishment of a practical plan that will meet the above three requirements, - (2) to select the processes that will most economically meet these requirements with minimum impact on system performance and logistics, and - (3) to organize these factors and processes into a sterilization plan. These study efforts included: selection of the basic approach to biological burden control; determination of the influence of all factors affecting burden; analyses to measure burden estimates as a function of clean room and control investigation of burden assay, terminal heat application procedures; and considerations of sterilization maintenance after terminal heating.

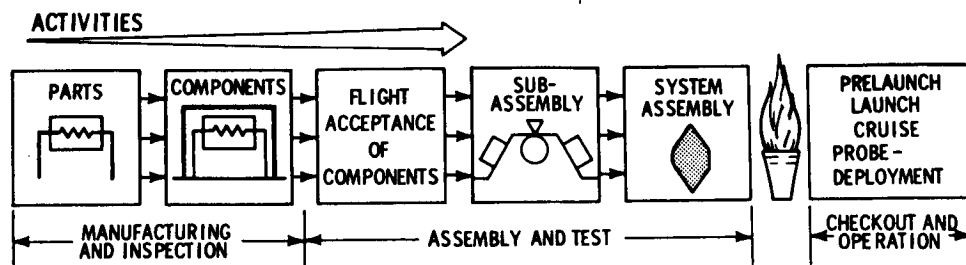
### 6.1 MAJOR CONSIDERATIONS IN SELECTION OF STERILIZATION TECHNIQUES

Figure 31 schematically presents the principal activities (factory through Probe deployment) that are affected by the planetary quarantine, and lists the factors which must be given consideration when establishing a sterilization plan.

In order to establish the biological burden of a system and determine if it can be controlled within acceptable limits, it is necessary to examine, quantitatively, the causes of contamination (manufacturing and assembly activities) and the effectivity of possible decontamination and handling procedures. A computer

---

\* A range of acceptable temperature-time combinations, all having a stated  $10^{12}$  kill effect have been authorized for use. This allows the probe designer to select a cycle most compatible with performance and reliability objectives.



- CAUSES OF CONTAMINATION
- DECONTAMINATION FACTORS
- SYSTEM PHYSICAL CHARACTERISTICS
- METHODS OF BIOLOGICAL BURDEN ANALYSIS
- BURDEN CONTROL AND CERTIFICATION METHODS
- PROOFS OF STERILIZATION
- REPAIR
- STERILIZATION MAINTENANCE

Logistics • Economics • Safety • Sterility Risk • Performance Risk

86-8677

Figure 31 CONSIDERATIONS IN THE SELECTION OF STERILIZATION TECHNIQUES

approach to the problem is indicated by the complexity of the system, the wide variation in required manufacturing assembly and test functions for the various components, the broad range of biological loading on parts and components, and the varying effectiveness of handling and decontamination procedures.

Potentially defective components must be eliminated by flight acceptance tests (environmental exposure) prior to assembly. These acceptance tests should include heat-cycle tests and possibly ethylene oxide (ETO) tests, since terminal sterilization is a future environment and, as developed in the body of the report, ETO cleaning after assembly can be desirable to reduce surface biological burden.

#### 6. 1. 1 Contamination and Decontamination Factors

NASA, the scientific community, and industry were consulted to establish, from completed experiments and many still in progress, specific values for the several factors necessary to compute system burden estimates. The primary factors that affect biological burden, and the specific values used in the study are listed in Table XVI.

Piece parts such as resistors, transistors, and transformers, have been found to have internal burdens ranging from 0 to 100,000 microorganisms, depending on the particular manufacturing process involved and the nature of acceptance test procedures employed. In some cases, as for acceptance of high reliability transistors, which are burned in and stabilized for long periods at temperatures more severe than the specified terminal sterilization cycle, internally sterile parts result. The heat shield too, because of its manufacturing cure cycle, is another example of this situation. Transformers on the other hand have been found to employ quite "dirty" operations that result in high biological loadings. With the recognition that many different types of parts are required in a system, all of which are fabricated in different ways by hundreds of different suppliers, it becomes clear that use of conventionally made parts (with perhaps a few exceptions) is mandatory, if the impact of sterilization on cost and schedule is to be held within reasonable bounds. Table XVII lists the expected internal burden on typical Probe parts.

Exposure to flight acceptance sterilization temperature conditions should be first in the flight acceptance sequence if done at a component level, and the heat cycle should be equal or higher than the terminal sterilization cycle. This will result in sterile component interiors, and if the components are sealed, their interiors will remain sterile throughout the remainder of assembly. To minimize reliability and performance degradation, the flight acceptance and the terminal sterilization heat cycles should be optimized simultaneously. This optimization is as important to sterility maintenance as it is to performance, as it will reduce post-sterilization repair requirements and thereby recontamination risk.

TABLE XVI

**BIOLOGICAL BURDEN CONTAMINATION AND DECONTAMINATION FACTORS**

<u>Contamination Factors</u>	<u>Consensus Value</u>	<u>Study Value</u>
Internal burden of parts	0 to 100,000/Unit	Same
Fallout on surfaces		
Normal facilities	32 to 128 org/in. <sup>2</sup> /day	40 org/in. <sup>2</sup> /day
Bio-clean facilities	0.32 to 1.28 org/in. <sup>2</sup> /day	4 org/in. <sup>2</sup> /day
Handling		
Normal facilities	1900 org/in. <sup>2</sup> (handled)	Same
Bio-clean facilities	19 org/in. <sup>2</sup> (handled)	190 org/in. <sup>2</sup> (handled)
Electrostatic factor	1 to 10	5
<u>Decontamination Factors</u>		
ETO effectiveness	4D(10 <sup>-4</sup> )	Same
Flight acceptance heat test effect	12D(10 <sup>-12</sup> )	Same
Die-off		
Normal facilities	30 to 99 percent	90 percent
Bio-clean facilities	30 to 99 percent	90 percent

TABLE XVII

PART AND MATERIAL BURDEN ESTIMATES

<u>Type</u>	<u>Estimated Internal Burden Range</u>
Balsa wood	1-10/in. <sup>3</sup>
Battery cell	0
Capacitor	10-1000
Coaxial cable	0-100/ft.
Connector	100-10000
Crystal	0-10
Diode	0
Duplexer	0
Evacuation bellows	0
Explosive	1000/gm *
Explosive trains	0-200/ft.
Fiberglass	0
Foam	1/ml **
G-M tube	0
Inductor	1000-10,000
Magnetic core	0
Magnetron	0-10
Metal	0
Nylon, Dacron	0
Optical system	10-100
PbS detector	0
Photomultiplier	0
Relay	100-1000
Resistor	0-10
Silicone int'd circuit	0-10
Silicone oil	1/ml
Silicone rubber	0
Teflon insulation	0
Thermal control	0
Transformer	10,000-100,000
Transistor	0
TWT	0

\* Weight of solid fuel  $0.059 \text{ lb/in}^3 = 26,800 \text{ org/in}^3$

\*\* Foam -  $16.2 \text{ org/in}^3$

ETO flight acceptance tests should be performed after heat flight acceptance tests. The effectiveness of ETO as a decontamination process has been substantiated by experiment; however, it is important to recognize that ETO cleaning will not reach and decontaminate occluded Probe surfaces or interiors of sealed components.

Cleaning by ETO would affect the interiors of components if they are not sealed. However, as will be discussed later, it may not be necessary to decontaminate the interior of components or "black boxes." Therefore, designers can be given the option of sealing components against ETO penetration whenever this course of action will result in a higher system reliability.

Experiments have shown that microbial fallout in existing aerospace assembly and test facilities is on the order of 30 to 50 organisms/inch<sup>2</sup>/day depending on the number of workers present and the degree of worker activity. Further, natural death (die-off) of organisms occur continually and has been found to be as high as 99 percent of the total population over a period of one year.

Burden attributable to individual hand contacts will be very low in a bioclean room if proper clothes and gloves are worn but, for conservatism, a value of only one order of magnitude less than that for normal conditions is assumed in burden estimate calculations. The analysis takes into account the numbers of contacts, estimated as a function of required operations.

The burden on plastic surfaces may be multiplied above that of normal fallout if the surfaces are electrostatically charged. Accurate values for this factor are not available, and estimates vary widely. A value of five is considered conservative for this factor. Experiments under artificial severe conditions have reported results as high as thirteen. Since its impact on total burden magnitudes can be substantial, an accurate value should be established by experiment under anticipated conditions.

#### 6. 1. 2 System Physical Characteristics

The physical characteristics of the Probe that are of significance to presterilization burden loadings are summarized in Table XVIII. The number of parts, the wide variety of contamination and decontamination factors, and the number of calculations necessary to burden analysis, clearly emphasize the need for an automated data handling system with flexibility to vary alternatives, in order to establish the sensitivity of estimates to process variables, and to establish their effectiveness.

#### 6. 1. 3 Methods of Analysis

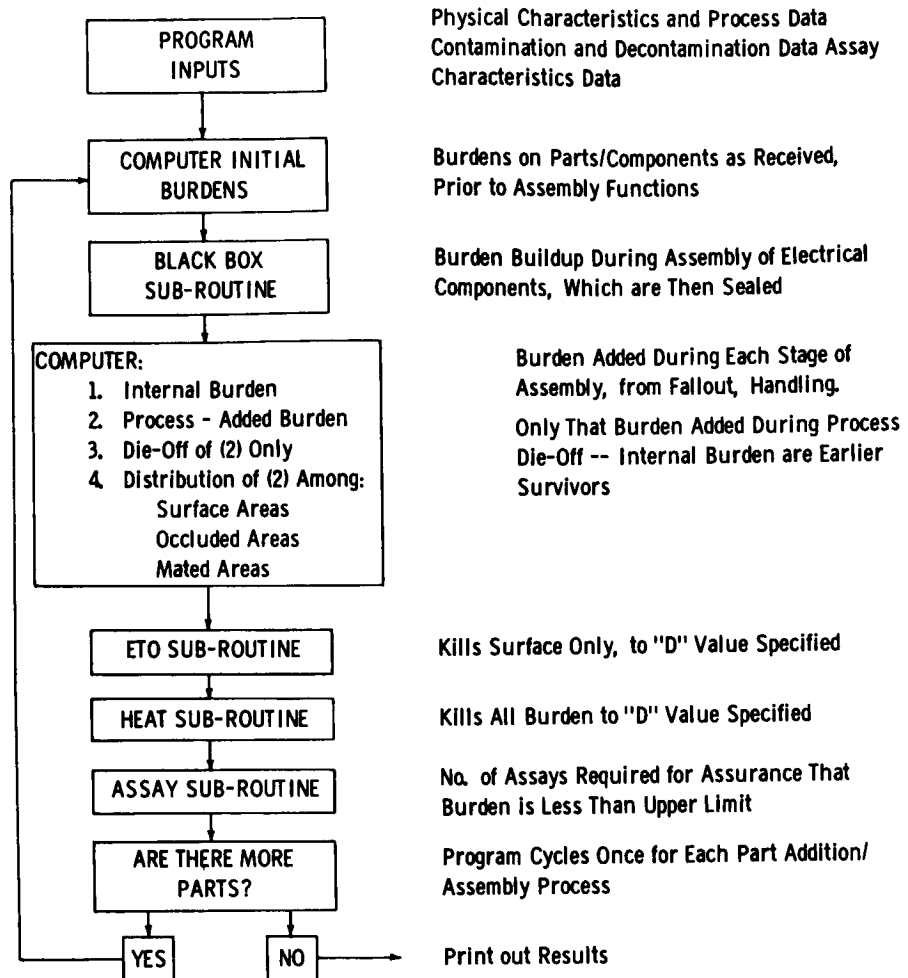
Early burden analysis and prediction methods were applied manually to the Probe design in order to provide a burden estimate while the computer program then under development was completed.

TABLE XVIII

PHYSICAL CHARACTERISTICS OF THE MARS PROBE SYSTEM

Weight	125 pounds
Diameter	36 inches
Electronic parts	1500
Magnetic cores	$6 \times 10^3$
Volume: (in. <sup>3</sup> ) heat shield	84
Propellant	20
Plastic (sterilization container)	1500
Components: quantity	60
Surface area: (in. <sup>2</sup> )	
Occluded	24, 000
Component interiors	20, 000
Electronic	19, 000
Other	1000
Mated	4000
Exposed	15, 000

The computer program shown schematically in Figure 32 accepts as input information the data listed in Table XIX for each part and assembly process. Part/component inputs are required for each element that is a new addition in the order of assembly. Where these elements are electronic components, a separate card, as shown in column two of Table XIX, is required for each type of part in the component, such as resistors and diodes. For any given run the



86-8678

Figure 32 COMPUTER PROGRAM SCHEMATIC

**TABLE XIX**  
**COMPUTER PROGRAM INPUTS**

(1) Part/Component Inputs	(2) Electronic Part Input/Part	(3) Constants for Given Run	(4) Assay Requirements	(5) General Inputs
Level Control point Part number Facility code Percent plastic Initial surface area Initial occluded area Initial volume Assembly mated area No. personal contacts Area contacted ETO "D" value Heat "D" value Assay technique	Level Control point Part number Facility code Part area No. parts Internal burden Percent plastic	Subroutines: Black box Assay Die-off ETO use Heat application Die-Off rate Heat subroutine: Growth rate Death rate ETO subroutine: Growth rate Death rate Initial burden levels Metal, surface Metal, occluded Plastic, surface Plastic, occluded Plastic, internal Electrostatic factor Personnel contamination rate Fallout rate Duration exposed factor Master facility code	No. of assay types Upper burden limit Confidence level code Assay accuracy for subassemblies Confidence level required	Table of assay types and accuracies Table of "t" Distribution values for different confidence levels

data in the third and fourth column are then used the same way at each point in the assembly process. The fifth column identifies and catalogs information used in the calculation of the required number of assays. The program is designed to cycle completely for each assembly process during which new parts may be added, or two or more assemblies may be put together without the addition of new parts. During each cycle, burden factors such as die-off, ETO application and heat application are accounted for.

## 6.2 RESULTS AND CONCLUSIONS

### 6.2.1 Biological Burden Estimates

It is necessary at the onset of the hardware phase of the program to apportion the biological burden among the major elements of the Probe such as each electronic component and each functional component. Knowing this distribution, it then becomes necessary only to exercise proper controls on the environment handling of the elements to assure a pre-sterilization burden of less than  $10^8$  viable organisms.

The basic requirement which makes possible these burden assignments is that of estimating the burden on the complete Probe prior to sterilization.

Table XX shows the results of twenty-four burden estimates based on a permutation of four clean room and six control options. These estimates range from a high of 15.26 million organisms in the case of no controls in a normal environment, to a low of 110,000 organisms in the case of full control in the widest use of bioclean facilities. There are two points of major importance which should be understood when evaluating these results.

These are:

- a. Because of the small size, relative simplicity and relatively short assembly time, the total Probe burden (including that on the inside surface of the sterilization canister), even under the worst likely conditions, will probably not exceed 10 to 15 percent of that which may be permitted, based on a 12D terminal sterilization heat cycle.
- b. Use of clean rooms and burden controls can result in burdens that are on the order of less than one tenth of one percent (three logs) less than allowable, thereby permitting acceptance heating levels and sterilization heating levels which are significantly lower than those presently considered necessary. It is important to note, in addition, that the clean rooms considered in this study are taken to be ten times as clean as a normal uncontrolled area. In fact, it may be easily possible to achieve a cleanliness of one hundred times a normal area in which case the required terminal sterilization cycle may be as low as 8D, or that required to kill 100,000 organisms with a probability of one survivor being  $10^{-4}$ .

**TABLE XX**  
**SUMMARY OF BIOLOGICAL BURDEN ESTIMATES**  
(millions of organisms)

<u>Clean-Room Options</u>					
				A	B
				C	D
				Funct. Compt.; Electr.; System	Funct. Compt.; System
				System Assembly Only	No Clean-Room
				Control Options	
10.53	10.72	11.54	15.26	No Controls	1
7.25	7.41	7.57	8.60	Final System ETO	2
0.52	0.60	1.42	5.16	Flight Accept. Heat	3
0.41	0.45	1.81	4.13	FA & Component ETO	4
0.14	0.19	0.35	1.40	FA + ETO <sub>F</sub>	5
0.11	0.13	0.27	1.15	FA + ETO <sub>C</sub> + ETO <sub>F</sub>	6

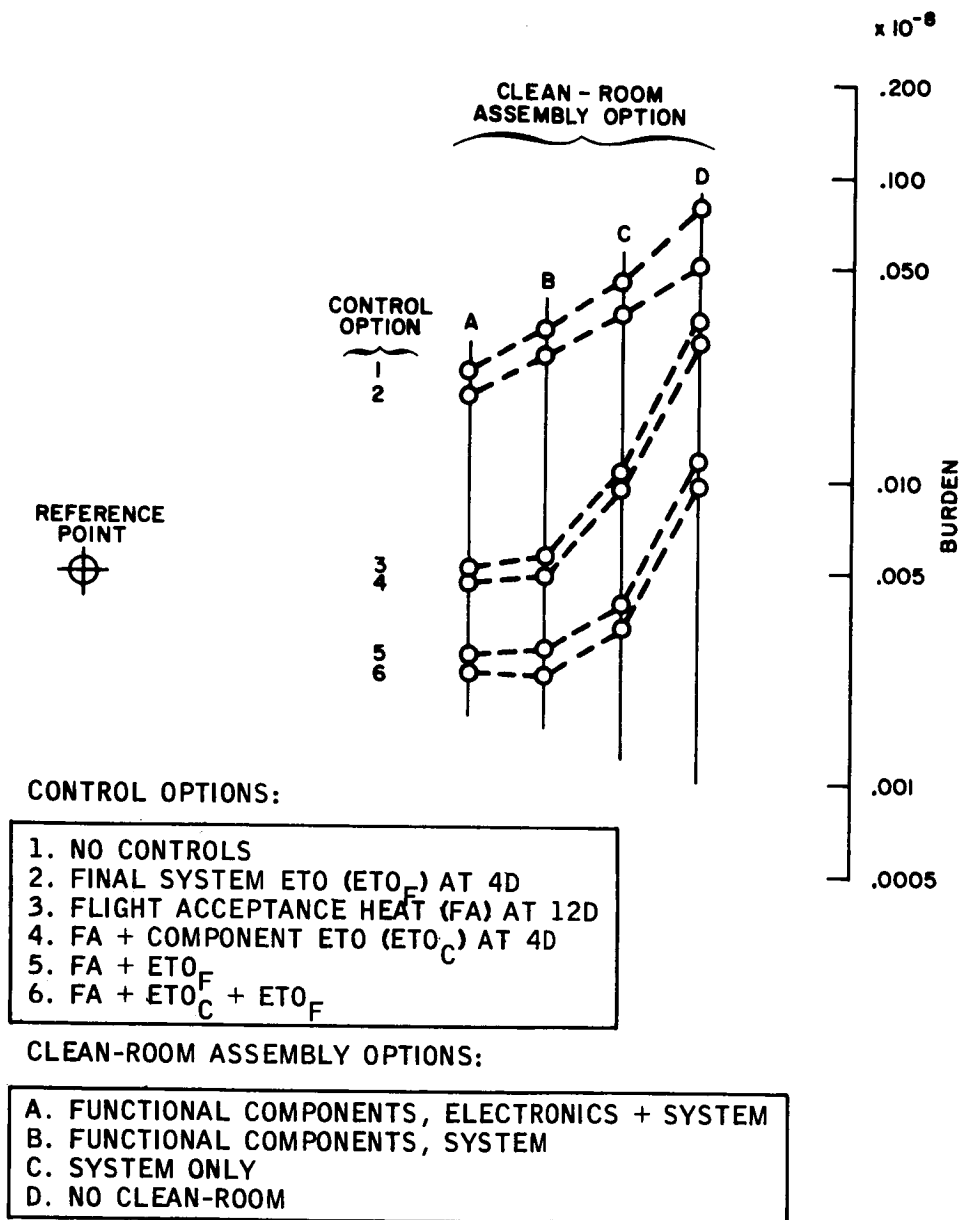
The burden estimate results are shown graphically in Figure 33. The figure is a combination carpet plot and nomogram such that the burden resulting from any conditions of clean room and control may readily be estimated. To determine the burden under a given set of conditions, the options are chosen, and a point on the carpet plot is therefore determined. (The control options, being discontinuous functions, are connected with dashed lines to avoid confusion.) A straight line drawn from the reference point through the point thus determined will intersect the right-hand burden scale at the burden level for the conditions defined.

Several interesting conclusions may be quickly drawn from the figure. Control options 3 and 4, as well as options 5 and 6 are relatively close to each other, indicating that the use of 4 instead of 3, or 6 instead of 5, does not result in a very significant burden reduction. In each case the additional burden reduction is a function of ETO at a component level. It may therefore be concluded that while ETO may be required at a component level for acceptance purpose, its impact on burden levels is relatively minor. Its level of application may therefore be determined from acceptance criteria rather than from sterilization criteria.

Control options 3 through 6 all imply the use of flight acceptance heating, and account for introduction into the assembly area of essentially sterile components. The subsequent addition of burden is a function of the level of cleanliness of the area. It follows that for these four control options, the burden values for clean room option A are always 10 percent of those for option D, since for this study clean rooms were taken to be 10 times cleaner than normal, uncontrolled areas. It is very simple, when considering these control options, to determine the effect of a better clean room having only 1 percent the contamination of a normal area, since the burden on the Probe would be either 10 percent of that for option A, or 1 percent of that for option D. For example, if options A and 6 are assumed, the burden indicated is 110,000 viable organisms. In a room ten times as clean, the burden would therefore be 11,000 organisms. Since present clean room technology indicates that this is reasonable, it makes quite clear the fact that an 8D terminal sterilization cycle can be adequate for this Probe.

In view of the fact that both heat and ETO acceptance will almost certainly be required, the most realistic control options indicated are 4, 5, and 6, the major difference being the application of final system ETO for options 5 and 6. It becomes immediately apparent that while the burdens indicated for both are fairly low, the application of final system ETO accounts for as much as 500 percent reduction, the equivalent of a 0.5D increase otherwise required for terminal heat sterilization.

It is interesting to note that for clean room D, as opposed to the others, final system ETO (control option 2) has a greater impact than control options 3 and 4. The reason for this is that in a non-clean room situation, the fallout and handling



86-6856

Figure 33 PRE-STERILIZATION BURDEN ESTIMATES

burden during assembly are high enough that the reduction due to final surface ETO only, is greater than the combined reduction of surface, occluded and internal burden at the component level, as a result of heat and ETO acceptance.

#### 6.2.2 Assay Requirements

In order to verify the selected sterilization plan, it is necessary to certify that the factors used are the correct ones, namely: internal burden of parts and fallout rates. This raises the question, "What types of assays are required and in what quantities are they necessary?" To answer this question it is necessary to establish the accuracies of possible assay methods.

A prediction can be made using the Student's "t" distribution technique for small sample sizes. Table XXI summarizes this statistical method. The assay recoveries in Table XXII, reported by the indicated references, were modified for conservatism and the values established in Table XXIII were used to indicate overall accuracy of each assay technique. A sub-routine for assay analysis was constructed and coupled to the burden estimate computer program. Results are shown in Figure 34, and indicate that very few assays of equipment are needed to establish that the burden contribution of components is acceptable, the criterion being that they have low burdens compared to the kill effectiveness of the flight acceptance conditions to which they will be exposed.

Those assays which are considered necessary must be conducted during the development program to verify apportionment values used in the sterilization burden control plan. Once values have been verified, it is then necessary only to monitor fabricators of equipment to certify that changes to procedures are not undertaken that will strongly increase burden. Values of fallout and handling contamination in assembly operations should, however, be measured and established within the particular facilities to be used, then monitored continuously to guarantee that limits are not violated at any time.

#### 6.2.3 Terminal Sterilization

The Probe, with a biological burden controlled to less than  $10^8$  organisms during assembly, shown schematically in Figure 35, is subjected to dry heat applied externally by a forced convection oven, and by internal heaters strategically located to allow heat application in a balanced fashion and to shorten the rise time to temperature. Studies show that if heat is applied only externally, the rise time for a system of this size is on the order of 20 hours. Internal heaters reduce this by nearly an order of magnitude. Investigations of other time-shortening techniques such as forced internal convection of different inert gases, or by external temperature cycle overshoot, provide additional improvement. After a dwell at maximum temperature, cool-down takes approximately 20 hours to reach ambient conditions for highly insulated elements. However, the external canister surface reaches room temperature conditions within a few hours.

TABLE XXI

## STATISTICAL METHOD DESCRIPTION

$\eta$ = No assays required	$\bar{x}_p$ = Upper control limit
$t$ = Value from standard "t" table	$A$ = Assay accuracy
$\bar{x}_s$ = Calculated value of burden	$\frac{\eta}{t^2} = \left( \frac{\sigma_s}{\bar{x}_p - \bar{x}_s} \right)^2 \cdot \frac{1}{A}$
$\sigma_s$ = Standard deviation of $\bar{x}_s$	

The right side is calculated, then equality is satisfied by iterating in "t" table, where associated values of  $t$  and  $\eta$  are found for any given confidence.

TABLE XXII

## ASSAY ACCURACIES

Surface Burden	Precision	Recoveries (percent)	Reference
Swabs	Poor	52 to 90	Angelotti, '58
Rinse or spray rinse	Fair	80	Buchbinder, '47 Angelotti, '58
Agitation	Fair	80	Wilmot Castle Co.*
Immersion with ultrasonics	Excellent	90 to 99	Wilmot Castle Co.*
Rodac	Good	41	Angelotti, '64
Internal burden			
Size reduction techniques	Very poor	1	Reed, '65
Filtration (for assay of liquids)	Excellent	99 to 100	Wilmot Castle Co.

\*Based on unpublished data

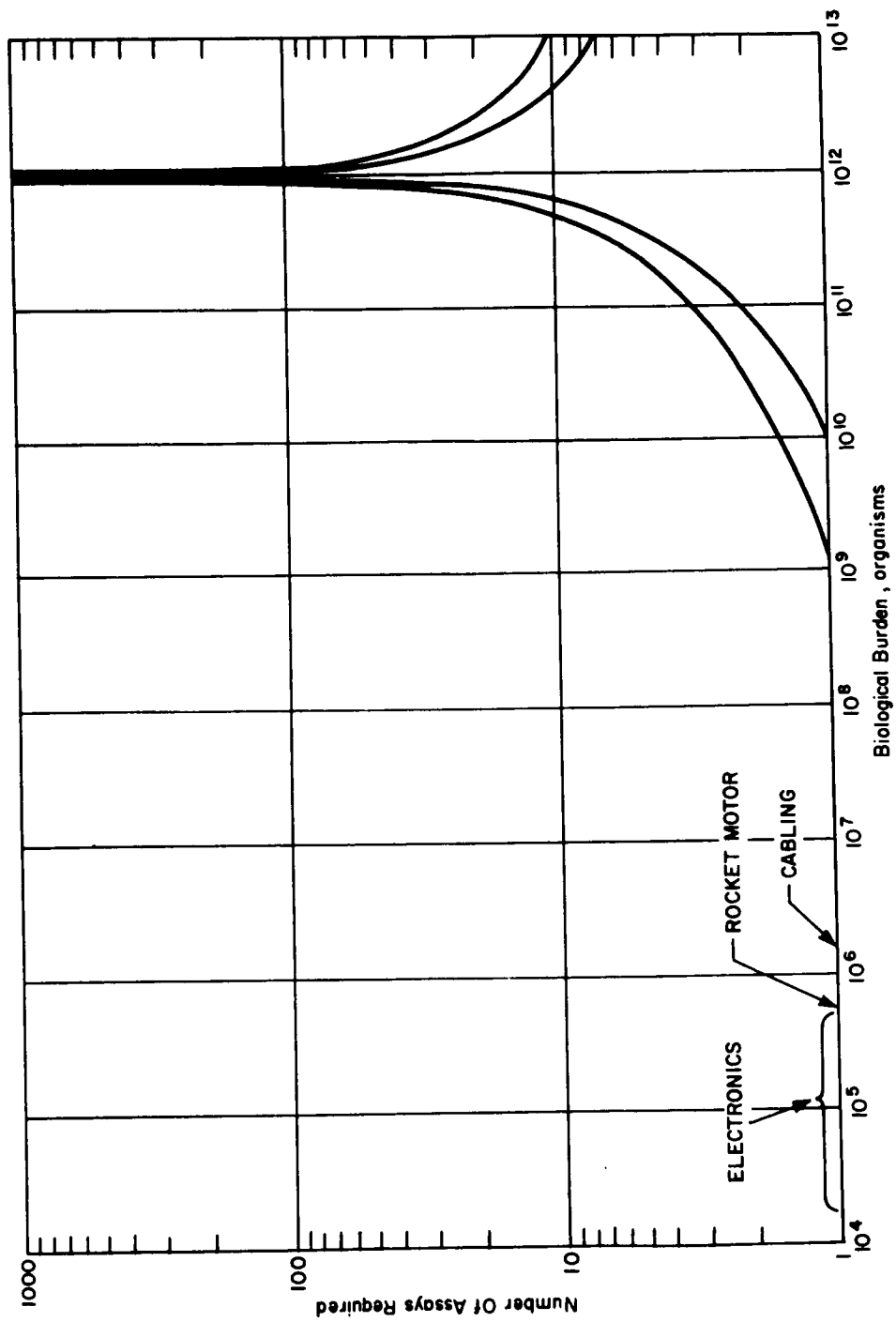
TABLE XXIII

## OVERALL ASSAY ACCURACIES

Swab	37%
Rinse	60
Agitation	60
Immersion	67
Rodac	30
Filtration	74
Internal	5
Black boxes	50*
Subassembly, general	30**

\*Mixture of Swab, Immersion and Internal

\*\*Mixture of Rodac, some Swab



86-6357

Figure 34 BURDEN ASSIGNMENT ASSAY REQUIREMENTS

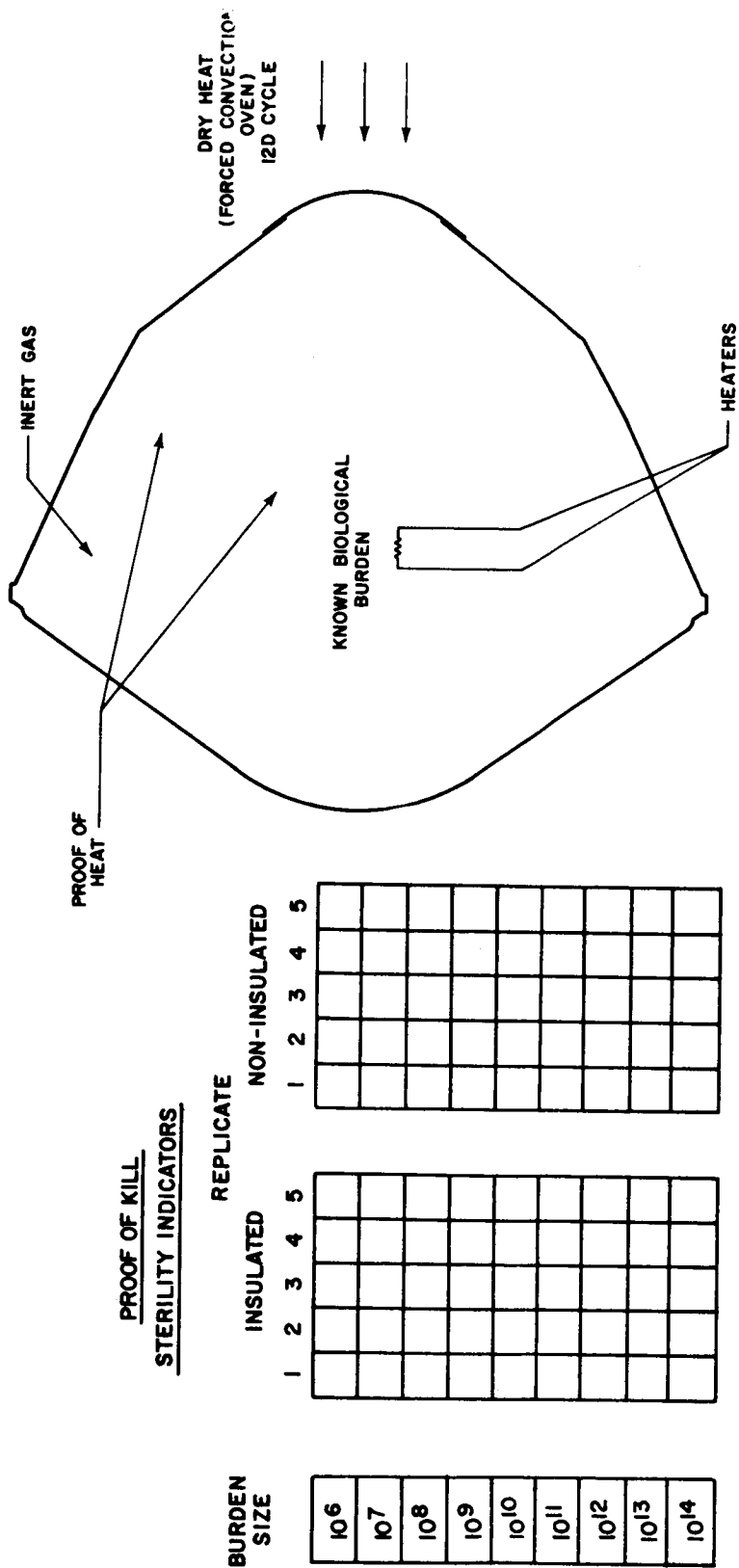


Figure 35 TERMINAL STERILIZATION CONFIGURATION

86 - 6858

The terminal cycle should be optimized to provide a total kill effect of 12D (or less if the burden during assembly is controlled to values significantly below  $10^8$ ) to minimize the impact on system performance and reliability during the heatup, dwell, and cool-down periods.

Heat application is verified by thermocouples installed within the Probe. Cycle kill effectiveness may be verified through the use of sterility indicators, in the form of known organism populations, which are simultaneously exposed to the heat cycle in the same oven as the Probe. Indicators can be designed to have the same insulation characteristics as remote Probe interiors. Non-insulated indicators can directly verify the effect of the cycle. If indicators with a range of population sizes are used, Probe sterility probability can be established.

#### 6.2.4 Post-sterilization Maintenance

Subsequent to terminal sterilization, the Probe System interacts with other project systems as indicated schematically in Figure 36. Sterility during these phases can be verified only indirectly, by measuring any leakage of a pressurized inert gas stored within the system. However, this does not guarantee that sterility is not compromised, since evidence indicates that organisms may be able to flow "up stream" if leak-hole sizes are large enough. Additional protection can be provided, if the Probe is stored within a handling container, by applying ETO within the handling container.

There is a finite probability that repairs, or at least adjustments, may be required during the time period from terminal sterilization to launch. This establishes the potential need for a method (equipment, facilities and procedures) to conduct such activities under sterile conditions. In the absence of such a method, if repairs are to be made, the Probe must be capable of tolerating additional sterilization heat cycles (a very severe penalty).

Little is known about the possible recontamination risk that may be encountered by the Probe during and after canister lid opening, but prior to ejection. This area requires substantial investigation to determine if recontamination is possible.

#### 6.2.5 Sterilization Effects on Materials and Components

To enhance the performance and reliability of the Probe, design recommendations for compatibility to environments imposed by the sterilization constraint should be made as early in the program as possible. These recommendations would include listings of preferred materials, parts, processes and design techniques. There is a considerable and growing amount of information on this subject in the field and this should be searched and organized to initiate the preferred listings. Section 5.0 of Volume IV briefly highlights the more

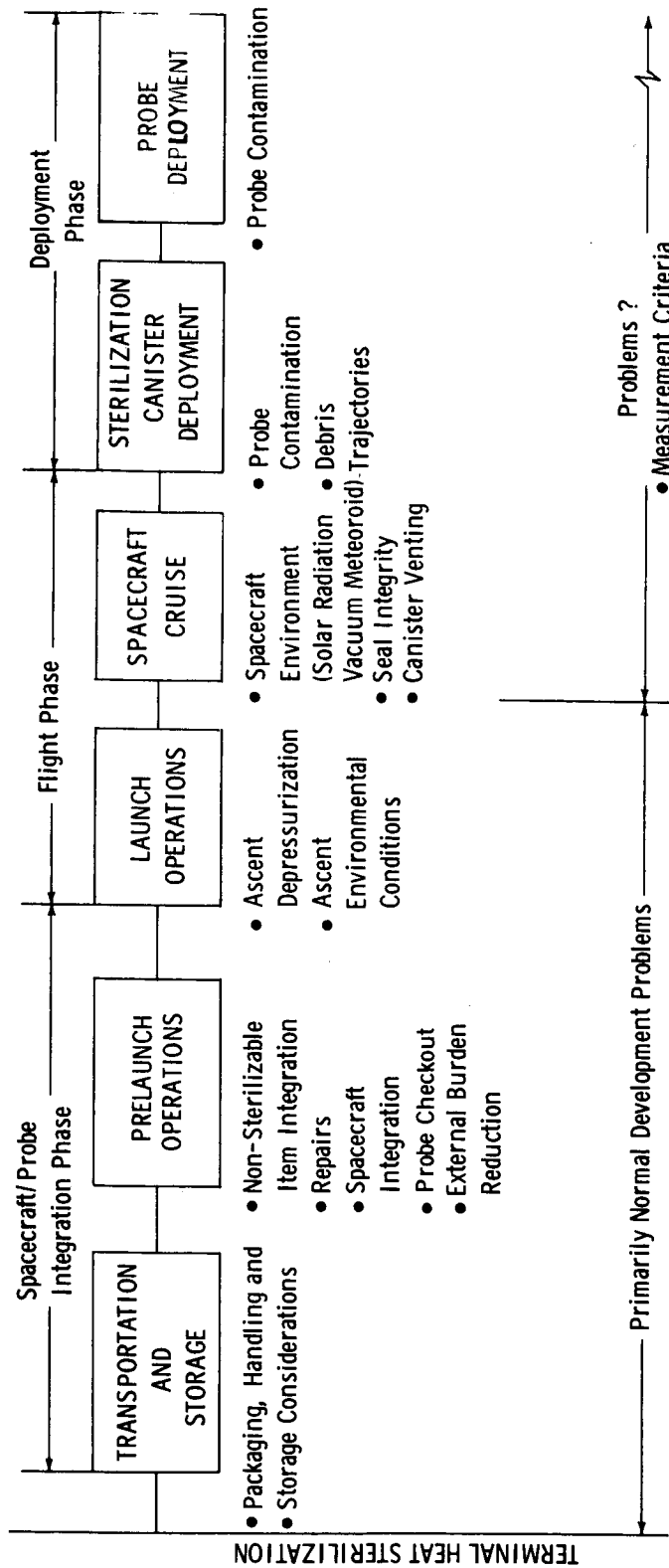


Figure 36 POST-STERILIZATION MAINTENANCE

significant effects which must be considered in the development of Probe elements, and lists specifically the major effects on Probe materials and components of the terminal sterilization cycle.

Particular care must be exercised in the selection of materials and components so as to minimize harmful outgassing during the heat cycle. Careful design is also needed to prevent misalignment due to thermal stresses. Certain instrumentation components (radiometer interference filters) are sensitive to temperature variations and some components (batteries) are predictably degraded by the heat cycle and must be overdesigned to compensate for this degradation. Although to date no insuperable problems have been uncovered due to the effects of the terminal sterilization cycle on Probe subsystems or components, it is clear that extensive development and testing would be required during the hardware phase of a Probe program to assure satisfactory Probe performance.

## 7.0 ALTERNATE MISSION MODES

The basic Probe mission consisted of deploying the entry Probe from the approach trajectory. For illustrative purposes, much of the detailed work was performed for the 1969 Type I trajectories launch window since it resulted in the highest entry velocities and thus governed the entry vehicle heat shield and structural design, as well as yielding lower limits on some of the relay communications link parameters (communications time available after blackout) and upper limits on the instrumentation dynamic range requirements.

In addition to this illustrative mission, several other mission modes were examined in some detail. Among these the most important were:

- A Probe mission for the 1971 launch opportunity
- A minimum payload, minimum ballistic coefficient Probe design
- Deployment of the Probe from a spacecraft in orbit around Mars

The principal results for these alternate mission modes are summarized below.

### 7.1 THE 1971 LAUNCH OPPORTUNITY

The basic Probe design for Probe deployment from the approach trajectory is not too sensitive to the launch opportunity since in all cases the basic measurement, separation, communications and housekeeping requirements are quite similar. Since the approach velocities for 1971 are considerably lower than for 1969, the heat shield requirements are eased so that a slightly lighter Probe can be designed. The structural weight, however, is always governed primarily by minimum manufacturing gage requirements and is therefore largely unaffected by the entry velocity.

The lower entry velocities (18-20,000 ft/sec as compared to 26,000 ft/sec) also result in longer entry flight times, longer communications times after blackout, and shorter blackout duration, which generally eases the  $M/C_D A$  requirements and the communications requirements. The lower g-loadings also ease the mechanical survival requirements on the payload components.

The most important consequence of the reduced entry velocity for the 1971 opportunity is its effect on one of the measurements, namely the optical radio-meter. This instrument operates only during the time that the shock-heated gas near the stagnation point radiates with sufficiently large intensity to be detectable. Since the radiation intensity is very strongly dependent upon the entry velocity, a decrease in entry velocity leads to a large decrease in radiation

intensity. Therefore, for the lower velocity entries the radiation measurements can be performed for only a very short period of time and very great demands are placed upon the sensitivity required of the instrument.

In summary, it is concluded that the 1971 opportunity is quite attractive in that it generally eases the design requirements imposed on the Probe mission with the exception of the radiometer measurement which is then significantly more difficult to accomplish.

## 7.2 MINIMUM BALLISTIC COEFFICIENT PROBE DESIGN

After the receipt of the Mariner IV occultation data, it became clear that stringently low  $M/C_D A$  requirements would have to be placed on the Probe vehicle to assure adequate relay communications performance. It was also recognized that to cope with the possibility of a very low density atmosphere, it may be desirable to target for an entry angle of less than 70-80 degrees. Since shallow entry angles somewhat degrade the accuracy of reconstruction of the atmospheric density profile, it was interesting to examine a low  $M/C_D A$  Probe design whose primary goal would be an accurate determination of the density profile. Thus the instrumentation complement consists of only the four accelerometers, five pressure gages and two temperature Probes.

The deletion of the mass spectrometer and radiometer results in a payload weight savings of about 10 pounds. In addition, since it is no longer required to achieve a non-ablating stagnation region, the removal of the heat sink and radiometer window from the front of the Probe results in some additional weight savings as well as a considerably simplified Probe design. The net result of these changes is that for the same 36-inch Probe diameter, the ballistic coefficient is reduced to less than 0.14 slug/ft<sup>2</sup>. Thus vertical entry into even very low pressure atmospheres (> 5 millibars) still results in adequate communications times. Larger Probe diameters result in still lower  $M/C_D A$ 's so that values as low as 0.10 - 0.12 could be considered for such larger vehicles.

The most attractive use of such low ballistic coefficient Probes appears to be in cases where a single spacecraft carries more than one Probe. Then the low  $M/C_D A$  Probe could be targeted for a vertical (or near vertical) entry while the full payload Probe would be targeted for a lower entry angle. Thus the first Probe would obtain very accurate density profile information, while the second Probe would obtain additional atmospheric composition data.

## 7.3 PROBE DEPLOYMENT FROM OUT-OF-ORBIT

Probe deployment from a spacecraft already in orbit about Mars was studied for a variety of orbits having a common periapsis altitude of 1800 kilometers and apoapsis altitudes ranging from 1800 to 30,000 kilometers. It was found that Probe deployment at a true anomaly somewhat later than periapsis (50

degrees after apoapsis) provided quite reasonable communications ranges and look-angles for all orbits. Furthermore, it was found that a fixed deorbit velocity increment and a fixed-thrust application angle could be used to cover the entire range of orbits and still achieve satisfactory entry conditions. To avoid skipout for the 1800 kilometer circular orbit, a minimum  $\Delta V$  of 1200 ft/sec is required, resulting in an entry angle of about -14 degrees. For the 1800 by 30,000 kilometer orbit, this same  $\Delta V$  results in an entry angle of -46 degrees. The corresponding entry velocities are about 11,000 and 14,000 ft/sec, respectively.

Ordinarily, this spread in possible entry conditions and the generally quite shallow entry angles would raise questions about the accuracy of the atmospheric reconstruction due to errors arising from uncertainties in the knowledge of the entry angle. It was found, however, that with the same separation and attitude control system, the dispersions in entry angle were much lower than those associated with deployment from the approach trajectory. Dispersions as low as 0.6 to 1.0 degree 3 sigma appear possible. Thus even at the shallow entry angles, the knowledge of the entry angle is sufficiently precise so that, if anything, slightly better atmospheric reconstruction can be accomplished with the out-of-orbit deployment as compared with the approach trajectory deployment.

The low entry velocities greatly reduce the heating and g-loads to the Probe vehicle and in combination with the shallow entry angles result in much less stringent ballistic coefficient requirements. In addition, the relay communications link requirements are considerably reduced since the communications ranges are less than 4000 kilometers, the look-angles are favorable (the spacecraft elevation angle does not go below 40 degrees at Probe impact for any orbit and model atmosphere considered) and communications blackout is greatly reduced or perhaps eliminated altogether.

The only undesirable effect of the low entry velocities is the elimination of the radiometer experiment which does not function at such low velocities. The mass spectrometer, however, is easier to utilize at these lower velocities thus somewhat compensating for the loss of the radiometer experiment.

## 8.0 EARTH-ENTRY TEST PROGRAM

As part of the development of the Mars Probe System and to demonstrate the performance and adequacy of the Probe design, it is very desirable to perform earth-entry flight tests which simulate the Mars entry conditions in several important respects.

The following sections cover the booster and trajectory selection for the earth-entry tests, the mission profile flown and the integration of the Probe with the earth-entry test booster together with any Probe design changes necessary to accommodate the tests.

### 8.1 BOOSTER AND TRAJECTORY SELECTION

The objectives of the earth-entry test (s) are to evaluate the performance of the total Probe System and to assess the accuracy with which the Probe data can be used to reconstruct the atmospheric properties.

The trajectory selection is based on the desire to simulate the heating and loading environment characteristics of Mars entry and to simulate, wherever possible, the proper geometry between the Probe transmitting antenna and the ground based receiver system (which serves as the simulated Probe-to-spacecraft relay link).

Because of the small size and weight of the Probe, the Scout booster system is considered quite applicable for this purpose. As discussed below, this low cost booster can achieve the desired trajectory conditions.

To simulate the worst integrated heating inputs, reconstruction accuracy at off-vertical entry angles, and longest flight times encountered in the large scale-height-model atmospheres, it is necessary to fly relatively shallow ( $\approx 20$  degree) earth-entry trajectories. For entry velocities of up to 23,000 ft/sec this can be accomplished with the three-stage Scout (two stages fired on the ascent trajectory, one stage fired down). A schematic of the trajectory profile is shown in Figure 37. Subscripts "1" and "2" refer to Probe antenna look-angles and communications ranges at entry to Wallops Island and Bermuda, respectively.

To simulate the worst heating rates, highest g-loadings, and shortest flight times, it is necessary to fly steep earth-entry trajectories as illustrated in Figure 38. Such trajectories result in large look-angles between the Probe antenna and the ground stations.

$\gamma_{\text{ENTRY}} = -20 \text{ deg}$   
EARTH

$\alpha_{\text{ENTRY}} = 0 \text{ deg}$   
EARTH

SCALE: 1 INCH=100 STATUTE MILES

$\beta_1 \approx 37^\circ, R_1 \approx 1060 \text{ km}$

$\beta_2 \approx 85^\circ, R_2 \approx 158 \text{ km}$

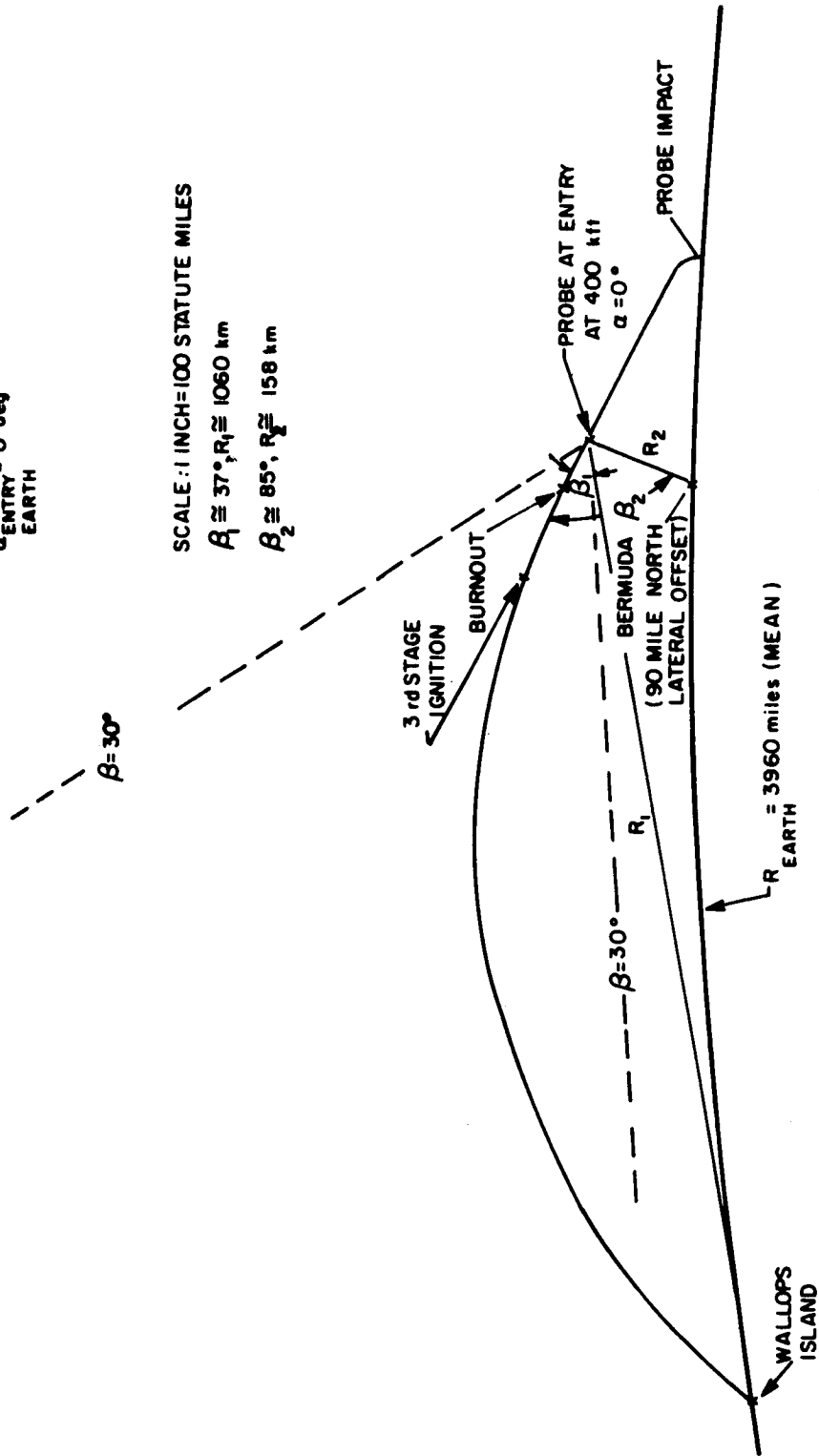
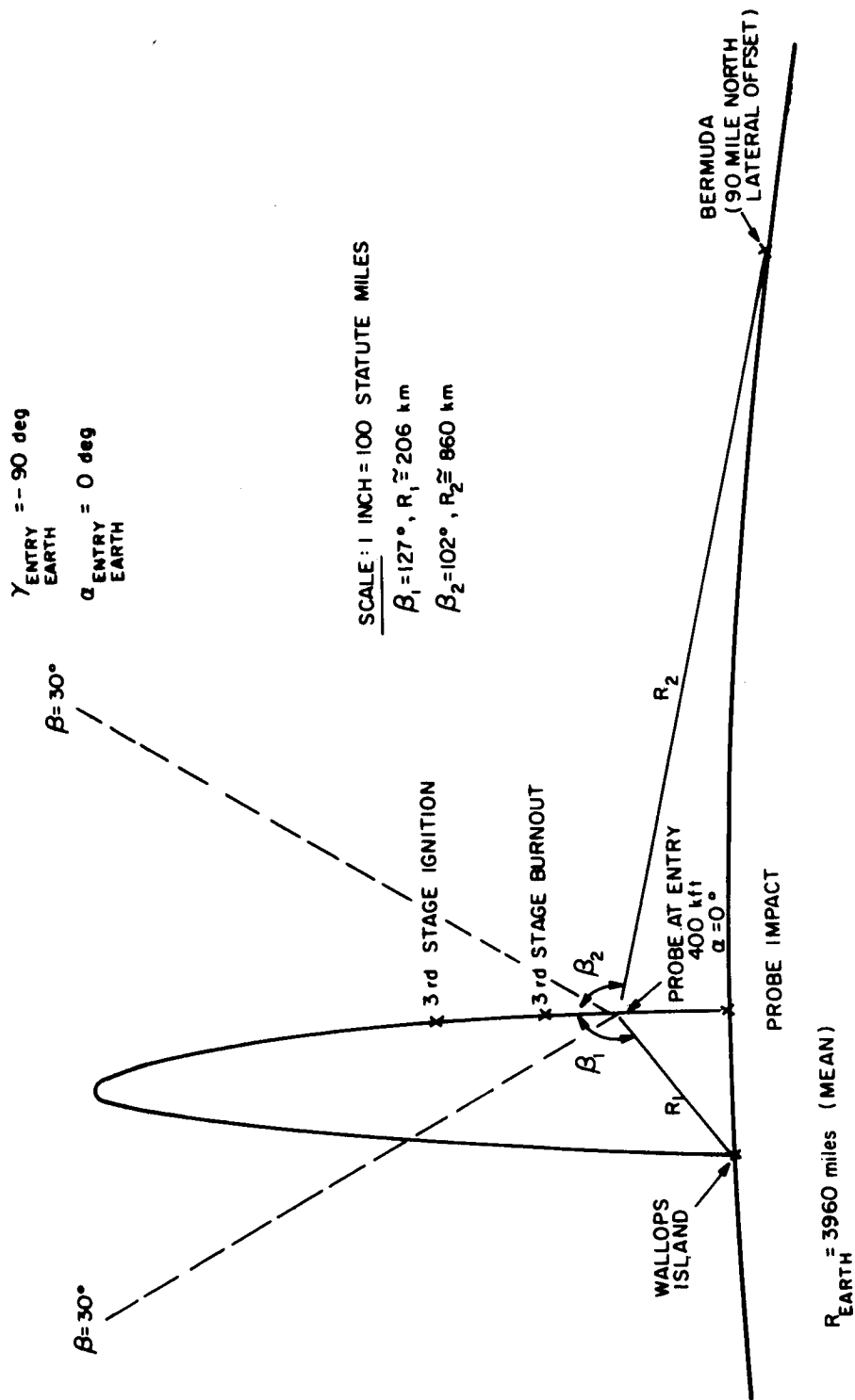


Figure 37 EARTH-ENTRY TEST TRAJECTORY (SHALLOW ENTRY, THICK ATMOSPHERE SIMULATION)

86-8679



86-8680

Figure 38 EARTH-ENTRY TEST TRAJECTORY (VERTICAL ENTRY, THIN ATMOSPHERE SIMULATION)

## 8.2 PROBE DESIGN AND BOOSTER INTEGRATION

It is intended that the earth entry test should be conducted with a Probe System which is very similar (and even identical) to that used for the Mars flight. The integration of the Probe into the Mars spacecraft and the Scout booster is compared in Figure 39.

The Probe System is assembled to the Mariner spacecraft via an adapting spacer bolted to the aft sterilization canister flange. For the earth entry test, the same hardware is bolted to the earth-entry test booster via another adapting spacer designed to mate with the booster mechanical and electrical interface. The earth-entry booster-ascent heat shield is modified to accommodate the maximum diameter of the Probe System.

The Scout consists of three booster motors, a spin table, a fourth-stage motor, a payload adapting "E" section and a payload separation system based on the V-band coupling principle. It also provides an ascent heat shield. For this application, only the first three booster motors are required; two for ascent and the third for Probe acceleration into the earth's atmosphere. The spin table is removed since the spin-stabilized fourth-stage motor is not used. Other Scout components removed are the adapting "E" section and the payload separation system. The "E" section is not used since it would adapt to the fourth-stage motor.

The Scout payload separation system is removed since the Probe System is equipped with its own separation assembly which is being development tested as a part of the flight test. The Scout ascent-heat shield is locally modified to meet the Probe maximum diameter requirement. The Scout ascent heat shield is 34.1 inch in outside diameter. A 36-inch diameter Probe is required to meet the payload and communication time requirements. The Scout heat shield can be modified to accommodate this larger dimension as shown in Figure 40. This radial extension of the heat shield has been reviewed both mechanically and aerodynamically. Mechanically, LTV can provide a radial heat shield modification similar to that shown. Aerodynamically the design limit is not one of axial drag but rather of side loading due to wind load against the projected area of the ascent heat shield. Since the modified configuration only increases the projected area one percent, the modification is deemed feasible and practical. This is the only significant Scout modification needed to accommodate the Probe System.

A mechanical stabilizing bumper is used between the Scout fourth-stage motor and the ascent-heat shield for standard applications. Since the fourth-stage motor is not used for this application, a corresponding bumper is supplied as an extension to the forward flange of the Probe-adapting spacer. The spacer is bolted to the forward flange of the third-stage motor, replacing the Scout spin-table aft flange.

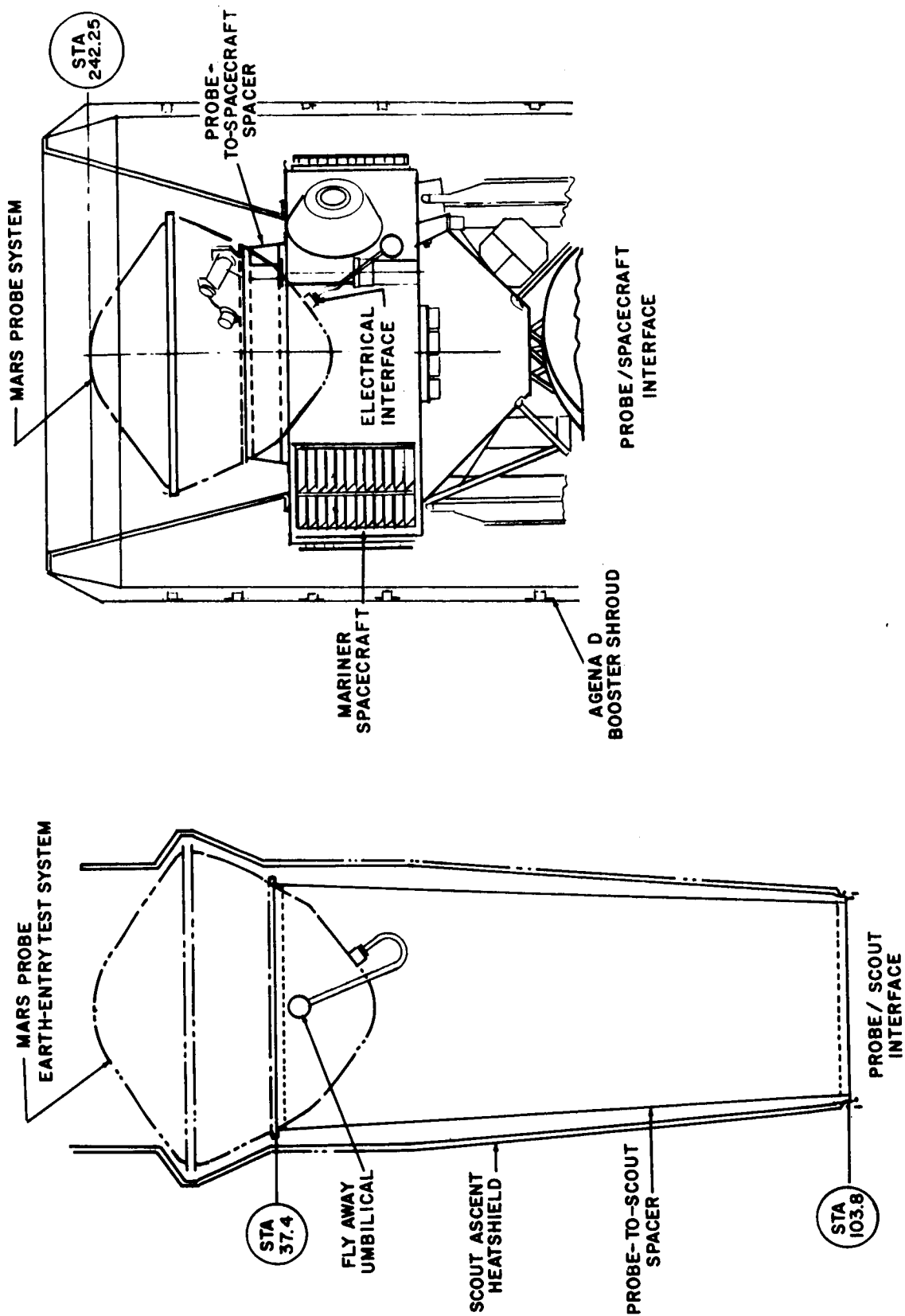
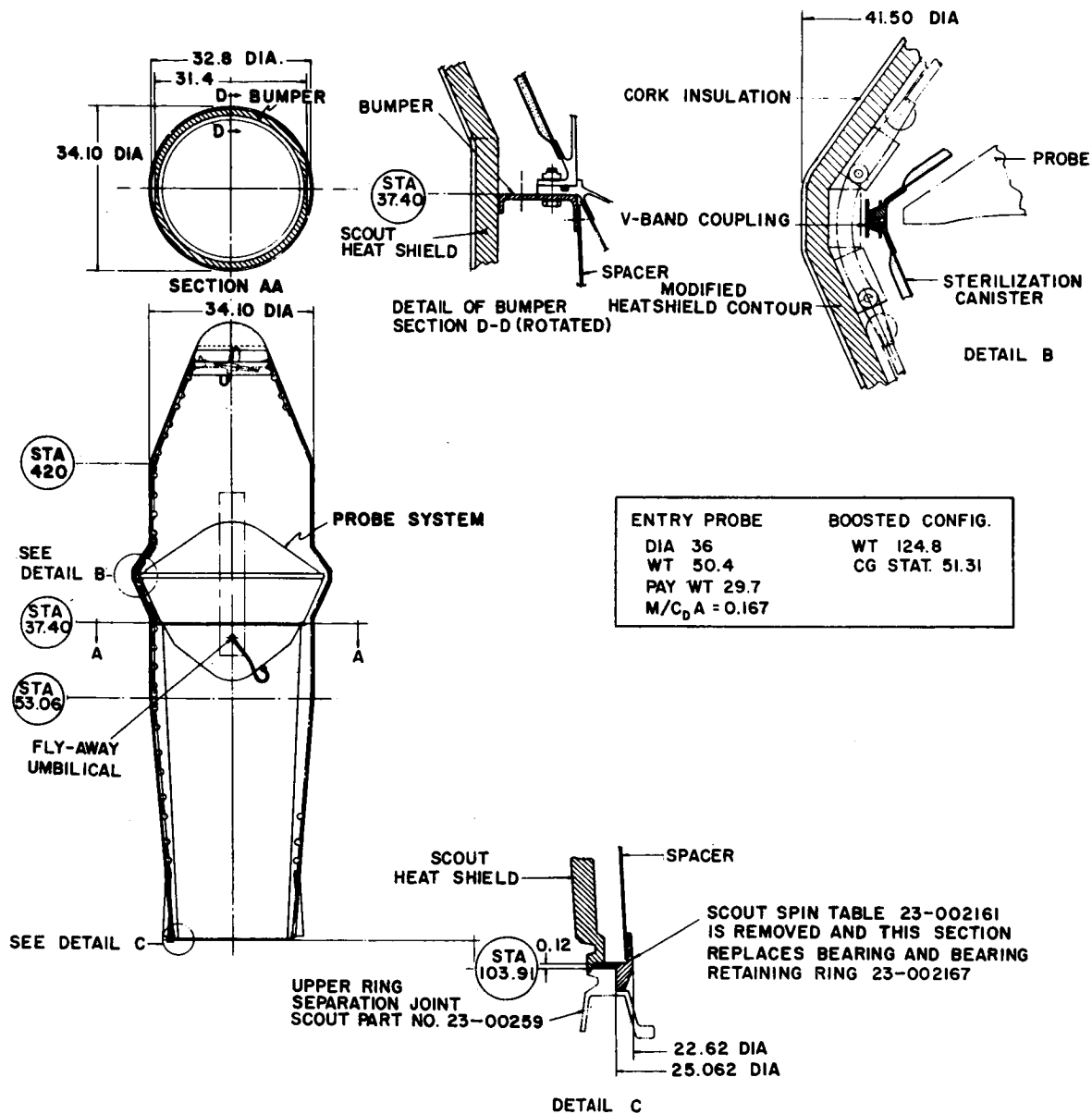


Figure 39 PROBE-SCOUT AND PROBE-MARINER SPACECRAFT INTEGRATION COMAP

86-8681



86-6877

Figure 40 PROBE-SCOUT MECHANICAL INTERFACE DIFINITION

Finally, the elevation of the Probe System within the Scout heat shield is determined by the location of the launch facility flyaway umbilical. It must be located within the rectangular area shown on the inboard profile to prevent facility modification.

## 9.0 REFERENCES

1. Seiff, A., Some Possibilities for Determining the Characteristics of the Atmospheres of Mars and Venus from Gas-Dynamic Behavior of a Probe Vehicle, NASA TN D-1770 (1963).
2. Seiff, A., and D. E. Reese Jr., Defining Mars' Atmosphere -- A Goal for the Early Missions, *Astronautics and Aeronautics*, Vol. 3, No. 2 (February 1965).
3. Seiff, A., and D. E. Reese Jr., Use of Entry Vehicle Responses to Define the Properties of the Mars Atmosphere, Preprint 65-25, American Astronautical Society Symposium on Unmanned Exploration of the Solar System, Denver, Colorado (8-10 February 1965).
4. Peterson, V. L., A Technique for Determining Planetary Atmosphere Structure from Measured Accelerations of an Entry Vehicle. NASA TN D-2669 (1965).
5. Peterson, V. L., Analysis of the Errors Associated with the Determination of Planetary Atmosphere Structure from Measured Accelerations of an Entry Vehicle. NASA TR R-225 (July 1965).
6. Reese, D. E., and S. Georgiev, Design Problems and Experiments for Mars Atmosphere Probes, Proceedings of the AIAA/AAS Stepping Stones to Mars Conference (28 to 30 March 1966).
7. Lavin, G. M., D. E. Evans, V. Stevens, NASA Engineering Models of the Mars Atmosphere for Entry Vehicle Design, NASA TND-2525 (November 1964).
8. Kraus, A., The Helical Antenna, Proceedings of the IRE (March 1949).

*"The aeronautical and space activities of the United States shall be conducted so as to contribute . . . to the expansion of human knowledge of phenomena in the atmosphere and space. The Administration shall provide for the widest practicable and appropriate dissemination of information concerning its activities and the results thereof."*

—NATIONAL AERONAUTICS AND SPACE ACT OF 1958

## NASA SCIENTIFIC AND TECHNICAL PUBLICATIONS

**TECHNICAL REPORTS:** Scientific and technical information considered important, complete, and a lasting contribution to existing knowledge.

**TECHNICAL NOTES:** Information less broad in scope but nevertheless of importance as a contribution to existing knowledge.

**TECHNICAL MEMORANDUMS:** Information receiving limited distribution because of preliminary data, security classification, or other reasons.

**CONTRACTOR REPORTS:** Scientific and technical information generated under a NASA contract or grant and considered an important contribution to existing knowledge.

**TECHNICAL TRANSLATIONS:** Information published in a foreign language considered to merit NASA distribution in English.

**SPECIAL PUBLICATIONS:** Information derived from or of value to NASA activities. Publications include conference proceedings, monographs, data compilations, handbooks, sourcebooks, and special bibliographies.

**TECHNOLOGY UTILIZATION PUBLICATIONS:** Information on technology used by NASA that may be of particular interest in commercial and other non-aerospace applications. Publications include Tech Briefs, Technology Utilization Reports and Notes, and Technology Surveys.

*Details on the availability of these publications may be obtained from:*

SCIENTIFIC AND TECHNICAL INFORMATION DIVISION  
NATIONAL AERONAUTICS AND SPACE ADMINISTRATION

Washington, D.C. 20546